FATIGUE BEHAVIOR AND DESIGN OF HEAVY DUTY RIVETED STEEL GRATINGS IN BRIDGE DECKS

A Dissertation

Presented to

The Graduate Faculty of The University of Akron

In Partial Fulfillment

of the Requirements for the Degree

Doctor of Philosophy

Godwin Addiah Arthur

December, 2014

FATIGUE BEHAVIOR AND DESIGN OF HEAVY DUTY RIVETED STEEL GRATINGS IN BRIDGE DECKS

Godwin Addiah Arthur

Dissertation

Approved:

_____	
Advisor Dr. Craig Menzemer	
_____	
Committee Member Dr. Anil Patnaik	
_____	
Committee Member Dr. David Roke	
_____	
Committee Member Dr. T.S. Srivatsan	
_____	
Committee Member Dr. Desale Habtzghi	

Accepted:

_____	
Department Chair Dr. Wieslaw Binienda	
_____	
Dean of the College Dr. George Haritos	
_____	
Dean of the Graduate School Dr. George Newkome	
_____	
Date	

ABSTRACT

A heavy duty riveted steel grating is an open grid deck system used in movable bridge construction and rehabilitation projects. They are lightweight and easy to install when compared to conventional slab systems and is thus preferred when the load carrying capacity of an existing bridge needs to be increased. Empirical methods have been used in the past due to limited information about their design and behavior. Open grid decks have been used in a number of bridges with the majority being welded decks. A major problem encountered with these decks is the development of fatigue cracks resulting in increased maintenance cost. Observations in the field when heavy duty riveted steel gratings are used and results from experiments indicate better fatigue performance than welded decks. The fatigue characterization of the heavy duty riveted grating has not been established and there are no provisions to govern the design in the AASHTO LRFD Specifications.

The current research examines the fatigue behavior of heavy duty riveted steel decks under AASHTO H20 truck loading and also establishes an effective width to be considered during design. Preliminary tests were conducted on two large panels of 37R5 lite to investigate the static behavior and the nature of stress distribution on major components of the grating. A 3D finite element model was calibrated to laboratory data

to simulate experimental tests and used for parametric studies in estimating stresses in various components. Fatigue testing of six structural panels with simulated H20 design truck tire loads and of 26 smaller panels at stress ranges of 20ksi, 25ksi, 30ksi and 35ksi was performed. A fracture mechanics approach was used to estimate the fatigue life of the gratings. Results showed that the primary strip width provided in the AASHTO LRFD specifications for the design of open grid decks under predicted the stresses on main bearing bars. An effective width is proposed and involves the length or width of the tire patch perpendicular to the direction of main bars plus twice the spacing of the main bearing bars. The intermediate bars, if present, contribute towards the load carrying properties of the heavy duty riveted gratings but not the connecting bars. Results from smaller panel specimens correlated well with that of the large panels during fatigue testing. The mean fatigue S-N curve for test data was close to that of a category B with a constant amplitude fatigue limit of 16ksi. The heavy duty riveted steel grating can conservatively be designed as a category D detail but with a constant amplitude fatigue limit of 12ksi. Results from the research were used to develop a guide towards the design of heavy duty riveted steel gratings.

DEDICATION

This work is dedicated to my family for the continuous support and encouragement throughout my education.

Mum: Although you didn't live to see this day, I know I made you proud.

ACKNOWLEDGEMENTS

I have been fortunate enough to receive a lot of encouragement and support from my family, colleagues and friends in the cause of my doctoral research. This work wouldn't have seen the light of day without the guidance, advice and support of my graduate advisor, Dr. Craig Menzemer. I owe a lot of gratitude also to Mr. Brett Bell, Mr. Dave Mcvaney and Mr. Steve Paterson for helping me with my laboratory set-ups for testing.

I would like to thank my committee members for their help and input towards the completion of this research. My fellow friends both in Ghana and the United States for your prayers and encouragement throughout my studies and not making me feel home sick.

Finally, I want to thank God for the strength, wisdom and blessings bestowed on me for the successful completion of this research.

TABLE OF CONTENTS

LIST OF TABLES

LIST OF FIGURES

CHAPTER I

INTRODUCTION

1.1 Background

Open grid decks are structural systems employed in a number of applications to successfully transfer loads. Worthy of mention is in the area of bridge engineering where they find their use in the construction of new bridges and in rehabilitation projects to increase the live load capacity of existing bridges. A common form of open grid decks occur as metal bar gratings which is an assembly of metal bars which are welded, riveted or pressure-locked where the principal load bearing bars run parallel in one direction, and are spaced equally from each other either by rigid attachment to cross bars running in a perpendicular direction, or by attachment to reticuline (connecting) bars extending between them. (National Association of Architectural Metal Manufacturers, 2009)

Grid decks were employed in several bridges built in the 1920's and 30's and may also be found on a number of bridges constructed in the 1950's and 60's. Their use had been dwindling, until reintroduction in the 1980's. They possess enough structural capacity to support applied loads and are mostly designed using empirical methods due to limited research into their behavior under both static and fatigue loads. A problem observed with the reintroduction of these grating systems, the majority of which are welded, has been the development of fatigue cracks. Contrary to the current trend, open

grid riveted steel decks have performed satisfactorily during service and some examples are presented which include riveted steel decks that are almost in new condition after 15 years in service and others that are still in good condition after nearly 60 years of service without evidence of significant damage or deterioration. Current bridge renovations have seen the re-emergence of the use of metal gratings with some limitations.

1.2 Problem Statement

Information on the design of open grid decks is limited and provisions in the AASHTO LRFD specifications apply mainly to welded decks. A major concern with the use of welded decks is with the development of fatigue cracks. The AASHTO LRFD specifications classify the fatigue detail of an open grid welded deck as a category E (Article 9.8.2.2). This is true for welded decks but bridge inspections and results from some experiments (Gangaroo, 1987), (Fetzer, 2013) has highlighted the enhanced performance of heavy duty riveted steel gratings under fatigue loading. The current design method provided by NAAMM uses allowable stress design principles which necessarily lead to design inconsistencies if used in conjunction with current AASHTO LRFD Bridge Specifications. Heavy duty riveted gratings will serve as a better alternative if their behavior under both static and fatigue loading is established.

1.3 Justification

Bridge owners are hesitant to approve of heavy duty riveted gratings as a deck system due to limited information on the design and detailing of these decks. The focus of this

research is to better understand the behavior with respect to static and fatigue loading of the heavy duty riveted steel decks in order to improve on existing design procedures. This will include the establishment of an effective width and a proposed guide for the design of heavy duty riveted steel gratings. Estimation of the fatigue life of the gratings will be addressed by results from the research program and will lead to a better characterization of the fatigue detail category.

1.4 History of Heavy Duty Riveted Gratings

The Heavy duty riveted steel deck was among the first types of gratings developed in the early 1900's. There are many examples of riveted decks that have been in service for decades with no evidence of fatigue cracks. A number of examples exist for the usage of both riveted and welded type decks on some bridges in the United States with the average annual daily traffic unknown. The Veterans memorial bridge in Bay City, Michigan carries the four lane MI highway 25 over the Saginaw River. This Bascule Bridge was originally constructed in 1957. In 1994, the deck was replaced with a heavy duty riveted grating during a major renovation. Figure 1.1 shows a photo of the bridge taken in February 2009 with the deck still in good condition after about 15 years of use.

The historic LaSalle Street Bridge in Figure 1.2 is in the heart of Chicago and was built in 1928. During renovation in 1971, a new riveted steel bridge deck was installed. This bridge is exposed to average daily traffic of about 27,000 vehicles per day. An

examination in June 2008, demonstrated that the riveted grating is still providing good service after over 37 years of heavy use.

Figure 1.1 - Veterans Memorial Bridge, Bay City with Heavy duty riveted gratings

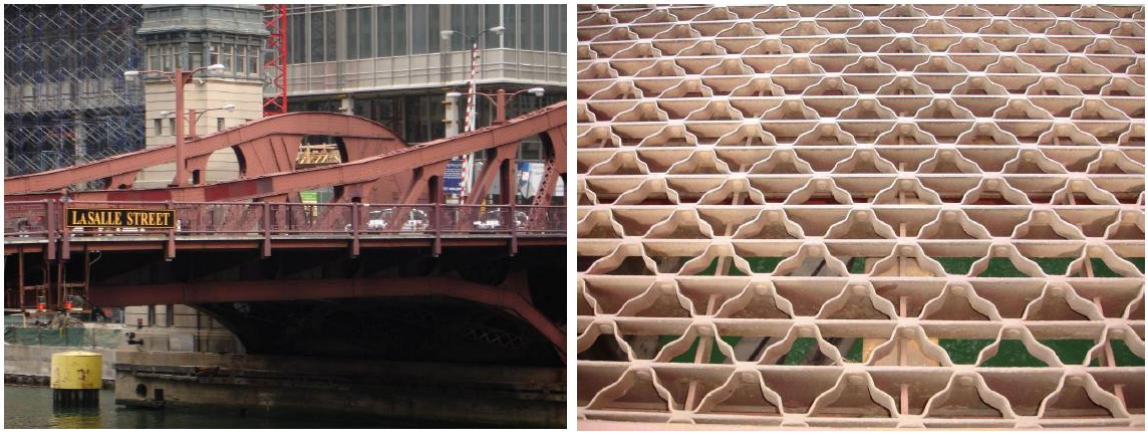

Figure 1.2 - The LaSalle Street Bridge in Chicago installed with riveted deck in 1971

The bridge shown in figure 1.3 is located on the Island of Grosse Ille, Michigan. It has a 1,400 ft span over the Trenton branch of the Detroit River. Most of the span is fixed, with a 340 ft swing portion near the east end. The bridge was built in 1930 with a

concrete deck surface. In 1980, a welded steel deck was installed in order to lessen the dead load to accommodate heavier trucks. By 2006, when the photos below were taken, many cracks had developed in the bars of the bridge deck. Some sections had missing bars with patch plates installed for maintenance. In addition, the bridge deck was noisy as vehicles crossed. In 2007, the deck was replaced with a heavy duty riveted steel bridge deck as shown in Figure 1.4

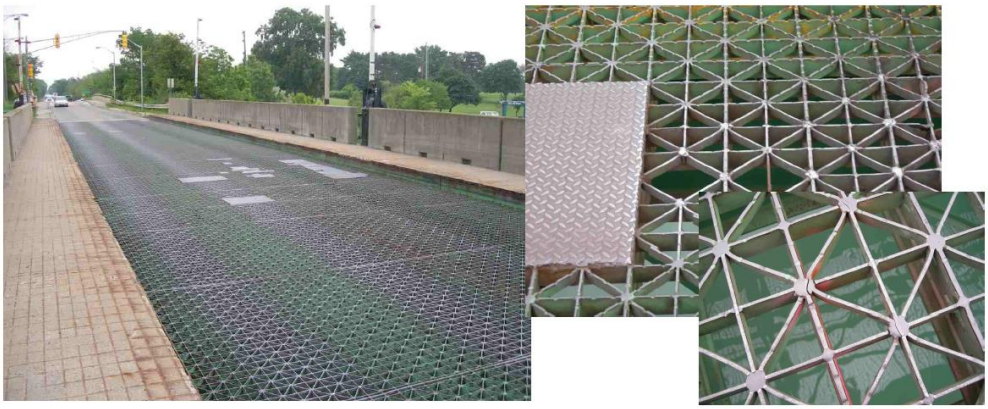

Figure 1.3 - Grosse Ile Bridge, welded deck with patches in 2006

Figure 1.4 - Grosse Ile Bridge, Heavy Duty Riveted Grating installed in 2007

1.5 Objectives

Earlier attempts at the study of open grid decks involve work by Gangarao (1987) who tested 26 open grid decks with most of the panels having welded connections. His work concluded that allowable fatigue stresses for commercially available welded grid decks were close to Category E in the AASHTO specification and that riveted decks performed better than the most common welded decks. Fetzer (2013) highlighted the improved performance of riveted grating decks subjected to fatigue loads than most of the welded gratings tested but attributed the better performance to the relatively short spans that limited the stress range. The current research is part of a comprehensive program underway at the University of Akron with the following objectives:

- Investigating the stress distribution on sub components of the grating as a result of the application of static loads. This will also lead to the establishment of an effective width to be considered for design
- Exploring various analytical methods and procedures towards the design and estimation of stresses on the heavy duty riveted gratings.
- Development of a proposed S-N curve for heavy duty riveted steel gratings based on experimental testing of full size panels under H20 loading and smaller panel specimens with varying stress ranges.
- Finite element analysis and parametric studies on the panels using ABAQUS CAE calibrated to laboratory data to investigate the effect of main bar spacing, bearing bar cross – section and contribution of intermediate and connecting bars.

- Fatigue detail category for the estimation of the fatigue life of heavy duty riveted steel decks and the development of fatigue life prediction equations
- A fracture mechanics approach towards estimating the fatigue life of heavy duty riveted steel gratings
- Modifications and improvements to current methods of design with a proposed guide towards the design of heavy duty riveted gratings using LRFD principles

1.6 Outline of Dissertation

In studying the fatigue behavior of heavy duty riveted gratings, a number of tasks were completed and are presented. Chapter 1 introduces the usefulness of open grid decks particularly heavy duty riveted gratings and their application in structural projects and also spells out the research problem and objectives. Chapter 2 explains the standard marking system employed by the NAAMM for the identification of heavy duty riveted gratings together with the advantages and disadvantages associated with the use of the gratings. A review of previous work done on fatigue life prediction of open grid deck systems is also presented.

Chapter 3 explores the properties and nature of stress distribution on the heavy duty riveted gratings through static testing and finite element analysis using a 3D model of the grating. Results are compared with experimental testing and a parametric study conducted. This provided input towards the design of an experiment for fatigue testing. Chapter 4 presents information on fatigue testing of the heavy duty riveted gratings and involved testing of six large panels of the 37R5 Lite and 37R5 L-series. Twenty six

smaller samples of the 37R5 Lite and L-series were also tested. The results from the fatigue testing and its analysis are presented in Chapter 5 together with the development of an S-N curve for the design of the heavy duty riveted gratings. Linear elastic fracture mechanics (LEFM) principles are employed considering two failure mechanisms in bearing bars based on experimental results. The critical details are used in Chapter 6 to study the fatigue behavior of the gratings. Results from both experimental and analytical methods are used to develop a guide towards the design of heavy duty riveted gratings considering the limit states of strength, serviceability and fatigue in Chapter 7. A summary of the results from the research together with recommendations for future work are presented in the last chapter.

CHAPTER II

LITERATURE REVIEW

2.1 Introduction

Grid decks have primarily been used in bridges either as open, filled or partially filled. They have performed creditably under service loads on a variety of projects. Heavy duty riveted steel grating is among the oldest, and is still in use due to its reliability, durability and strength. As with many open grid decks, heavy duty riveted steel gratings are made up of an assemblage of main bars with or without intermediate bars, with reticuline bars riveted at equal intersections along the main bars (NAAMM, 2009). The main bars usually occur as flat bars or structural shapes with varying cross sections based on the strength and fatigue requirements. Metal gratings occur in various forms with intersections of sub-components welded, pressure locked or riveted.

2.2 Metal Bar Gratings as a Flooring System

Metal gratings are capable of supporting both pedestrian and vehicular loads. The Heavy Duty Grating manual of the National Association of Architectural Metal Manufacturers (NAAMM) sets guidelines for their design. The usefulness of heavy duty gratings in bridge deck construction as compared to other decking types is as follows:

- Riveted gratings are light weight and of high strength in supporting applied vehicular loads
- Simple installation procedures compared with other decking types providing less disruption to traffic on rehabilitation projects making their use economical
- Maximum quality control during fabrication under factory conditions.
- Open Grid decks are advantageous in terms of aerodynamic stability and cost reduction in long-span bridge construction when used in conjunction with box girders on cable-stayed bridges
- They are also useful in bridges constructed in snowy areas since it reduces the amount of snow to be removed from the deck

Current problems associated with the use of these decks include the high level of noise generated with time due to the development of cracks. There is also an inherent problem of components cracking over time as a result of fatigue and thus routine maintenance is required to keep them in service. Plates used for patching, results in aesthetically unpleasing decks. Welded decks have in recent years been preferred, being used extensively on a number of bridge rehabilitation projects due to improved welding methods and the ease of fabrication. Issues associated with welded decks include the presence of high residual stresses and common welding flaws which provide sites for crack development resulting in early development of fatigue cracks as compared to a riveted deck used under similar conditions (Gangaroo, 1987).

2.3 Standard Marking of Heavy Duty Riveted Gratings

Heavy duty riveted steel gratings can be characterized by the name or mark they bear as a result of the standards developed by NAAMM. Gratings involved in this study include R37-5 (5”x ¼”) steel and modified forms provided by the Ohio Gratings Inc. Each parameter in the five part name of the heavy duty riveted steel grating gives information about its geometrical properties.

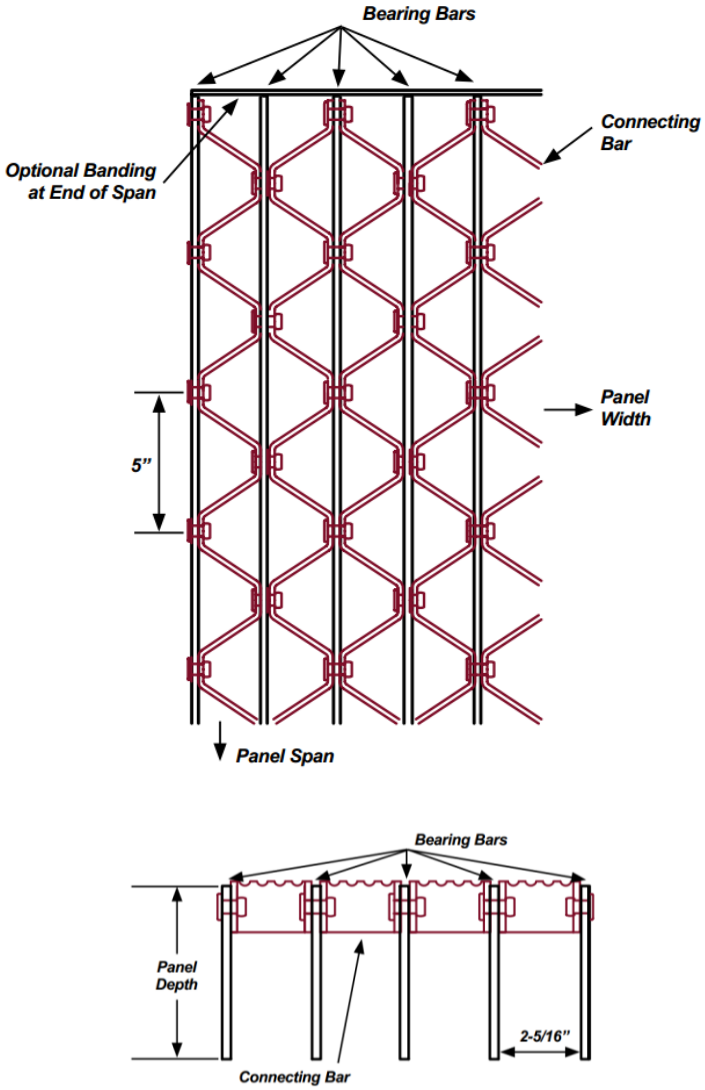

Figure 2.1 - Standard marking of Heavy Duty Riveted Gratings (Ohio Gratings Inc.)

The first parameter, R, describes the type of grating which in this case is riveted. The second (37) represents the spacing between bearing bars and it is the distance measured between the faces of the bearing bars in riveted panels. It provides the spacing in terms of 1/16th of an inch. The third parameter (5) describes the spacing of the rivets with connecting (reticuline) bars in inches. The fourth (5 x ¼) indicates the dimensions of the cross-section of the bearing bars. The size of the bearing bar is specified in inches of depth and thickness. The fifth parameter (Steel) is the type of material used for the grating. Table 2.1 provides a summary of the standard marking of riveting gratings.

Table 2.1- Standard Marking of Heavy Duty Riveted Steel Gratings

Parameter	Standard Marking	Description
1	R	Riveted
2	37	Bearing bars spaced 2 -5/16 between faces
3	5	Rivets spaced 5in on centers
4	5 x ¼	Bearing Bar size
5	STEEL	Material

2.4 Background

Rivets were the preferred mode of connection and were in use for decades until the advent of high strength bolts. They provide enough structural capacity in connections by safely transmitting applied loads. Rivets still find common use in the aerospace and rail industries. The focus of this research is towards the better understanding of the

behavior of the heavy duty riveted gratings under static and fatigue loads using the standard H-20 truck for bridge applications. There has been a decrease in the use of rivets due to the presence of high strength bolts, but the configuration of open grid decks and the fabrication methods employed make the use of rivets attractive. The current design method used for heavy duty riveted gratings are those provided by the NAAMM Manual which uses an elastic analysis approach following allowable stress design concepts. When highly stressed sections of a continuous structure yield, they merely transfer additional moments to less stressed areas through redistribution in order to carry the load more efficiently. Stresses other than calculated service stresses can be used as long as there is no danger of low cycle fatigue or brittle failure.

Other analysis methods have been employed in the design and analysis of open grid decks in order to fully take advantage of the extra strength occurring after yield. A plastic method of analysis uses the collapse behavior of the structure as a basis to proportion members. Such collapse is accompanied by large deformations with structure behavior departing from elastic theory. The yield line analysis method with the principle of virtual work has been shown to adequately predict the strength of open grid deck systems (Cannon 1969).

Cannon (1969) tested two grid deck systems and used yield line theory to determine the collapse load of the grids consisting of single sized flexural members. Moment design equations were generated both for a square grid system and a rectangular system which depend on the spacing of the grid and the member plastic moment capacity. It was determined that grids had less reserve strength than slabs since slabs invariably

exhibited greater strength than that predicted by yield line theory. The report indicated that the theoretical yield line collapse load provides a good, upper bound, measure of the true collapse load of grids.

Vukov (1986) presented an upper bound approach to the analysis of orthogonal grid systems applying the kinematic or mechanism method. The corresponding virtual work equations were formally written and used to determine the ultimate capacity of a grid system. Work equations were developed for different beam layouts with grid decks. Results from the work was compared to lab results from Cannon (1969) and showed good correlation.

Approximate methods can be used in the analysis of decks according to Article 4.6.2.1.1 of the AASHTO LRFD specifications. The deck is subdivided into strips perpendicular to the supporting components. When this method is used, the extreme positive moment in any deck panel between girders shall be taken to apply to all positive moment regions, similarly, negative moments over beams or girders shall be taken to apply to all negative moment regions.

Baker (1991) conducted experiments and tested four concrete filled grid decks to investigate the twisting and bending stiffness of an orthotropic plate. A line load was involved in measuring the bending stiffness in the three orthogonal directions. The twisting stiffness was measured by supporting the three sides of the plate and loading the unsupported end at a corner where load and deflection were recorded. The inputs were used for finite element analysis and the model produced deflections comparable to the

experiments (within 15%) for concrete filled grid decks subjected to line and concentrated loads.

Huang (2001) sought to better understand the behavior of grid decks by using analytical, experimental and numerical methods. Four open and three filled grid decks were tested to quantify their structural behavior experimentally. Grid decks involved in the study were welded decks. The analytical procedures included the use of the classical orthotropic thin plate theory and the theory of beams on elastic foundation. Three dimensional finite element models were developed for both the open and filled grid decks and calibrated to laboratory data. Results from the finite element analyses were compared with classical orthotropic plate theory. Parametric studies were conducted on major components that affect deck behavior. Concrete filled decks were stiffer than their open grid counterparts by about 33%. Results from the FEM models also showed general agreement with experimental results and thus FEM can be used as a tool to analyze and design open grid decks and that classical orthotropic theory gives reasonable results for filled grid decks but not open grid decks.

Mahama (2003) examined the current metal bar grating design provisions using analytical, numerical and an experimental approach. Major emphasis was placed on developing finite element models of welded gratings using ANSYS, incorporating both material and geometrical nonlinearities to predict the collapse load of the grates. Data from both analytical and finite element analyses were compared with results from physical tests, which provided an insight into the limit behavior of metal gratings.

Bejgum (2006) did an assessment of the current design methods of metal bar gratings and tested four heavy duty riveted and two welded metal gratings under static loads. The gratings were simply supported and a tire patch of 20in x 20in was used to simulate applied loads. Strain and deflection data was acquired as loads were applied until LVDTs went offscale. At 50kips, deflections of about 0.30in were recorded in both riveted and welded gratings. A nonlinear finite element analysis based on models created for design loads was developed and calibrated with laboratory data. Collapse loads of the gratings were found to have corresponded well with analytical predictions (within 20%) and the finite element model.

2.5 Fatigue Behavior of Riveted Decks

With the use of grid decks occurring either as open or filled in a number of bridge applications, attempts have been made to better understand their behavior, thereby improving and optimizing design methods and rules. A number of open grid decks in service have developed fatigue cracks with the situation more predominant in welded decks. The inherent problem with the development of these cracks and the subsequent failure due to fatigue can be avoided based on a better understanding of the fatigue behavior and resistance of these gratings. Grid decks were used on older bridges and at a time when the current AASHTO fatigue design requirements had not been established. Based on current code requirements and consideration of the fatigue limit states, the detail category of the critical detail of the heavy duty riveted grating has to be established in order to estimate their fatigue life from S-N curves.

2.5.1 Detail Category of Riveted Connections

The fatigue life of a structural detail is usually governed by the applied stress range at the critical detail, the number of cycles of loading to failure and the detail category. Major detail classification exists for riveted connections in different codes and standards but they cannot be directly applied to grid decks due to differences in their behavior. The American Association of State Highway and Transportation Officials Specification (AASHTO) designate riveted shear splices as Category D. At 2 million cycles, the permissible stress range of 10ksi for redundant load path structures and 8ksi for non-redundant structures is to be used. The American Institute of Steel Construction (AISC) manual categorizes a riveted shear splice connection as a Category D detail and a member with drilled or reamed hole containing bolts for attachment of light bracing as a Category C. The American Railway Engineering and Maintenance of Way Association (AREMA) also categorize the same as a Category D.

In estimating the fatigue life of a riveted connection, crack initiation is assumed to have occurred and thus the fatigue life is considered as the number of cycles to propagate the crack to a dominant size. This assumption is common in current specifications and U.S design practice. The behavior of grid systems under loading has been studied in the past with much emphasize placed on welded connections. Different design methods have been proposed as a result of the studies. One structural detail of interest in a riveted grating system includes bearing bars with drilled or punched holes containing rivets that hold the parts together. The fatigue properties of steel have been extensively studied and are not the focus of this research. The behavior of the various geometries of steel

members connected at their intersections with rivets is assessed in the determination of the appropriate design category for heavy duty riveted gratings. The AASHTO Guide proposes a fatigue design category for sections connected with rivets and can be used in estimating the number of cycles permitted by a particular stress range.

2.5.2 Experimental Research on Fatigue Behavior of Grid Decks

Gangaroo et al (1987) studied the fatigue behavior of open grid steel decks with emphasis on welded decks. It was established through his study that the load distribution procedure in use at the time for the design of grid decks was in error. Gangaroo developed more "realistic" load distribution procedures to prevent cracking of grid deck bars and plug welds. The work dealt with the effects of main bar spacing, direction with respect to traffic flow, load position, composite action and fatigue. They also investigated the effect of residual stresses in grid decks during fabrication, braking and accelerating forces, galvanization and composite action between the deck and stringers. Twenty six grid decks were tested under static and fatigue loading. Allowable fatigue stresses for commercially available welded grid decks were found to be very close to a Category E. However, under fatigue loading, riveted decks performed better than the most common welded decks.

Mangelsdorf (1996) in his final report on the static and fatigue strength determination of grid decks tested five full size panels of welded and filled decks under fatigue loads. There was cyclical loading on the test panels and tests were terminated when at least two components of each deck had cracked. Fourteen smaller size samples

were also tested with only two main bars under a cyclic load of constant amplitude strain until either the specimen survived 10 million of cycles of loading or at least one of the bars cracked. Based on his findings, he categorized the filled grid panels as a category C according to the AASHTO LRFD Specifications.

Murakoshi et al (1998) tested full size panels of welded gratings under running wheel loads to investigate the fatigue behavior. Three different welded decks with both main bars and cross bars were investigated. The surface members (main bar and cross bars) were connected to supporting stringers using high strength bolts. Running loads of 100KN were applied initially, followed by an increase of 20KN for every 40,000 cycles applied. Static response of the deck under loading was measured every 20,000 cycles. Major cracks developed along the welds after about 250,000 cycles to 300,000 cycles of loading.

Fetzer (2013) performed different tests on eight types of open grid decks which involved both welded and riveted decks. Full scale tests involved configurations of both simple and continuous spans subjected to patch loads. The tests established the flexural and torsional stiffness parameters of the decks for use in a finite element model. The model was used to develop LFRD compatible design moment equations for strength and fatigue. Subcomponent fatigue test were conducted with isolations on weak-direction fatigue behavior for welded decks. Design moment equations were developed for strength as well as to predict for fatigue life of the welded decks.

2.6 Fatigue Limit States

A limit state defines the condition of a structural member or an entire structure beyond which it fails to perform the function expected of it. The limit state to be evaluated as part of this study is the fatigue limit state. The fatigue limit state represents the occurrence of fatigue damage in a structure due to the complex nature of stresses and damage accumulation under the action of repeated loading.

2.6.1 Loading

The nature of the loading to be used in a fatigue analysis shall be one design truck or axle with constant spacing of 30ft between 32 kip axles. An impact factor on the order of 15% is applied for the fatigue and fracture limit states. The frequency of the fatigue load shall be taken as the single lane average daily truck traffic ($ADTT_{sl}$), which shall be applied to all components of the bridge. The $ADTT_{sl}$ is given by equation (2-1)

$$ADTT_{sl} = p \times ADTT \tag{2-1}$$

p = fraction of truck traffic in a single lane

ADTT = the number of trucks per day in one direction averaged over the design life.

$ADTT_{sl}$ = the number of trucks per day in a single lane averaged over the design life.

The value of p depends on the number of lanes available for trucks, with a maximum of 1.0 for 1 lane to 0.80 for 2 or more lanes.

2.6.2 Steel Structures

In steel structures, fatigue is categorized as load induced or distortion induced. Force effects considered shall be the live load stress range. For load induced fatigue, each detail shall satisfy equation (2-2)

$$\gamma(\Delta f) \leq (\Delta F)_n \tag{2-2}$$

$\gamma =$ Load factor for fatigue load combination

Δf = force effect, live load stress range due to the passage of the fatigue load

$(\Delta F)_n =$ Nominal fatigue resistance

As applied to heavy duty riveted gratings made of steel, all the above requirements of the AASHTO LRFD Specifications apply. Based on classification, mechanically fastened connections with base metal at the net section of riveted joints are designated category D details. This provision does not necessarily apply for heavy duty riveted grating using rivets for connections in a grid. Fatigue Resistance is given by equation (2-3)

$$(\Delta F)_n = \left(\frac{A}{N}\right)^{1/3} \geq \frac{1}{2}(\Delta F_{TH}) \tag{2-3}$$

$$N = (365)\ (75)\ n\ (ADTT)_{sl}$$

A = constant depending on detail category

n= design life of 75 years

N= number of stress range cycles per truck passage.

$\Delta F_{TH} =$ Constant amplitude fatigue threshold

CHAPTER III

BEHAVIOR AND FINITE ELEMENT ANALYSIS OF RIVETED GRATINGS

3.1 Overview

The static behavior of the gratings was evaluated experimentally to develop improved procedures and provide input towards the design of an experiment for fatigue testing of the panels. The contribution of the various sub components of the riveted gratings were investigated with continuous spans as would occur in a typical bridge structure. The laboratory test set up was based on provisions in the AASHTO LRFD bridge design specifications with a few modifications. Test Panels were modified forms of the 37R5 standard heavy duty riveted gratings and included the 37R5 Lite and L-series. Results obtained from static testing were used to develop samples for fatigue testing of the gratings.

3.2 Experimental Set Up

The research program involved the study of the behavior of heavy duty riveted steel gratings under AASHTO H-20 loading as a basis for the fatigue testing of the heavy duty riveted gratings. Three different research programs involved static testing of riveted gratings at the University of Akron and are described as follows:

(1) Static testing of heavy duty riveted and welded gratings with simply supported spans. Test set-up reflected recommendations of the Standard Specifications for Highway Bridges, 17th Edition. (AASHTO, 2002). Strain and deflection data recorded. (Begjum ,2006)

(2) Static testing of heavy duty riveted grating with continuous spans of 42in described herein as Test Panel A – 37R5 Lite (White, 2009).

(3) Current program which involves static testing of continuous spans of 65in of the heavy duty riveted gratings, 37R5 Lite panel described as Test Panel B

The 37R5 lite panel is a modification of the standard heavy duty riveted grating for applications requiring a much lighter product. According to the manufacturers, weight savings can add up to about 30% when compared to the standard heavy duty riveted steel gratings.

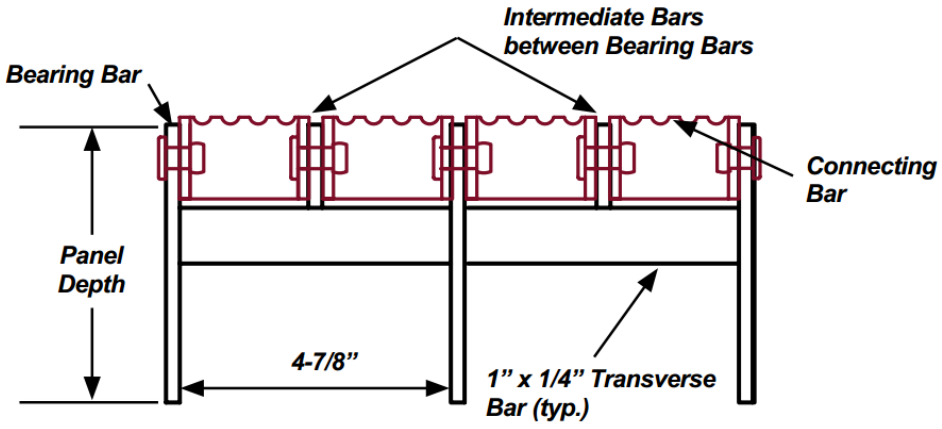

Figure 3.1 – Section through 37R5 Lite Panel

3.2.1 Test Panel A -37R5 Lite

Initial tests involved static loading of the 37R5Lite panel measuring 146.25 in x 41.25 in. The bearing bars are made of A36 steel and measures 5in x 0.25 in. Intermediate bars which occur between main bars are 1.5in x 0.25in. The connecting (reticuline) bars are made of A1011 steel and have serrations with the top surface 1/8" higher than the top of bearing bars. Support spacing was 42 in center to center of stringers. A spreader beam was utilized and loads were placed between the supports to simulate the condition of two trucks placed side by side so located as to provide the maximum negative bending response. Twenty inch long sections of steel "I" beam with reinforcement plates and a 10 in wide flange were used to provide the AASHTO tire patch for H20 loading. An impact factor of 30% was applied instead of the 15% in the LRFD bridge specification. High durometer rubber pads were placed between the 20in x 10in plate and the grating.

A total of eight tests were performed on the panel and the contribution of the various components of the grating was investigated and is presented in Table 3.1. Strain gages were attached on bearing bars over the central supports and connected to a Vishay system 5000 data acquisition system. Strain gages were placed 0.25in from both the top and bottom of the bearing bars over the central supports. An MTS actuator with a capacity of 55kips was used to apply the static load. Loads were gradually applied from 0 to 42.6kips at increments of 5kips. The panel was then unloaded and additional strain gages placed at other sub components of the grating of interest and the test repeated. Sub components involved in the study included the reticuline (connecting) bars and the intermediate bars.

Table 3.1 – Description of eight static test on heavy duty riveted Gratings (White ,2009)

Test No:	Description
1	Supports to deck were placed over the center main bearing bar (5") at 21" from center of supports to ground, on both sides from center. Original I-Beam supports were used with 5/8" rubber pads. Loading Foot-print equals 10" x 20" (20" side loaded parallel to longitudinal bearing bars.
2	Same as set-up in Test 1
3	Same as in Test Set-up 1, with additional strain gages added at one rectilinear bar and one intermediate bar on either side of the middle main bearing bar. Gages placed at top only.
4	Test Set-up 1 with the following additions. Strain gages were placed at the bottoms of the Intermediate bars to determine the proportion of the bars that were below and above the neutral axis. Additional Strain gages added at one rectilinear bar and one intermediate bar on either side of the middle main bearing bar. 4 gages total.
5	Test Set-up 1 with the following changes. Original I-Beam supports were replaced by Alternate Triangular supports used with original spreader beam with 5/8" rubber pads. Smaller Jack replaces larger Jack because of height change from supports. Supports to deck were placed over the center main bearing bar (5") at 21" from center of supports to ground (on both sides from center.
6	Test Set-up 5 with the following additions. Re-centered Jack and shimmed Triangular supports. Triangular supports have "cradle" like bottom.
7	Supports changed back to I-Beam Supports and placed so web is in line with Intermediate Bar 1. Large jack is replaced with small jack. Beam Supports still centered 21" from both sides of the center support in the longitudinal direction of the deck.All other conditions same as before
8	Triangular Support bottom surface ground down. Replace I-Beam with newly modified Triangular Supports.Replace large jack with small jack. Beam Supports still centered 21" from both sides of the center support in the longitudinal direction of the deck.All other conditions same as before.

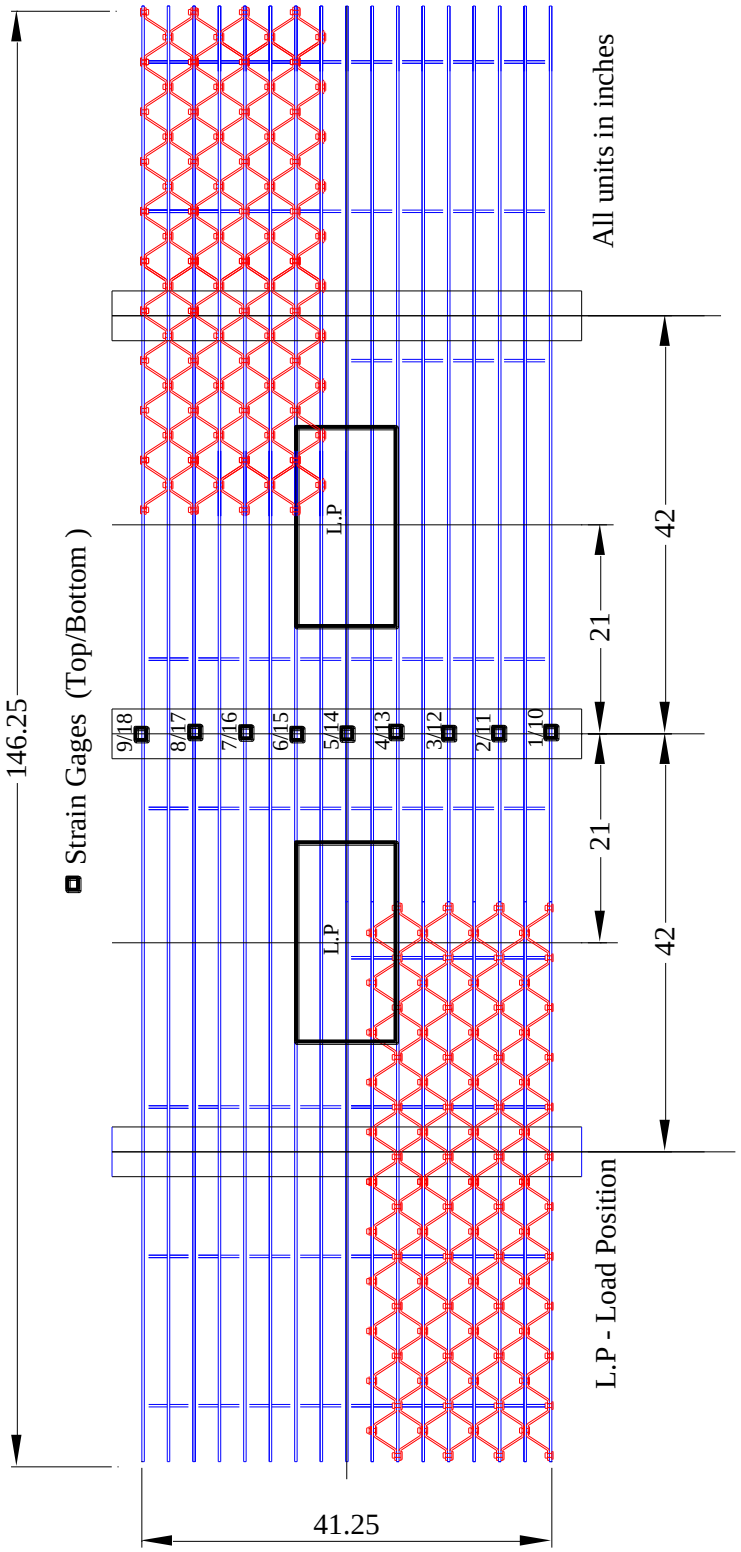

Figure 3.2- General Arrangement of Gratings with Strain gage positions for Test A

The heavy duty riveted grating was supported on pylons specially made for the purpose of testing. No permanent stringers were attached.

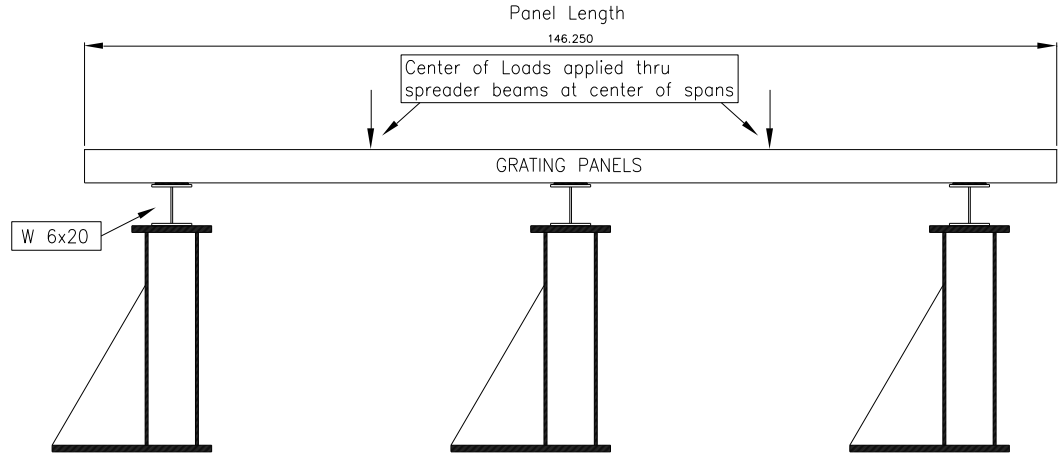

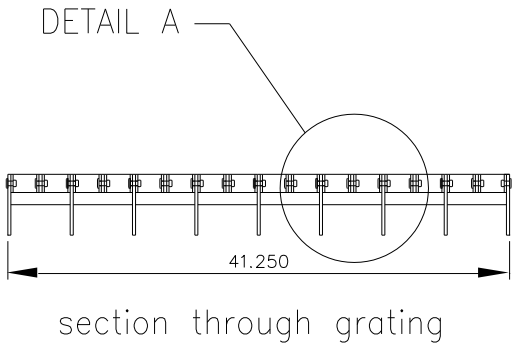

Detail A

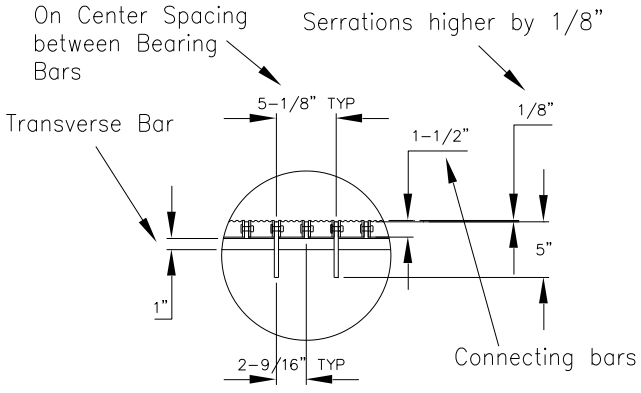

Figure 3.3- Layout for static testing of riveted gratings

3.2.2 Test Panel B -37R5 Lite

This involved the testing of a 37R5 lite panel fabricated and subsequently used for fatigue testing. A preliminary static test was performed to record both strain data for maximum values between supports as well as over the central supports. Deflections directly under the patch loading were also recorded. Panel dimensions were 126in x 36.2in with bearing bars made of A36 steel and 5in x ¼ in in cross- section. Intermediate bars which occur in between main bars measured 1-1/2" x ¼". The connecting (reticuline) bars are made of A1011 steel and have serrations 1/8" above the top of the bearing bars. Support spacing was 65 in center to center of stringers. The method used for attachment of the gratings to the stringers involved welding of attachment plates to both sides of the bearing bars. The attachment plates were then bolted to the stringers Menzemer (2010). Three W8 x 24 beams were used to simulate stringers. A spreader beam was utilized and loads were placed 3ft apart from the central support to simulate the condition of an AASHTO H-20 design truck so located as to provide the maximum negative bending response over the central supports.

Strain gages were attached 0.25in from the bottom of bearing bars directly beneath the load and also on all other bearing bars along the axis of loading to record tensile strains. Another set of gages were attached 0.25in from the top of bearing bars over the central support and on all bearing bars along that axis. Deflection measurements were taken with two LVDT's placed directly at the sides of the tire patch load. The strain gages and LVDTs were then connected to the Vishay System 5000 data acquisition

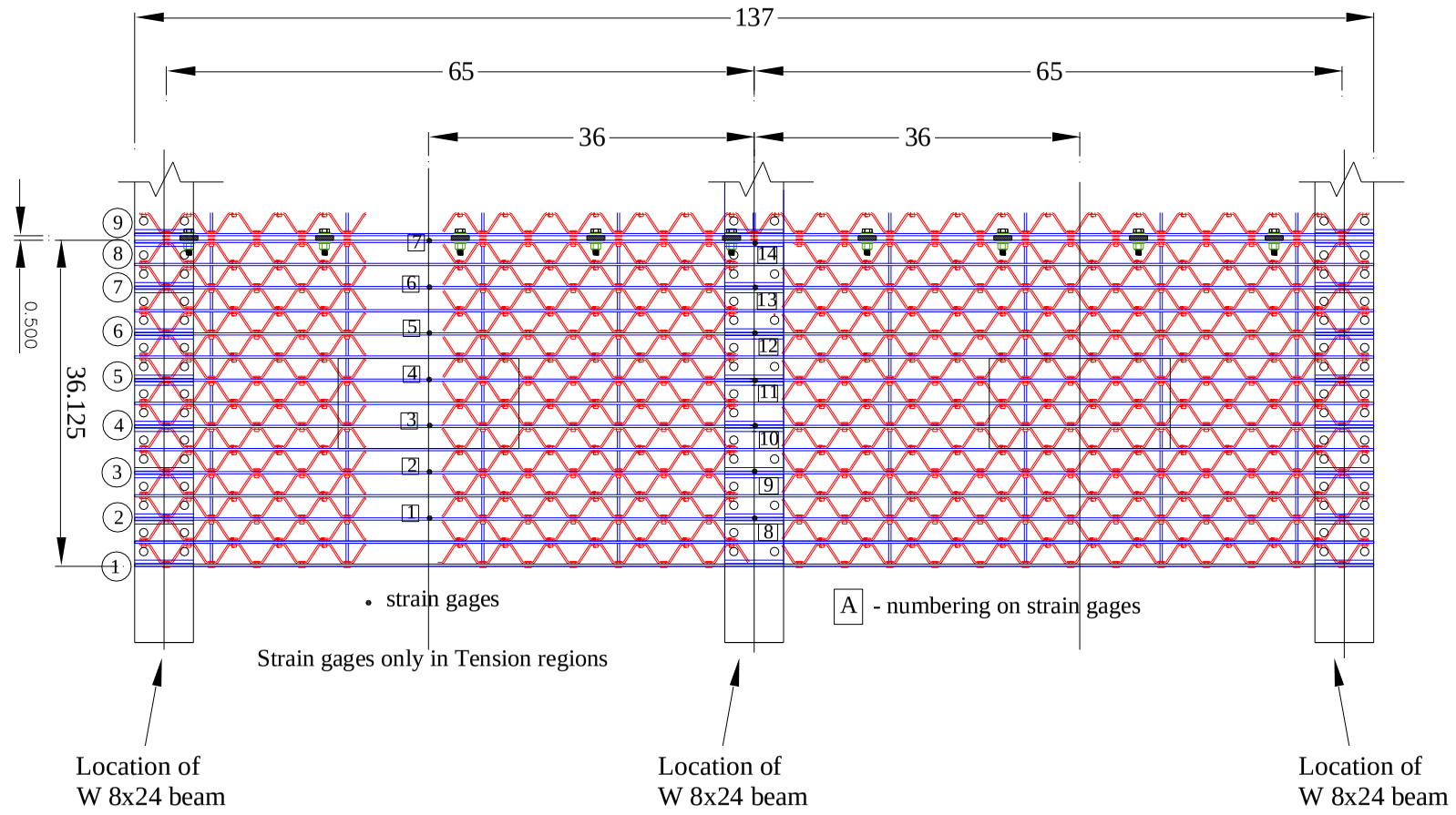

Figure 3.4 - General Arrangement of gratings with strain gage positions for test B

system. The MTS actuator was used to provide the loading from 1kip to a maximum of 42.6kips at major increments of 5kips till the maximum was reached. Figure 3.5 shows the test layout for panel B.

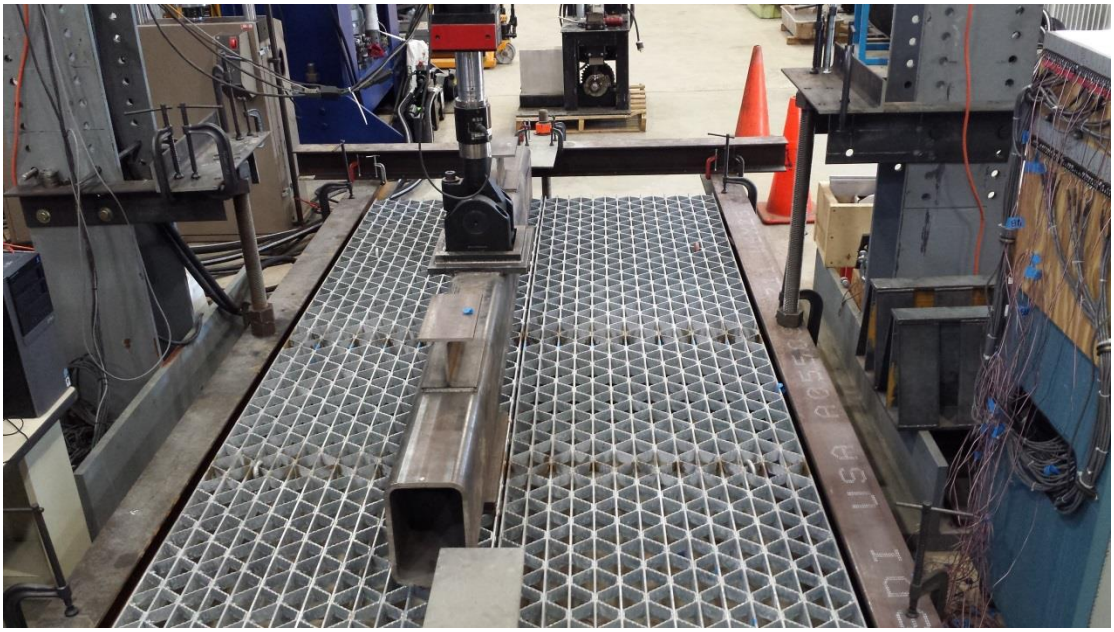

Figure 3.5- Layout for test panel B

3.3 Test Results and Discussion

The results from testing of panels A and B under static loading with varying conditions of loading, support conditions and span is presented. The variation of load with strain is presented for test panel A for the eight static tests performed. The effect of the varying conditions of loading, geometry and spacing of the main bearing bars on the behavior of the heavy duty riveted grating is reported with emphasis on the nature of stress distribution across the width of the grating.

3.3.1 Load – micro strain relationship

Both panels were loaded to a maximum of 42.6kips and then unloaded. Strain data was recorded by micro-measurements system 5000 Vishay data acquisition system at each load increment. Recorded data includes strains in both tension and compression at 0.25in from the top and bottom fibers of the bearing bars over the interior support. The load-micro strain relationship for the eight static tests performed is shown in Figure 3.5. There is a steady increase in micro strain with increasing load as expected. There is relative compression of the durometer pad under the simulated load to about 5kips of loading. This explains why a linear relationship is observed for the various tests after about 5kips of loading. There was a loss of stiffness in the grating as the test progressed.

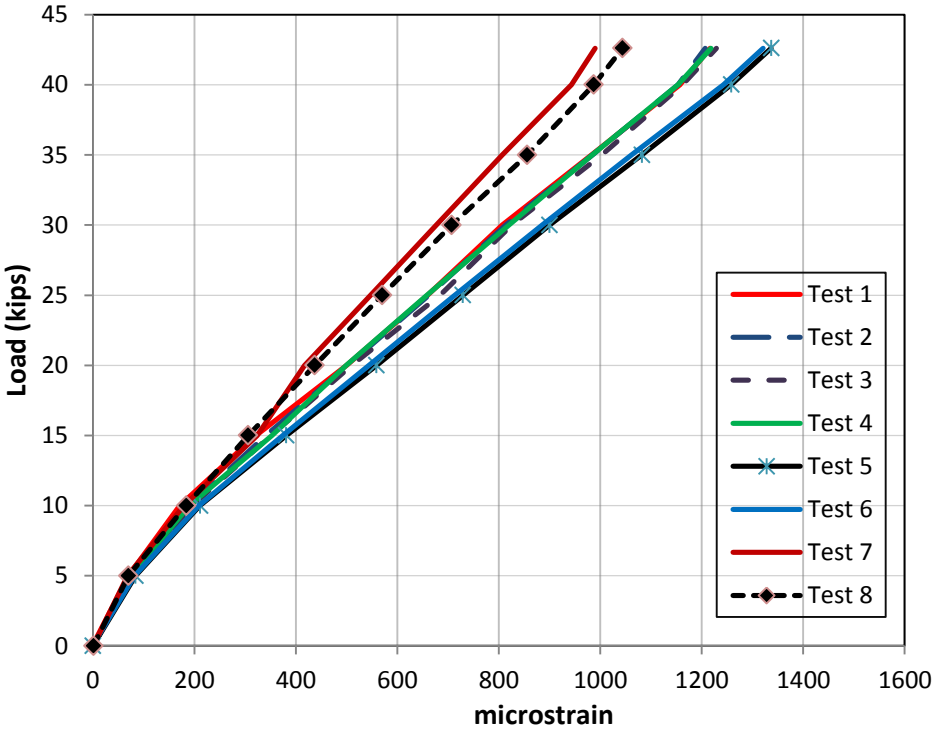

Figure 3.6 – Load- micro strain relation for static loading of panels in Static Test A

A major shift in the position of the load strain relationship for test 7 and 8 could be explained by the change in support conditions and the alignment of the support web so placed to be in line with intermediate bar 1, hence “distributing” the load evenly to the main bearing bars #22 and #23.

The pattern of strain distribution was studied both in tension and in compression. Strain gage data recorded for all strain gages placed 0.25in from the top and bottom of the main bearing bars gives an indication of the strain with respect to the position of the tire patch load applied. Figure 3.6 shows the longitudinal strain distribution on the gratings at 30kips which represents about 75% of applied AASHTO H-20 loading along the negative moment region of the continuous span for the 37R5 Lite. Based on the nature of the strain distribution, the resistance of the heavy duty riveted grating is supplied mainly by the bearing bars located directly under the load and the two bearing bars adjacent to those under the load on each side. Other components participate in carrying the load but to a lesser extent. The effective width of a heavy duty riveted grating that should be considered in analysis is taken as the tire contact width perpendicular to the direction of bearing bars in addition to twice the spacing of bearing bars for mid span loading.

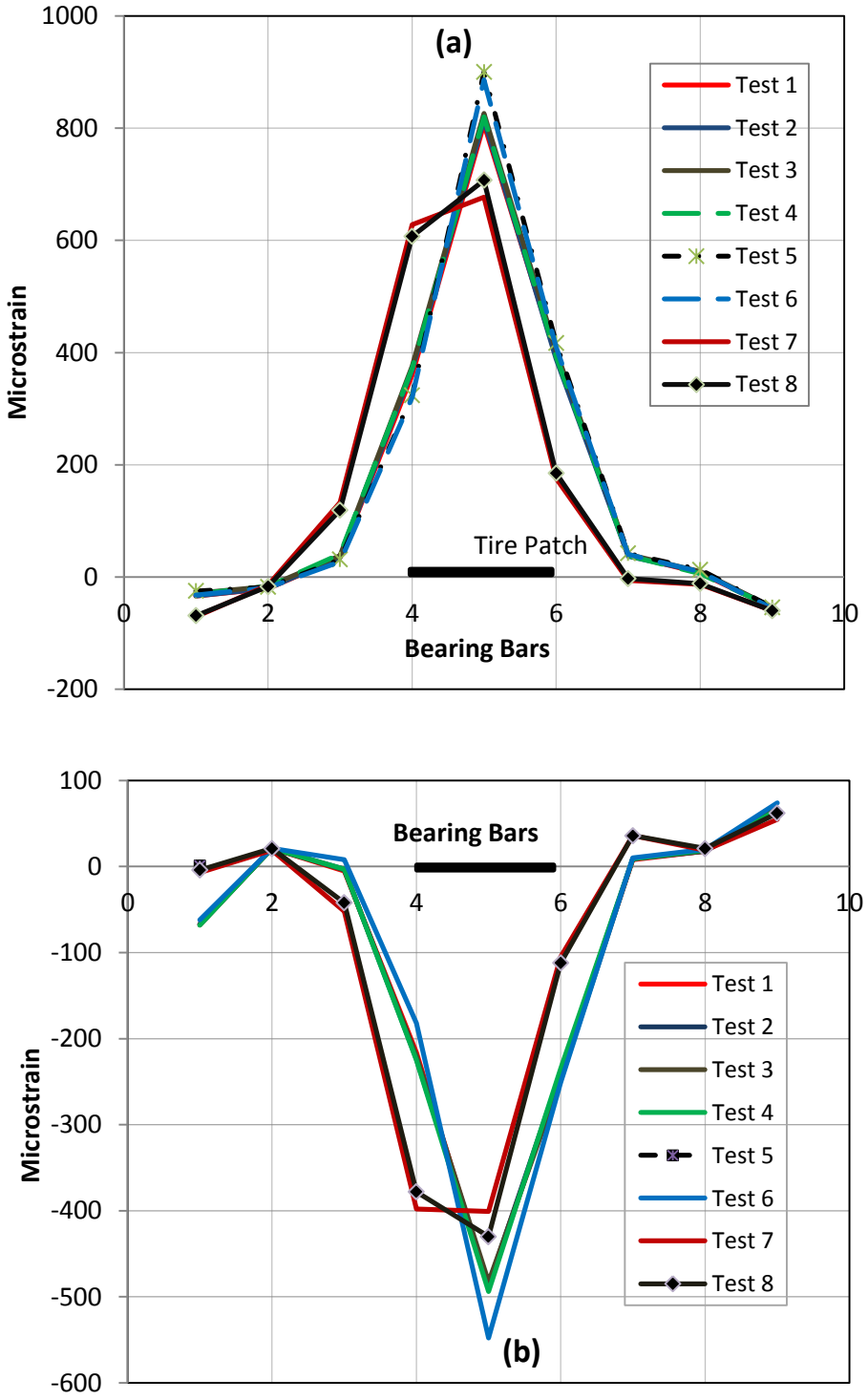

Figure 3.7 – Longitudinal strain distribution in (a) tension and (b) compression

3.3.2 Effect of Reticuline and Intermediate Bars

The various components of the heavy duty gratings provide both stability and structural capacity to carry applied loads. The main load carrying members are the bearing bars. The number of bearing bars per foot of a heavy duty grating may be reduced with the introduction of intermediate bars. This leads to different configurations based on the arrangement of the bearing and intermediate bars. The effect of loading on the intermediate bars and the presence of connecting bars on the load carrying capability of the gratings were explored. Strain gages were attached to intermediate bars and connecting bars over the supports. Five tests were run with loads from 0 to 42.6kips. Figure 3.8 shows the distribution of strain per foot of grating with three main bearing bars, two intermediate bars and two reticuline bars.

Reticuline bars had strains below 50 micro strain in all cases of loading and thus its contribution towards structural capacity may be ignored but must be present to provide some level of lateral stability to the grid. A thorough study of the behavior of the intermediate bars showed that two of such bars provided the same level of resistance as a main bearing bar. In heavy duty riveted gratings where intermediate bars are used to replace main bars, their contribution to structural capacity is significant and must be considered. A summary of the contribution of intermediate bars expressed as a percentage of total absorbed strain as compared to bearing bars within the vicinity of loading over the central supports is presented in Table 3.2. Bearing bars are the primary members providing load resistance for the heavy duty riveted gratings.

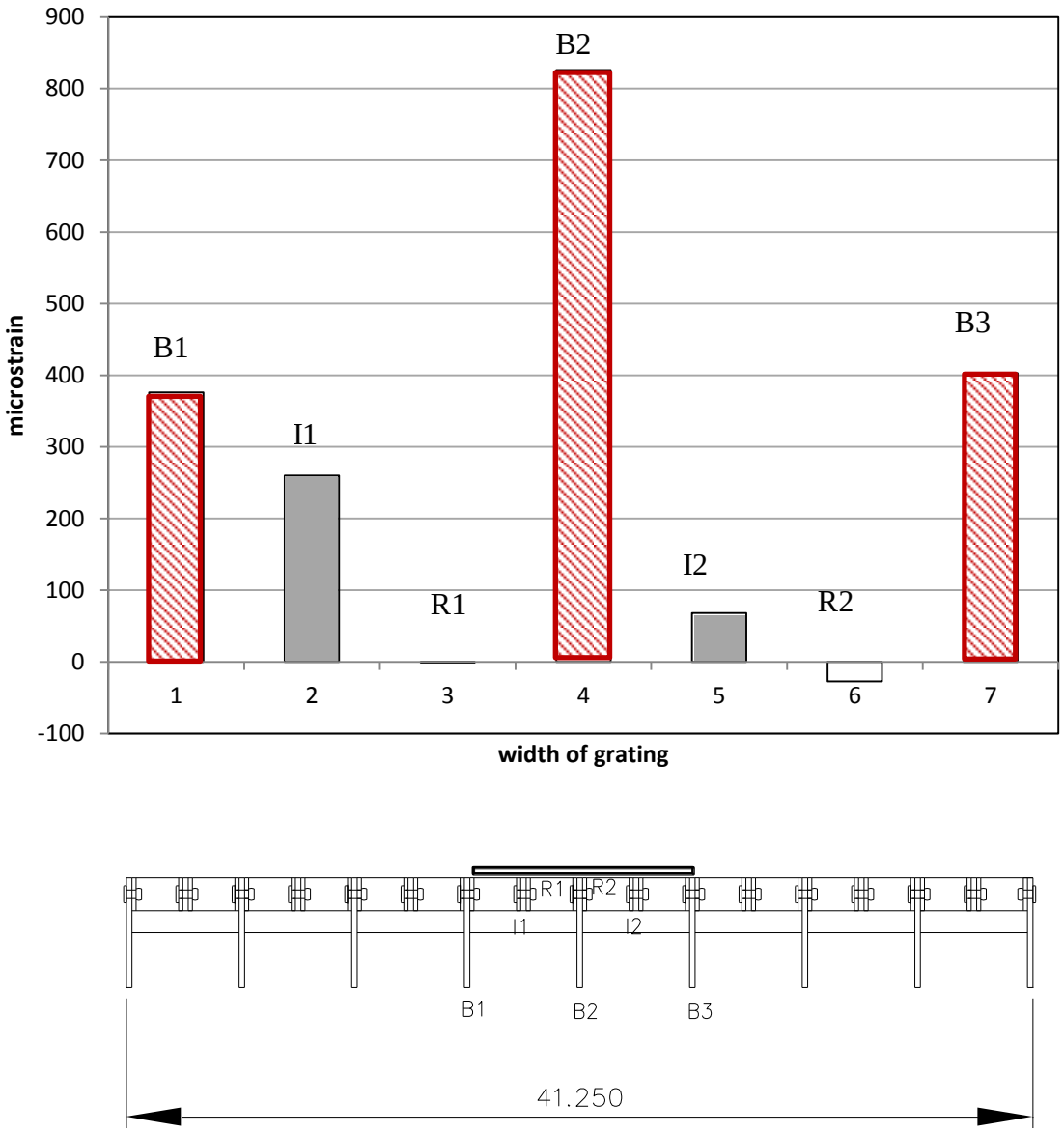

Figure 3.8 – Strain distribution per foot of grating showing contribution of components

Table 3.2- Contribution of intermediate bars of 37R5 lite panels

Test Number	B1 (%)	B 2 (%)	B3 (%)	I1 + I2 (%)
3	20	20	43	17
4	19	20	43	18
5	17	46	21	16

During testing of panel B, strains were also recorded and the results summarized in Figure 3.9. Strain gages were positioned along the tension regions of bearing bars at two positions over the span. The first set of strain gages were in between supports and the second set were positioned over the central support.

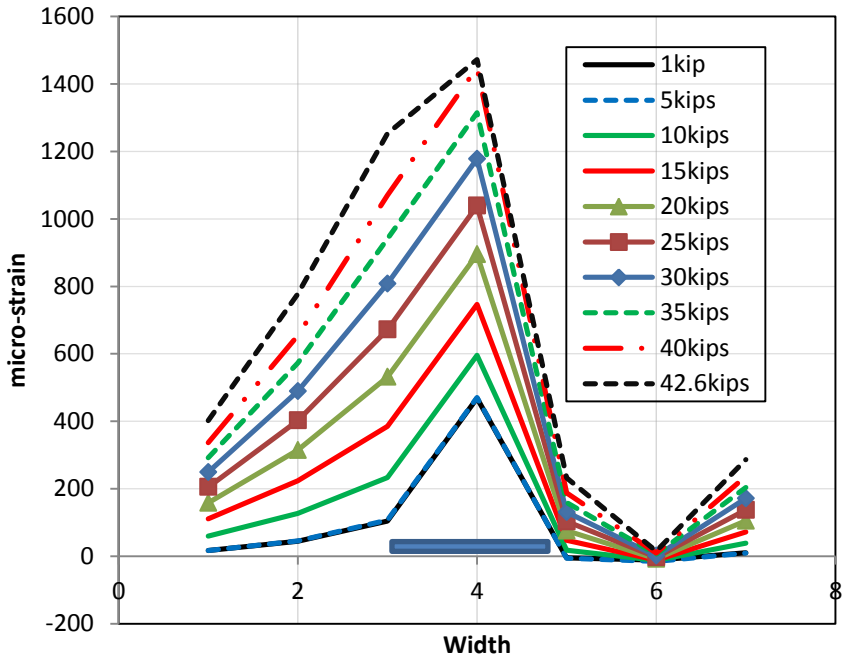

Figure 3.9 - Micro-strain distribution across width of riveted grating for Test B

Maximum strains recorded under loading were on the order of 1472 micro strain and that over the supports was about 818 micro strain. The strain distribution across the panel shows that higher strains are recorded in bearing bars directly under the load, with some strain carried by adjacent bars. The strain is also influenced by end support conditions of the panel. It is clearly seen that strain gradually decreases from area of loading towards the end of the panels. There is a slight increase at the end bearing bar influenced by the added stiffness of the adjacent panel.

3.4 Finite Element Analysis of Heavy Duty Riveted Steel Gratings

A three dimensional finite element model of the panel has been developed using ABAQUS CAE. Finite element analysis provides a way to study the behavior of structural systems with complex geometries. The finite element model developed has been calibrated with laboratory data of test panel A and involves the static loading of the 37R5 panel. A simplified modeling approach has been adopted to reduce both analysis time and also improve the accuracy of the results.

3.4.1 Modeling of Test Panel A

The finite element model of the heavy duty riveted grating involves the creation of parts for the main, intermediate and connecting or reticuline bars using shell elements. Only half of the panel was modeled but provisions were made to capture the continuous nature of the panels at both ends of the support. The modeled parts were assembled to represent the exact geometry of the heavy duty riveted grating as shown in Figure 3.10. A

constitutive model for structural steel was used with an elastic modulus of 29000ksi and a poison ratio of 0.3. Plastic behavior of the steel was not considered since stresses occurring as a result of the loading are primarily elastic. The various contact interactions occurring between individual components of the grating was adequately modeled using the contact property with the selection of both master and slave surfaces.

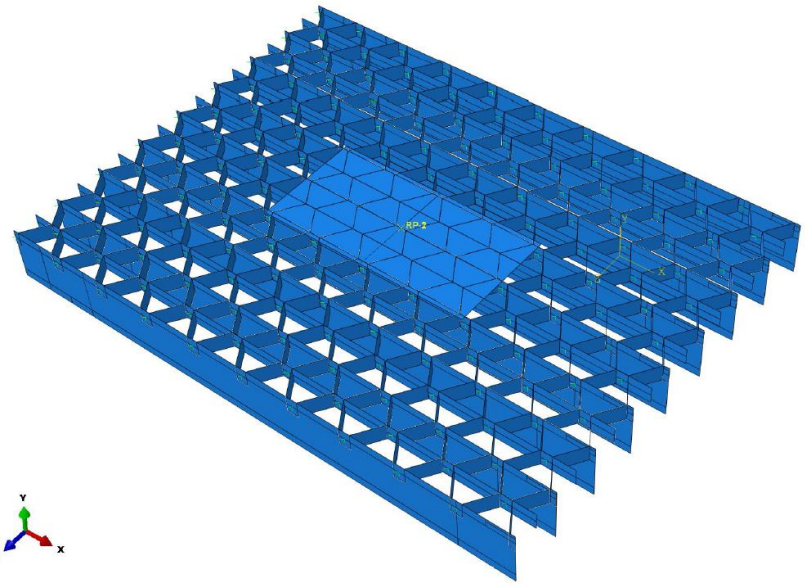

Figure 3.10 - Finite element model of the 37R5 lite panel

Rivets are modeled using the fastener property of Abaqus CAE with the definition of the various attachment points of the rivets. The beam connector property is used to describe the behavior of the rivets with a physical radius of 0.1875in. Boundary conditions were applied to the model at the initial step and included a fixed support to represent the continuous behavior of the grating and a pin support at the end. Loading was applied using a pressure of 0.11ksi/in^2 through a loading plate measuring 20in x 10in which represents the dimension for the tire patch and the load of an H-20 truck with a 30%

impact factor with some adjustments. The tire patch is tied to the grating during the assembly and interaction modules. The tire patch is assigned a property to behave as a rigid body through a reference point. Proper meshing techniques in a finite element model leads to an economic analysis with greater accuracy. The conventional shell elements, S4R was chosen from the element library and used to mesh all the parts with the mesh density varied depending on output data as shown in Figure 3.11

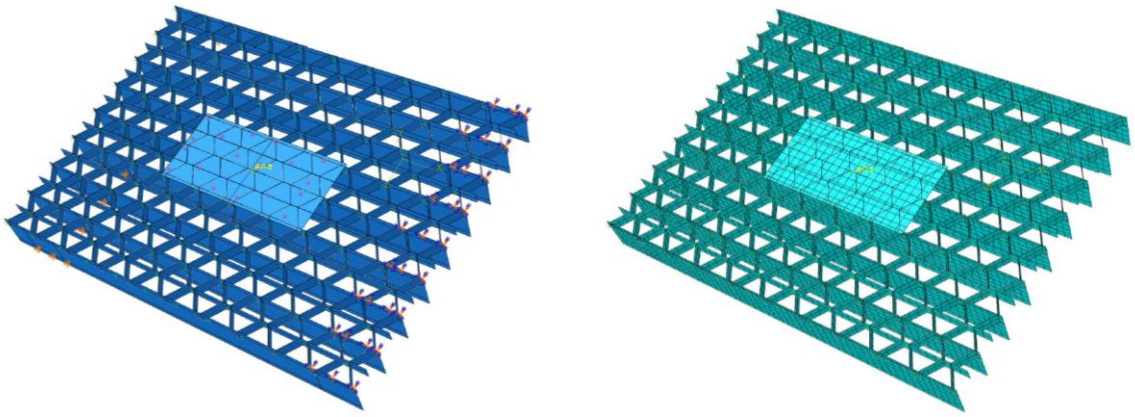

Figure 3.11- Boundary conditions, loads and mesh for the heavy duty riveted grating

3.4.2 Visualization of Results and Failure Patterns

The deformed shape of the heavy duty riveted grating Von mises stress contours is indicated in Figure 3.12. There are higher tensile stresses along the continuous support and directly under the load. Maximum deflections occur around the midspan of the loaded panels. The magnitude and nature of the stress distribution of the main bars is compared with the experimental output of test 1 of panel A and it is shown in Figure 3.13

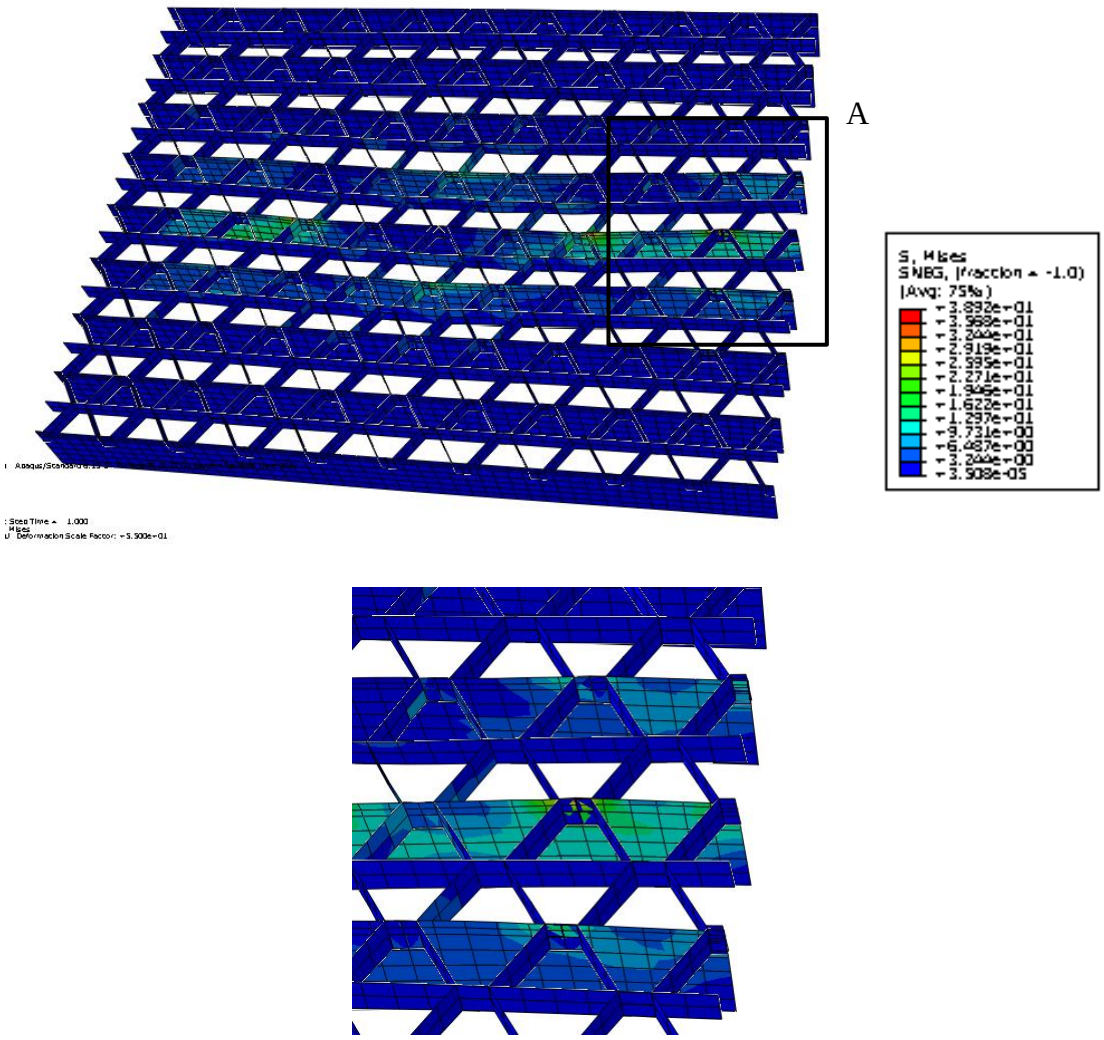

Detail A

Figure 3.12 – Deformed shape of the riveted grating showing stress distribution

A comparison of the graph from the finite element analysis with test results show that the behavior of the heavy duty riveted grating was adequately predicted using the finite element analysis. This provides a means to use finite element analysis to perform a parametric study on how different factors will affect the behavior of the heavy duty riveted grating.

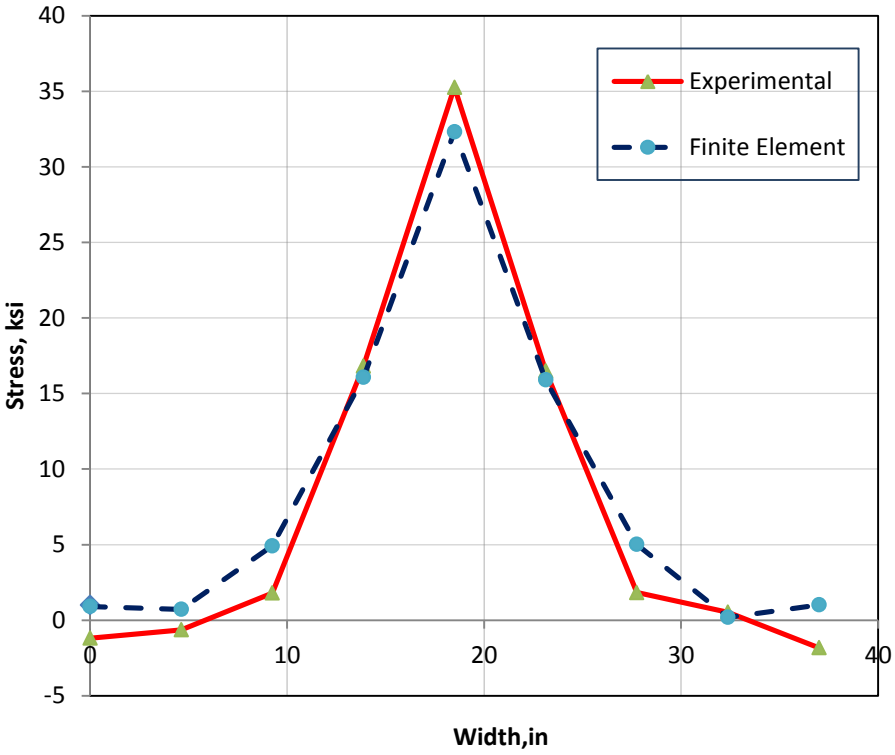

Figure 3.13 - Stress distribution across width of riveted grating

3.5 Parametric Studies

A parametric study was conducted on the heavy duty riveted gratings with different factors and modifications to the three dimensional finite element model. A significant factor is the spacing of the stringers which will lead to either an increase or decrease in both deflections and moments. The nature of the stress distributions and the magnitude of resulting stresses on the grating depend on factors such as the direction and position of loading in relation to orientation of the bearing bars, the presence of intermediate bars replacing main bars, the spacing and the cross-section of main bars. The cross-section of the main bars is related to the section modulus and the moment of inertia of the gratings. Under similar loading conditions, when the cross-section of the main bearing bar of the

37R5 Lite is replaced with a section which has a higher section modulus, the resulting moments and deflections will be reduced.

3.5.1 Effect of main bearing bar spacing

Bearing bars are the primary load carrying members in a heavy duty riveted grating. The spacing of the bearing bars therefore affect how load is distributed within the grating. Main bar spacing is investigated by replacing the intermediate bars in a 37R5 lite panel with bearing bars resulting in the standard 37R5 panel as shown in Figure 3.14.

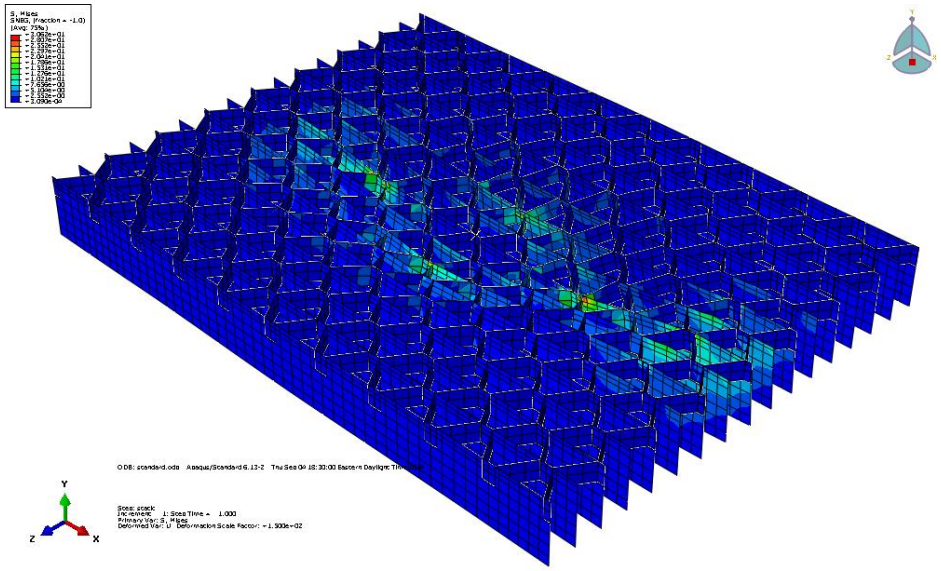

Figure 3.14 –Deformed shape of the riveted grating with reduced main bar spacing

It can be seen that decreasing main bar spacing results in decreased stresses on the main bars and vice versa. Reduced stresses on the members as a result of decreased main bar spacing will lead to better fatigue performance, but will increase the weight and cost per

square foot. When bearing bar spacing is reduced, the number of bars within the vicinity contributing to the load carrying capacity of the grating increases, therefore the effective stress on each bar is reduced. The stiffness of the grating will increase with reduced main bar spacing resulting in lower deflections and moments. The stress distribution pattern for the 37R5 lite panel is compared with that of the standard 37R5 panel. With reduced spacing of the main bars, there is a corresponding reduction in the stresses on the order of about 30% as shown in Figure 3.15

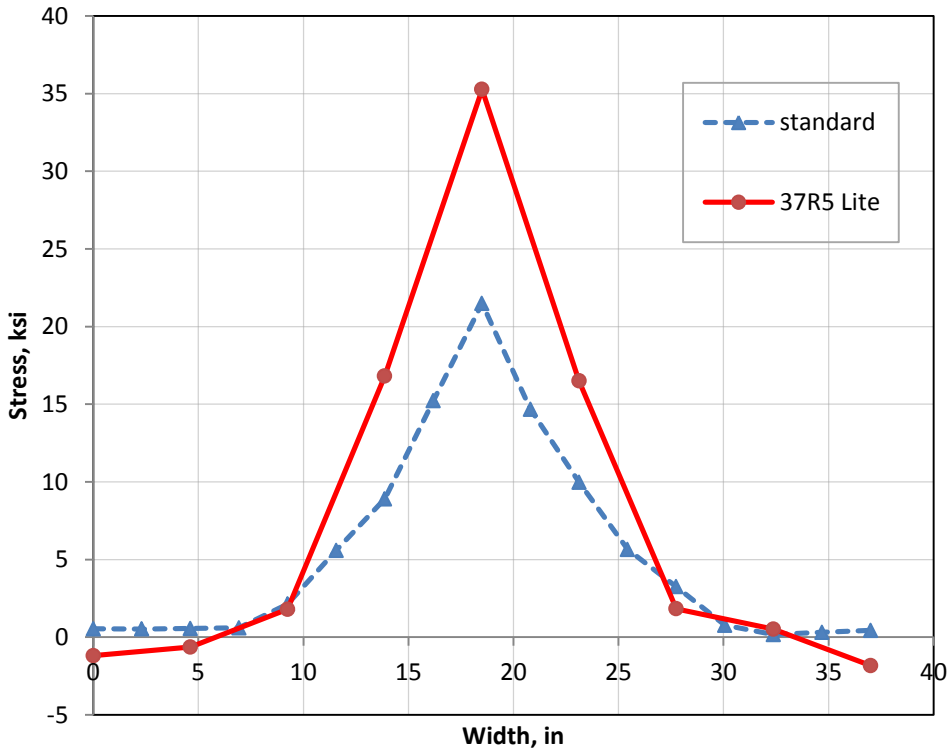

Figure 3.15 - Effect of main bar spacing.

3.5.2 Effect of Load Position and Direction

Main bearing bars in the heavy duty riveted gratings behave as beams when subjected to traffic loads. The behavior of the gratings is dictated by the number of bearing bars that are actively involved in transmitting the applied loads to the stringers. The magnitude of the stresses on the bearing bars therefore depends on the position of the loads in relation to the supports. It is determined the same way as an equivalent beam under load and specified support conditions. For maximum moment in a simply supported span, the load is placed at midspan and the stresses on each bar depend on the direction of traffic flow and the number of bearing bars actively involved in transmitting the load to the stringers. Under similar loading conditions, strain and deflections are higher when bearing bars are perpendicular to the direction of traffic than when they are parallel. This has been investigated with a modification of the three dimensional finite element model for the 37R5 lite panel with a change in the orientation of a tire patch as shown in figure 3.16. The tire patch is represented by a plate with dimension of 20in x 10in.

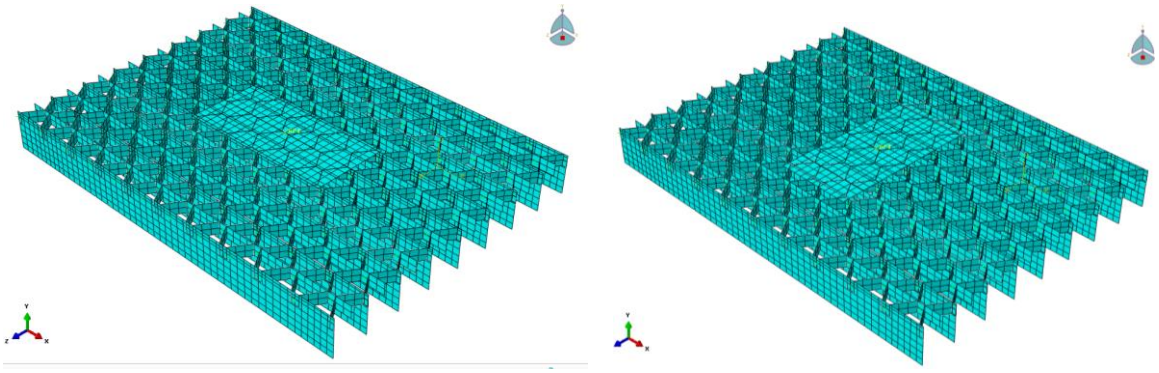

(a) perpendicular (b) parallel

Figure 3.16 – Effect of traffic direction on stresses

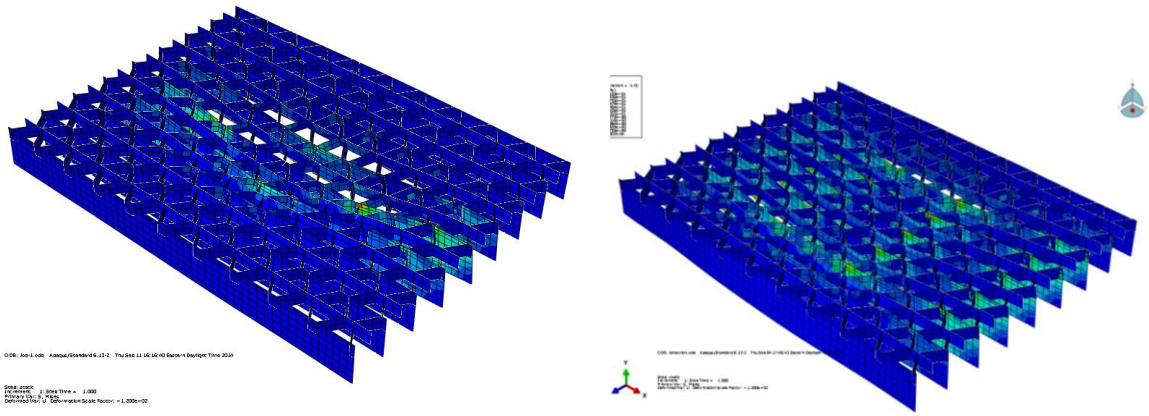

(a) Perpendicular (b)Parallel

Figure 3.17 – Riveted grating under load (a) perpendicular and (b) parallel to main bars.

Stresses are better distributed and reduced in the panel when traffic is oriented parallel to the direction of bearing bars. The critical situation for design involves the orientation of traffic perpendicular to the main bar directions.

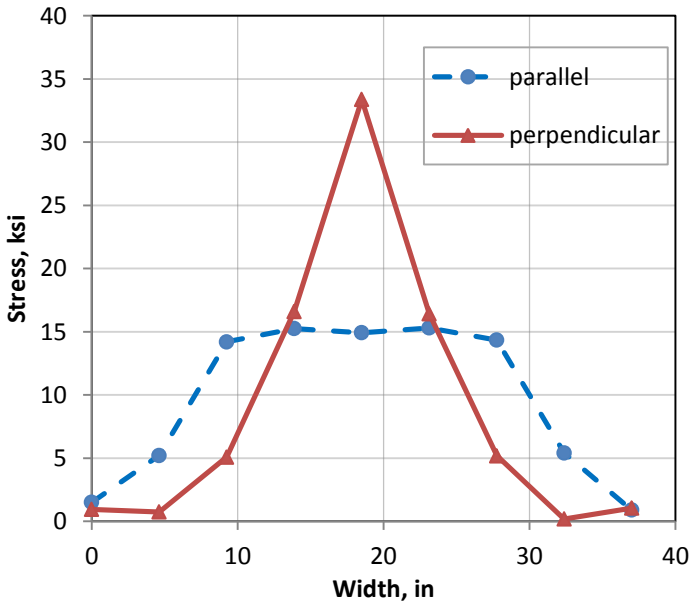

Figure 3.18 – Effect of traffic flow direction on riveted gratings

Resulting stresses are higher and localized with the panel oriented perpendicular to traffic. The stress distributions are compared for the same case of loading for the 37R5 lite panel but with different loading orientations as shown in figure 3.18.

3.5.3 Comparative study of the 37R5 L-series with the 37R5 Lite

The 37R5 L-series occur as a modified form of the 37R5 lite but with the cross section of the flat bearing bars replaced by angles, with two intermediate bars occurring between each of the main bars. A comparative study is done between the 37R5 lite and the 37R5 L-series by modifying the geometry of the finite element model and using it to study the behavior of the 37R5 L-series. Two cases have been considered in the analysis based on the position of the tire patch during loading. The first case occurs when the tire patch is placed directly in between two main angles with adjacent intermediate bars as shown in Figure 3.19 (a). The second scenario involves the loading of a main angle with adjacent intermediate bars occurring at both sides as shown in Figure 3.19(b)

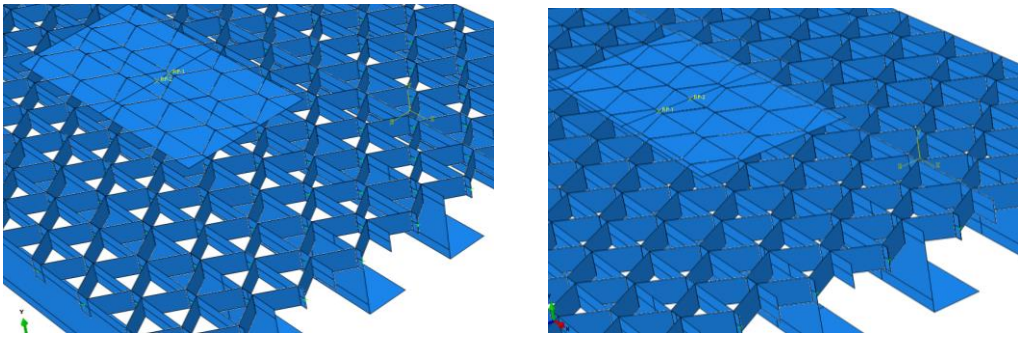

(a) Case 1 – two bearing bars (b) Case 2 - One Bearing bar

Figure 3.19 – Location of loading along width of riveted grating

All other parameters involved were similar to that used in the 37R5 lite model. The nature of the stress distribution in both cases is shown in Figure 3.20. There is better redistribution of stresses on bearing bars in case 1 as compared to case 2 which becomes critical for design.

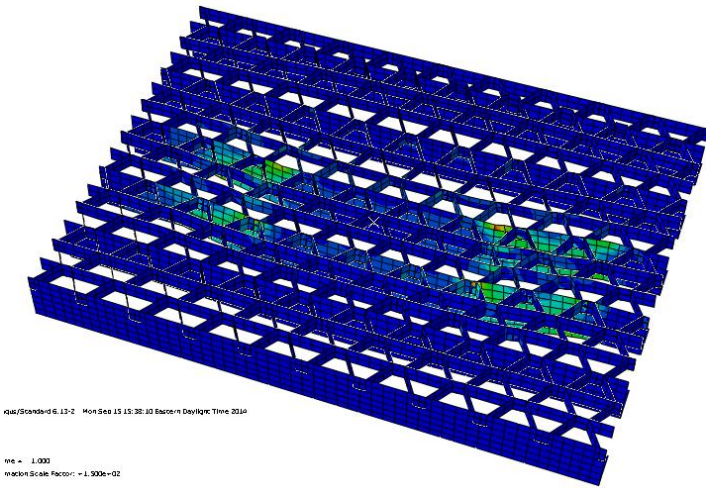

(a) Case 1

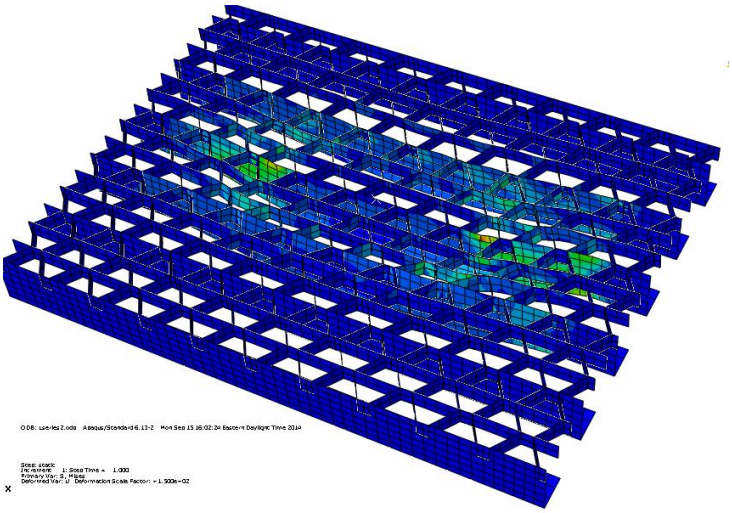

(b) Case 2

Figure 3.20 –Deformed shapes of the 37R5 L-series panel

Negative bending stresses in the angles over the supports are much higher and are therefore the controlling case for fatigue evaluation of the 37R5 L series. The stress distribution across the width of the grating for case 1 is shown in Figure 3.21. There is even distribution on both angles directly beneath the load with the magnitude of stress on the intermediate bars highest within that region. About 75% of the load is carried by the angles with the remaining 25% carried by the intermediate bars.

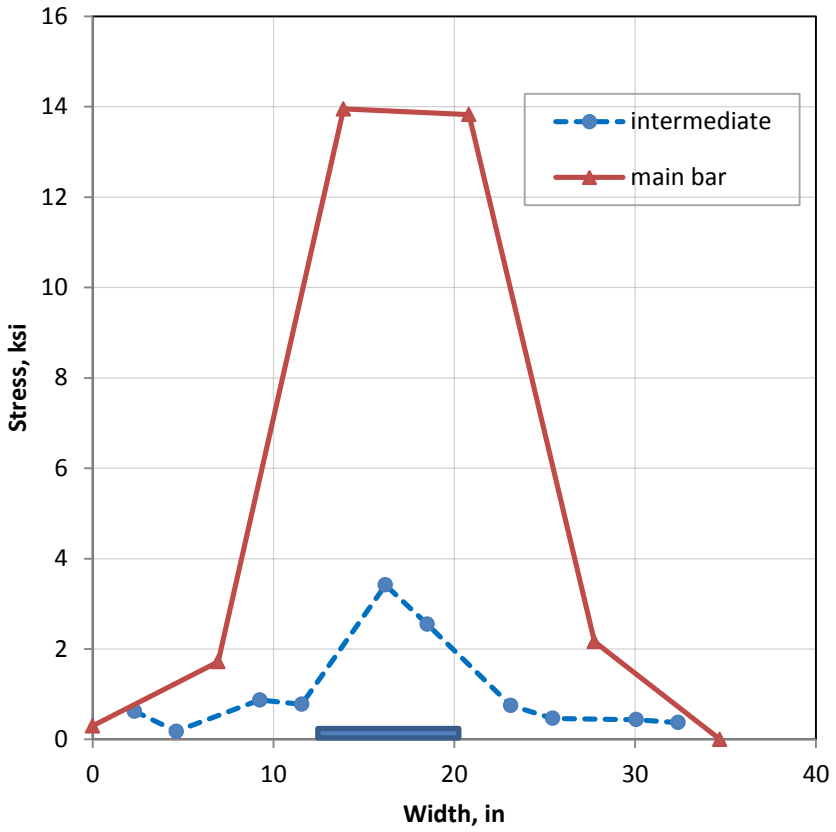

Figure 3.21 – Stress distribution pattern for case 1 loading of the 37R5 L-series panel

For case 2, with the tire patch placed directly on a bearing angle with adjacent intermediate bars, a much higher stress is observed and the nature of stress distribution is

shown in Figure 3.22 along with intermediate bars. Finite element results indicated that the contribution of the bearing angle was about 70% with the remaining carried by the intermediate bars.

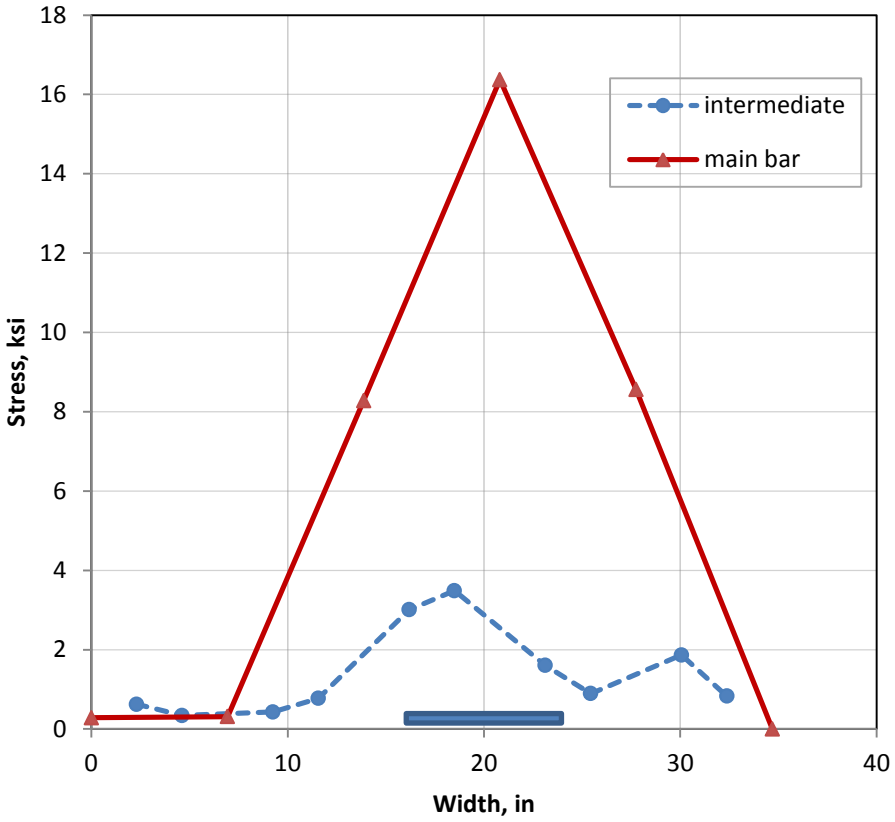

Figure 3.22 – Stress distribution for case 2 loading of the 37R5 L-series panel

3.6 Summary

Two panels of the 37R5 lite were tested under AASHTO H20 loading to study the nature of stress distribution across the grating and the contribution of the various subcomponents of the grating. Eight tests were performed on test panel A and the load strain relationships were established. The contributions of the various components of the grating were evaluated by attaching strain gages and recording strains during loading. A second set of

static tests was conducted on panel B, originally fabricated to be used for the fatigue testing of the gratings. A 3D finite element model was developed and calibrated to laboratory data. Results from the finite element analysis were compared with experimental results and showed good correlation. A parametric study was then performed to investigate how different geometric factors affected behavior of the grating. Results from the static and finite element analysis formed the basis for the design of the experiment for fatigue testing.

CHAPTER IV

FATIGUE TESTING OF HEAVY DUTY RIVETED STEEL GRATINGS

4.1 Introduction

The experimental program involved in the study of the fatigue behavior of the gratings consisted of testing of both large and smaller size panels. Fatigue testing of the large panels involved loads simulating the AASHTO H-20 design truck. Stresses in bearing bars of the grating and subcomponents were estimated based on the captured strain readings. The smaller samples were tested at different target stress ranges until failure occurred. All data obtained formed the basis for the development of S-N curve for heavy duty riveted grating. Six large panels of the 37R5 Lite and the 37R5 (L-series) and 24 smaller size samples were tested under varying loading and support conditions. A total of nine tests were conducted on the full panels and 24 test on the smaller panels. The critical detail for fatigue evaluation is the riveted detail in negative bending.

4.2 Experimental Set – up of the Large Panels

Large heavy duty riveted grating test panels were fabricated, taking into consideration findings from previous tests and observations published in literature about heavy duty riveted gratings. The fatigue behavior of structural systems is better captured when actual

configurations and testing are employed under both service and design loads. The large panels involved were cyclically loaded with AASHTO H-20 loading for the worst case scenario and maximum force effects. A total of nine tests were performed on six full size panels under various cases of loading and support conditions. Structural panels consisted of four 37R5 Lite (5in x ¼in) panels and two 37R5 –L Series (5in x 3in x ¼in) panels. Both are modified forms of the standard 37R5 grating.

4.2.1 - 37R5 Lite Panels (5”x1/4”)

Four large 37R5 lite panels were involved in testing. Bearing bars were rectangular in shape with dimensions of 5in x ¼in with intermediate bars measuring 1-1/2in x ¼in. The reticuline bars are serrated and have the same dimensions as intermediate bars. All the panels were galvanized were of 11’-5” in length and 3’-1/8” in width. Two panels of the 37R5 lite were connected at a side splice by 3/8in A325 bolts at 15in centers. Seven different test were performed on the panels based on differences in

i. support conditions and spacing of the stringers
ii. attachment system to the stringers
iii. magnitude and position of loading

The panels are classified in this report based on varying conditions. Strain gages were attached to bearing bars directly under the load at both the compression and tension sides as well as in the negative moment region. A total of 8 gages were used to capture strain data directly under the load and in the negative moment region. Table 4.1 gives a description of the various test performed

Table 4.1 – Description 37R5 (5in x ¼in) Lite panels based varying conditions

Test #	Panel	Description
1	37R5-A1	This is a 37R5 lite panel with stringer spacing of 50in. AASHTO H20 loading occurred at midspan. The attachment system involves the welding of attachment plates to each side of the bearing bars .The attachment plates were subsequently bolted to the stringers. This panel is attached to the 37R5-A2 panel
2	37R5-A2	This has similar properties and is bolted at the ends to the 37R5-A1 to form an adjacent span. Loading involves the AASHTO H-20 truck loading at the edge of the panel.
3	37R5 –A1	Maximum loading increased by 10kips to 52.6kips. No cracks detected in Test 1 after 2 million cycles of loading.
4	37R5 –A2	Maximum loading increased by 10kips to 52.6kips. No cracks detected in Test 2 after 2 million cycles of loading
5	37R5- B1	37R5 lite panel with stringer spacing of 65in. Attachment method is same as in 37R5-A1 but only to one side. H-20 design truck loading at mid span. Panel attached to 37R5-B1
6	37R5 -B2	Panel same as in Test 5. Attachment system employed is same as in panel 37R5-A1. H-20 design truck loading at edge adjacent to 37R5-B1
7	37R5- B2	H-20 Loading at free end of panel

4.2.2 -37R5- L Series (5”x 3” x ¼”)

Three tests were conducted on two 37R5 – L Series panels which were spliced together at the sides. The 37R5 angle product is a modification of the standard panel, but with 5”x 3” x ¼” bearing angles. Included are two intermediate bars measuring 1-1/2” x ¼” placed between adjacent bearing angles, thus reducing the number of bearing angles per foot of grating. The reticuline bars are serrated and have the same dimensions as intermediate bars. All the panels were galvanized and measured 126in x 38-5/8in. Both tests had the same support and stringer spacing of 65in, with only the load position varying as described in Table 4.2

Table 4.2 – Description of 37R5 – L series

Test	Sample	Description
8	37R5 –L1	H-20 loading at the midspan across the width of the 37R5-L series panel. Stringer spacing is 65in
9	37R5- L2	H-20 loading at the edge of the 37R5-L series panel

4.2.3 Gage Layout

The behavior of the riveted gratings under load was continuously monitored by strain gages attached at positions on the main bars of the gratings. Different gage layouts were used for each test. Strain gages were of the type CEA-06-125UW-120 manufactured by Vishay with a resistance of 120 ohms and a gage factor of 2.11 ± 0.5%. Panel 37R5-A1 and 37R5-A2 were connected at a side splice with high strength bolts to simulate in-field conditions. Each panel had 8 gages installed on the main bearing bars under the load and

in the negative moment regions over the continuous support. For the purpose of this study, gages are differentiated based on the lettering at the end of the gage number assigned. “T” is used to describe gages at or near the top of the bars while “B” is used for gages placed near the bottom of bearing bars. Gages were used to measure the longitudinal strains in the bars as this plays a critical role in deformation and cracking. A general layout of the gages is presented in figure 4.2

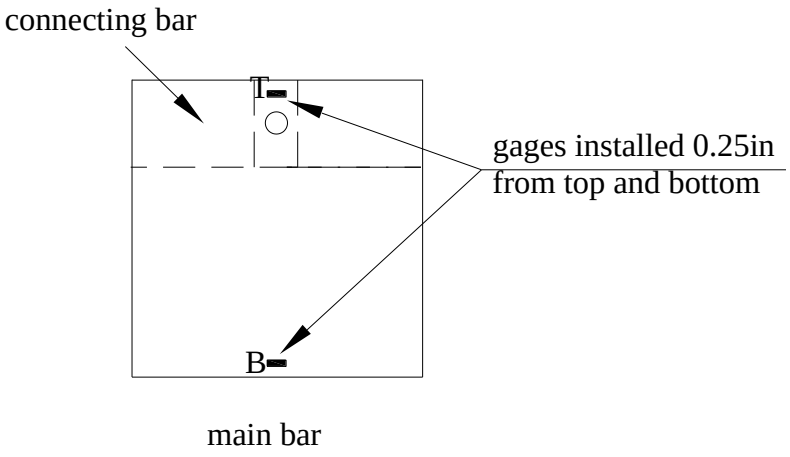

Figure 4.1- Gage layout of main bars

Panels 37R5-B1 and 37R5-B2 utilized a total of 26 gages, with 13 gages on each. Strain gages were placed only on the tension side of bearing bars in order to estimate the strain distribution across the width of the riveted grating. Gages were installed 0.25in from the bottom side of main bars at a distance of 3ft from the continuous support. Tensile strains over the support were recorded by gages installed 0.25in from the top of main bearing bars as shown in figure 4.1. Deflection measurements were taken on panel 37R5- B1 with linear variable differential transducers (LVDTs) mounted on two bearing bars directly

under the load. Figure 4.3 shows a layout of strain gauges for panel 37R5-B1. A total of 16 gages were used on the two panels of the L-series, 37R5-L1 and 37R5-L2. Strain gages were positioned at areas on bearing angles with expected high stresses. This included positions 3ft from the central support and directly under the load. Gage positions for the 37R5 L-series with a layout of gratings is shown in figure 4.4

4.2.4 Test Set Up

The test layout consisted of a box frame with which the grating was fixed to the strong floor. Stringers were already connected to the riveted grating panels using one of the attachment methods. In the case of the 37R5 lite panels, attachment plates were welded to either both or one side of the bearing bars and bolted to the stringers while the 37R5 L-series had bearing angles bolted directly to the stringers. A loading frame supports the MTS actuator used for fatigue loading and has a capacity of 55kips.

A spreader beam with pads 10in x 20in welded 6ft from each other was used to simulate the design truck wheel loads. MTS TestStar software was used to control the frequency and magnitude of loading by the actuator. A Vishay data acquisition system 5000 was used to collect strain data after the gages were connected. The Strainsmart software of the Vishay data acquisition system 5000 was used to zero, arm and calibrate the LVDT's and strain gages.

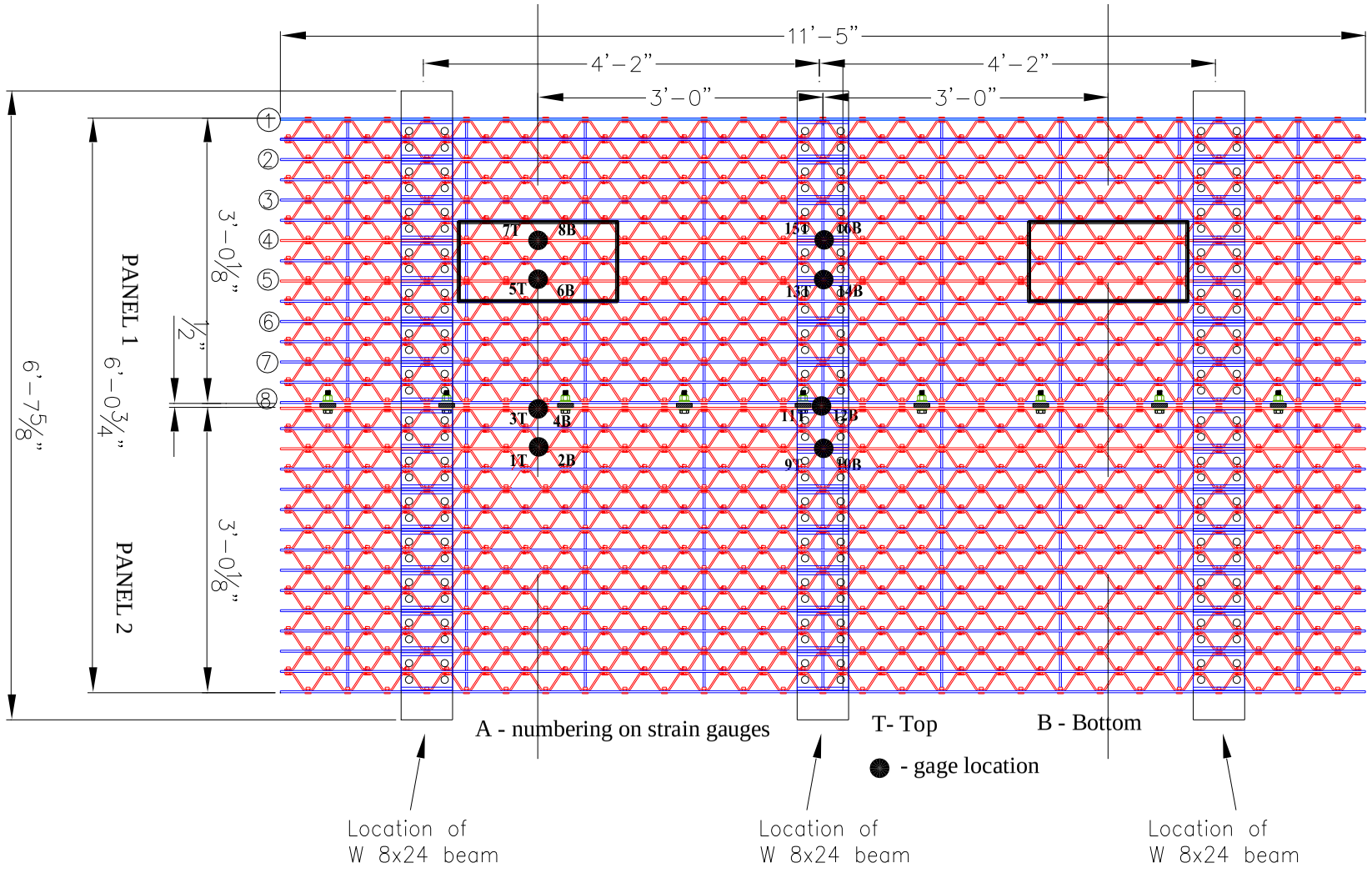

Figure 4.2 - General Arrangement of 37R5-A1 with gage and load positions for test #1 and #3

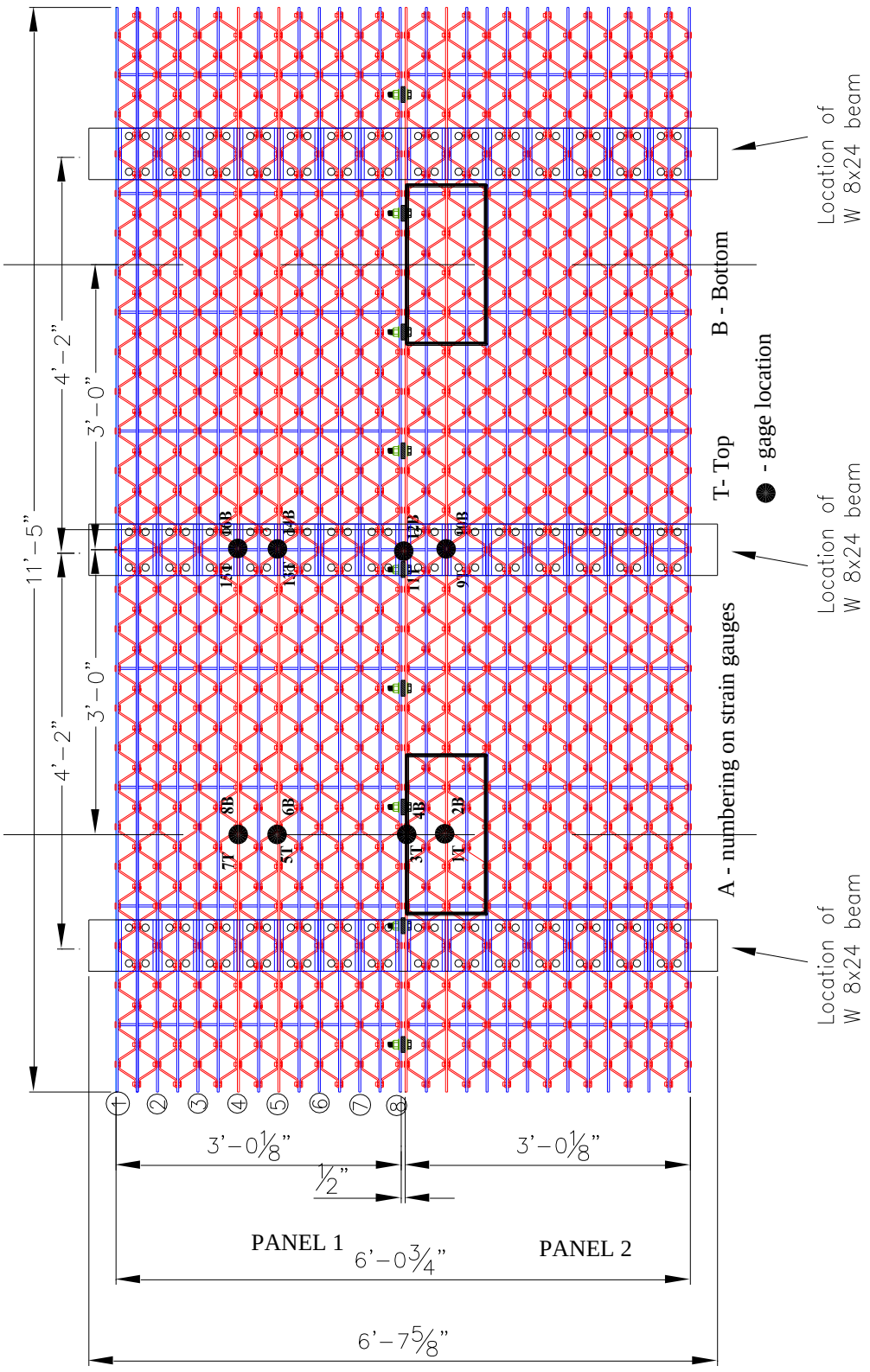

Figure 4.3 - General Arrangement of 37R5-A2 with gage and load positions for test #2 and #4

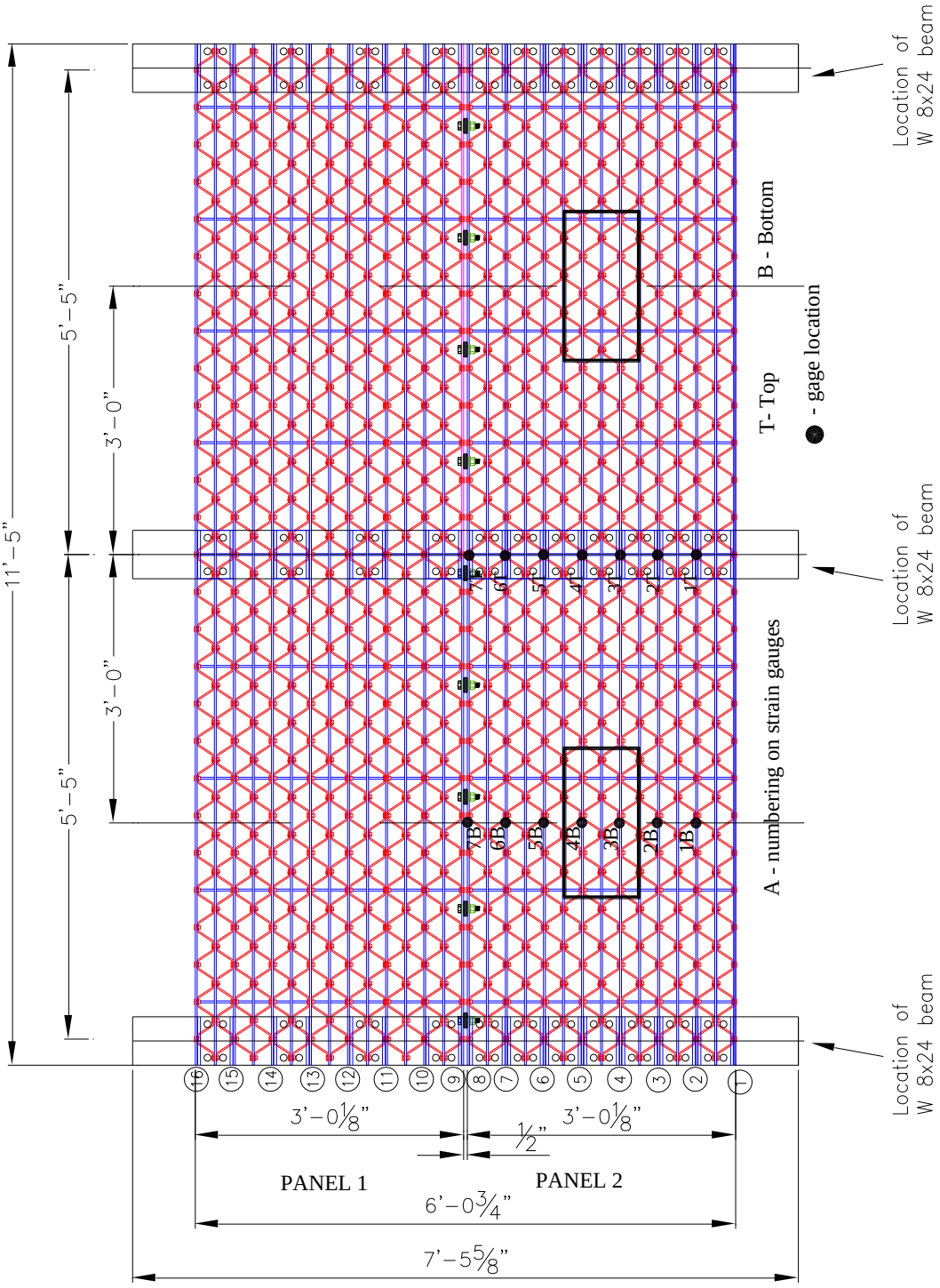

Figure 4.4 - General Arrangement of 37R5-B1 with gage and load positions for test #5

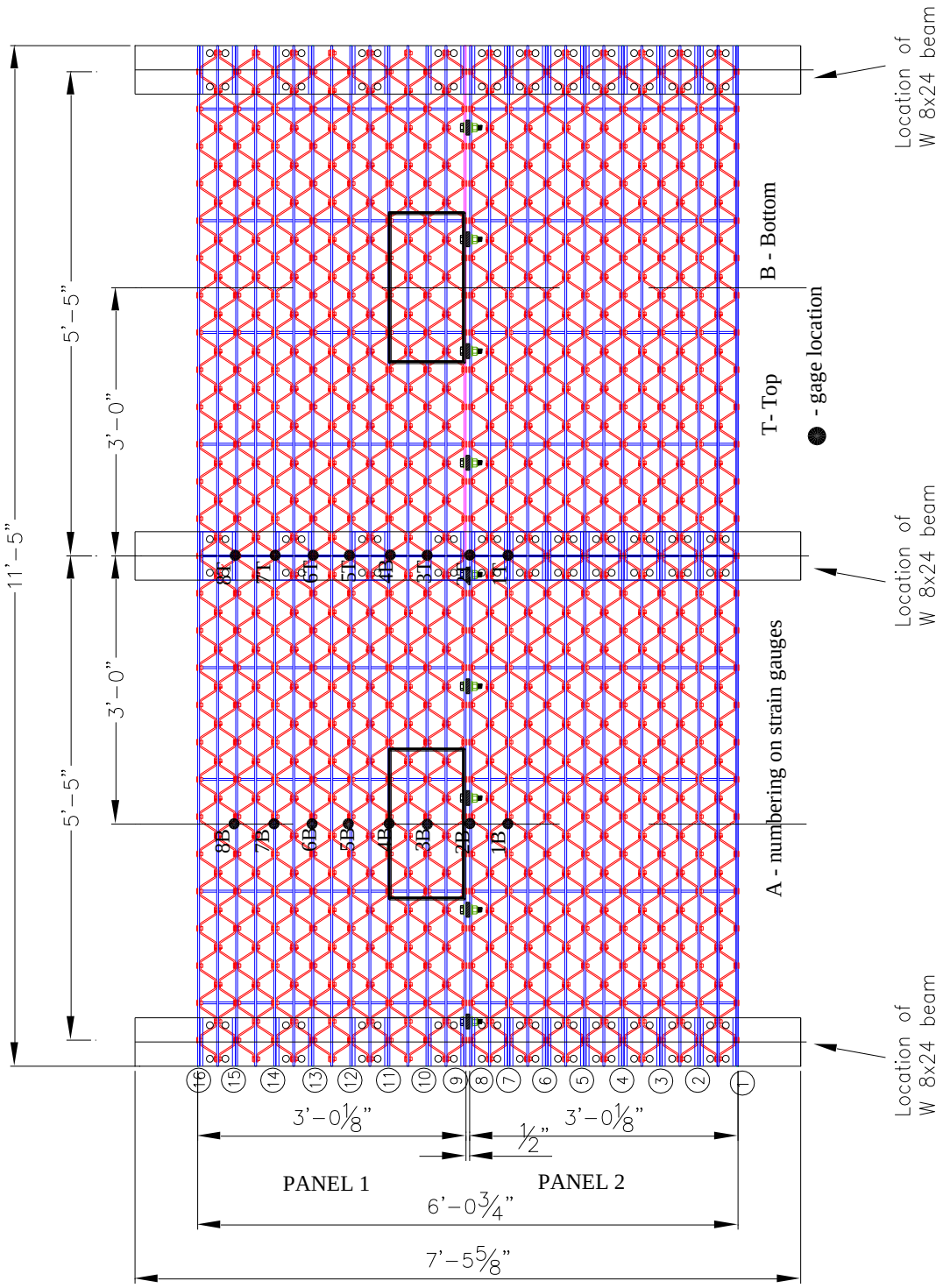

Figure 4.5 - General Arrangement of 37R5-B2 with gage and load positions for test #6

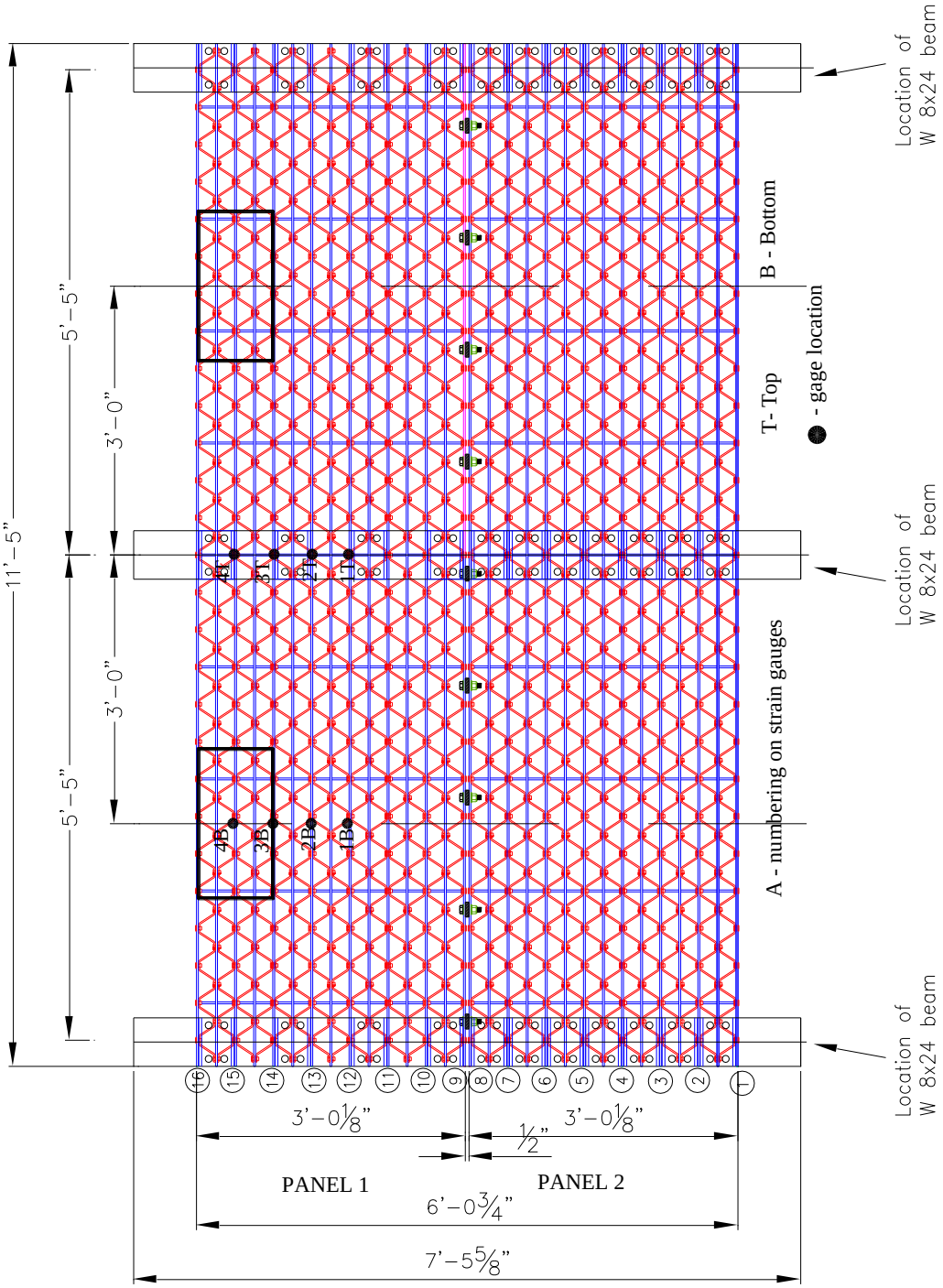

Figure 4.6 - General Arrangement of 37R5-B2 with gage and load positions for test #7

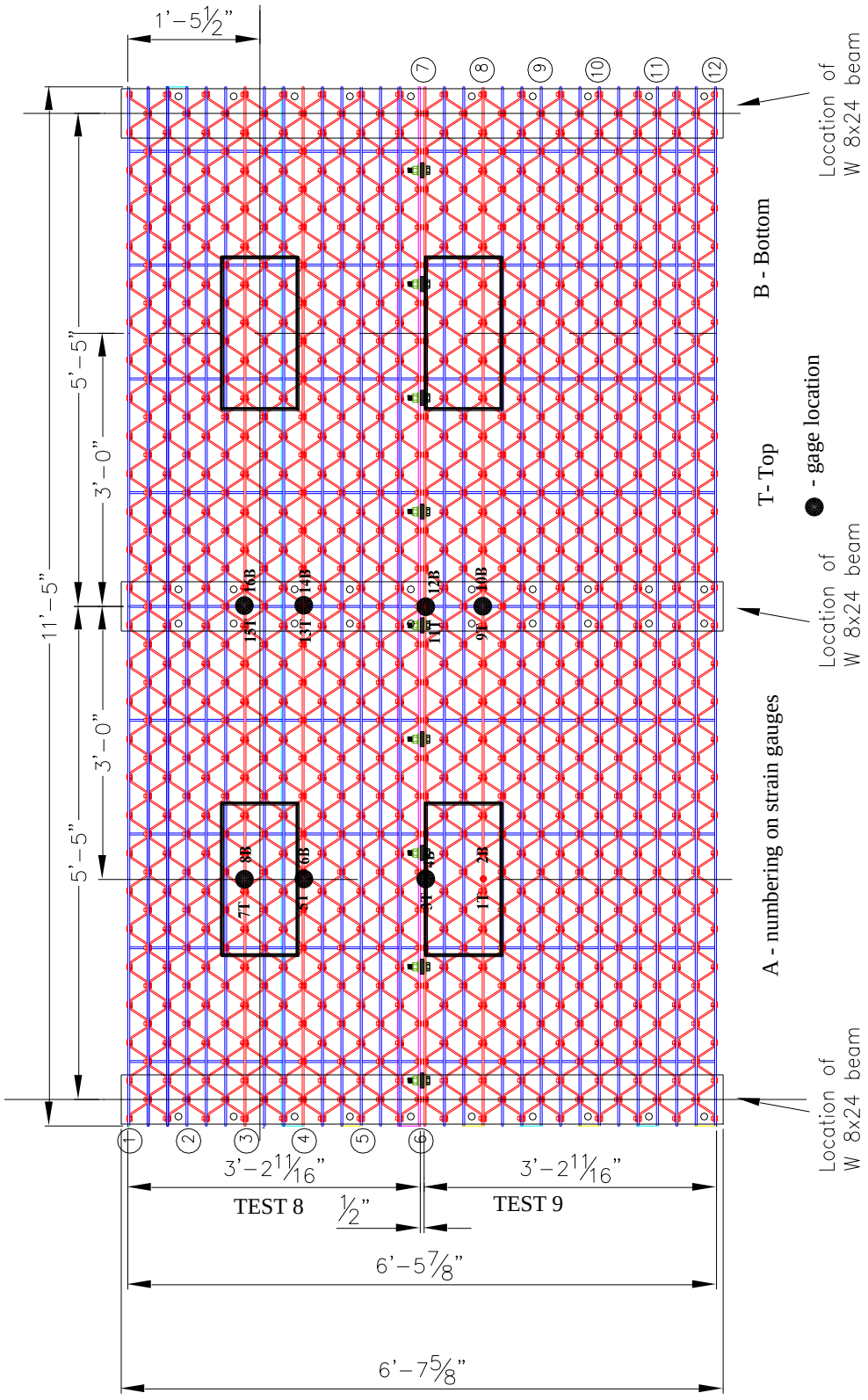

Figure 4.7 - Layout of 37R5-L series showing loading and strain gage positions for test #8 and #9

4.2.5 Loading

A test load simulating an H20 truck axle was applied by a 55 kip MTS actuator with an impact factor of 30%. An initial load of 1000lbs was applied on the spreader beams and gradually ramped to 42.6kips and cycled between the end points with a frequency of 1Hz. High durometer pads were placed under the patch plates to simulate a tire on the grating. At the end of testing of a panel where failure did not occur, the maximum load was increased by 10kips and the test restarted with a maximum load of 52.6kips

During testing of the 37R5 lite panels, loading occurred at different positions across the width of the grating. Test 1 involved loading across the mid span of the 37R5-A1 panel with a minimum load of 1000lbs and a maximum load of 42.6kips. Frequency of loading was 1Hz and 2 million cycles of loading was applied. The same magnitude and nature of loading was applied to the adjacent 37R5-A2 panel designated as Test 2. Loading occurred at the edge near the panel to panel joint. Test 3 and Test 4 were conducted after no failure occurred during testing of the 37R5-A1 and 37R5-A2 after 2 million cycles of loading. The panels were subjected to higher loads with the minimum maintained at 1000lbs and the maximum increased by 10kips to 52.6kips. Tests 5 and 6 involved two panels with a stringer spacing of 65in with loading conditions similar to earlier test. Loading of the simulated wheels occurred 3ft from the central support to each side of grating. Test 7 involved loading at the free edge of panel 37R5-B2.

37R5- L series panels had two different loading positions. In Test 8, loading was applied at the midspan of 37R5-L1 with characteristics as that of the H-20 design truck axle. A minimum of 1000lbs and maximum of 42.6kips was applied 3ft to each side of

the central support at a frequency of 1Hz. The test was completed after an acceptable level of failure had been observed in the grating. Test 9 had similar loading conditions as that of Test 8, with a change in location to the edge of the 37R5-L2 panel specimen

Figure 4.8 - Laboratory set-up for Test #1 with load at mid span of panel 37R5-A1

4.2.6 Test Procedure

All panels were set on a steel frame and held firmly to the strong floor. Load was applied through a spreader beam as shown in figure 4.9. Load was statically increased from 1000lbs to the maximum, and then cycled between the minimum load and the maximum load at a frequency of 1 Hz. Strain data was recorded by the Vishay data acquisition system for 10 seconds with 10 scans per second every 4 hours for strain gages mounted at various points of the bearing bars and angles. The panels were constantly inspected for

signs of failure or cracks. Where cracks developed in at least two of the members and propagated to a dominant size, the test was stopped and the sample deemed to have failed. If no failure occurred after 2 million cycles of loading, the maximum load was increased and the test specimen utilized again to examine other load locations or increased load magnitude.

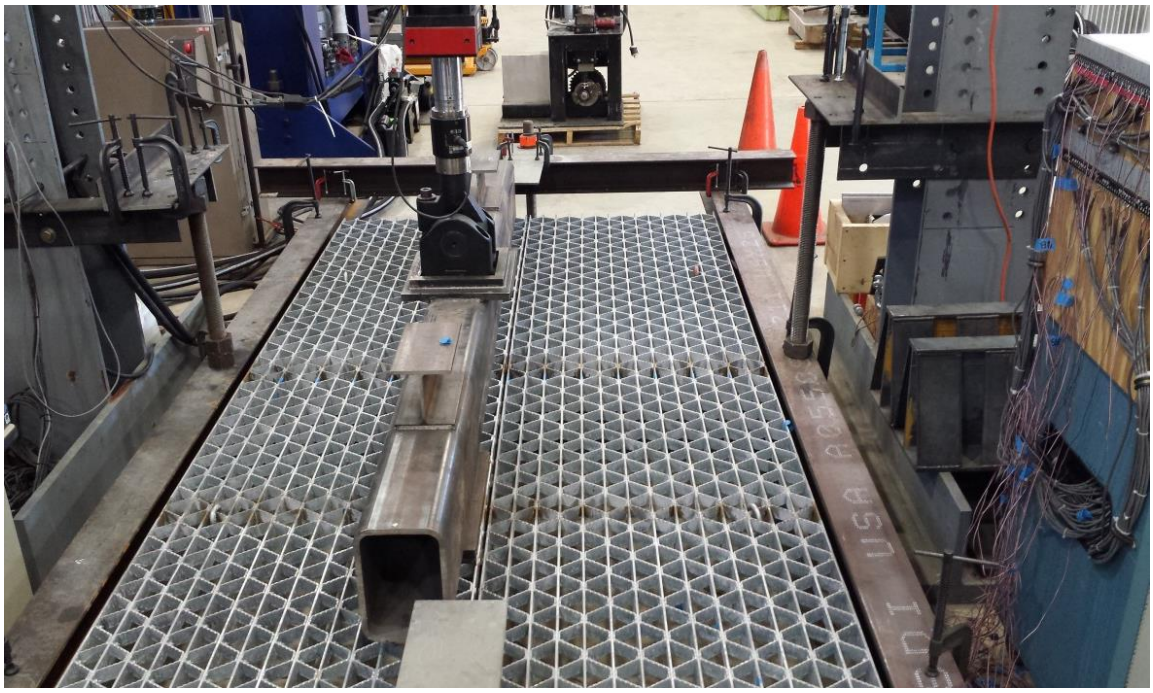

Figure 4.9 - Laboratory set-up for Test #6 with load at the edge panel of 37R5-B2

4.3 Experimental Set-up of Smaller Size Panels

The effect of varying parameters on fatigue behavior was further explored through an experimental study of different types of riveted gratings. This was achieved by testing smaller samples removed from full size grates, calibrated to the initial tests performed on

the large panels. Six sets of samples were tested under varying conditions of stress range, bar spacing, main bearing bar size, size of connecting bars and position of rivets.

4.3.1 Description of Samples

A sample classification system was adopted and gives information about the particular type of sample and the stress range with which the sample was subjected. There was a total of 4 sample types based on the 37R5 Lite geometry and 2 samples of the 37R5 L-series heavy duty riveted gratings. A summary of the section dimensions together with variations in the individual samples is presented in Table 4.3 and 4.4. Rivets are placed 3/4in from the top of bearing bars connecting reticuline bars to the intermediate and the bearing bars. Typically, for sample A which has an intermediate bar size of 1.5in x 0.25in and connecting bar size of 1.5in x 3/16in, rivets occur at 0.75in from the top of bearing bars as shown in figure 4.10. Different sizes of sub- components were explored during sample testing. All of the bars were galvanized. Table 4.3 and 4.4 are dimensions of the various subcomponents of the 37R5 lite and 37R5 L-series respectively.

Table 4.3 – Description of smaller size samples for 37R5 Lite

Sample	No.	Dimensions (in)	Main bar (in)	Intermediate bar (in)	Connecting bars (in)
A	5	37 x 10.5	5 x 0.25	1.5 x 0.25	1.5 x 0.1875
B	4	37 x 10.375	5 x 0.25	2 x 0.1875	2 x 0.125
C	4	37 x 11.125	5 x 0.375	1.5 x 0.375	1.5 x 0.0625
D	4	37 x 10.75	5 x 0.375	2 x 0.1875	2 x 0.125

Table 4.4 – Smaller size samples for 37R5- L Series

Sample	No.	Dimensions (in)	Main bar (in)	Intermediate bar (in)	Connecting bars (in)
E	4	37 x 15.625	5 x 3 x 0.25	2 x 0.1875	2 x 0.125
F	5	37 x 15.375	5 x 3 x 0.25	1.5 x 0.25	1.5 x 0.1875

4.3.2 Designation

A system was adopted to identify the individual samples during the test program. An alphanumeric system was used. A letter represents the type of sample with the number representing the stress range under which the sample is tested. An example is that of Sample A30 which represents a 37R5 Lite Sample of type A, tested under a stress range of 30ksi.

4.3.3 Support Conditions

The samples were supported at both ends with pylons specifically fabricated for the purpose. The pylons are 34in high and have bearing area of 36in x 12in. Samples were placed on elastomeric pads on the bearing area of the samples. A minimum bearing distance of 4in was used. Movement in the horizontal direction was prevented by the provision of side bars which are made of steel angle sections placed by the sides and clamped to the pylons.

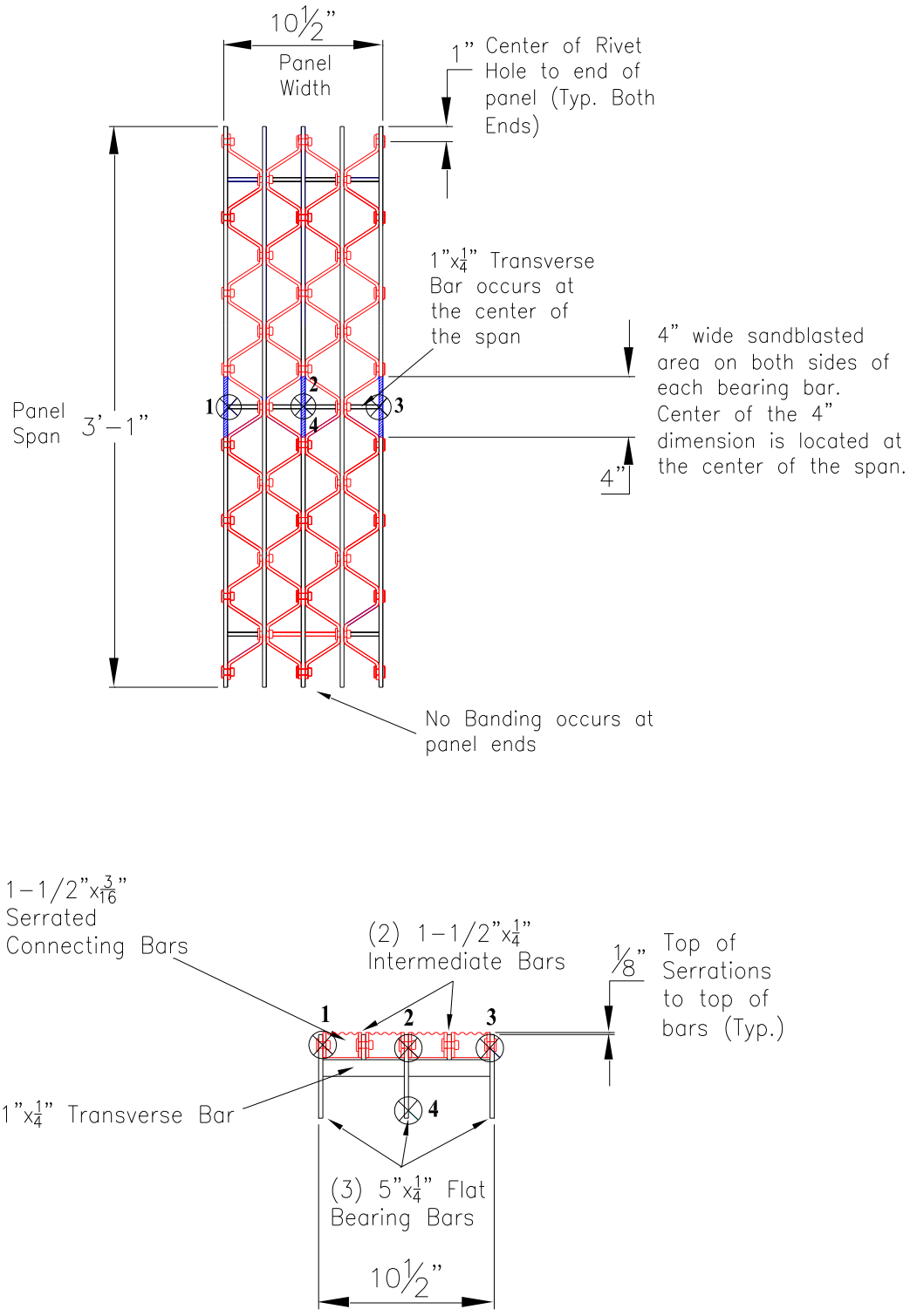

Figure 4.10 - Sample A of a 37R5 lite panel

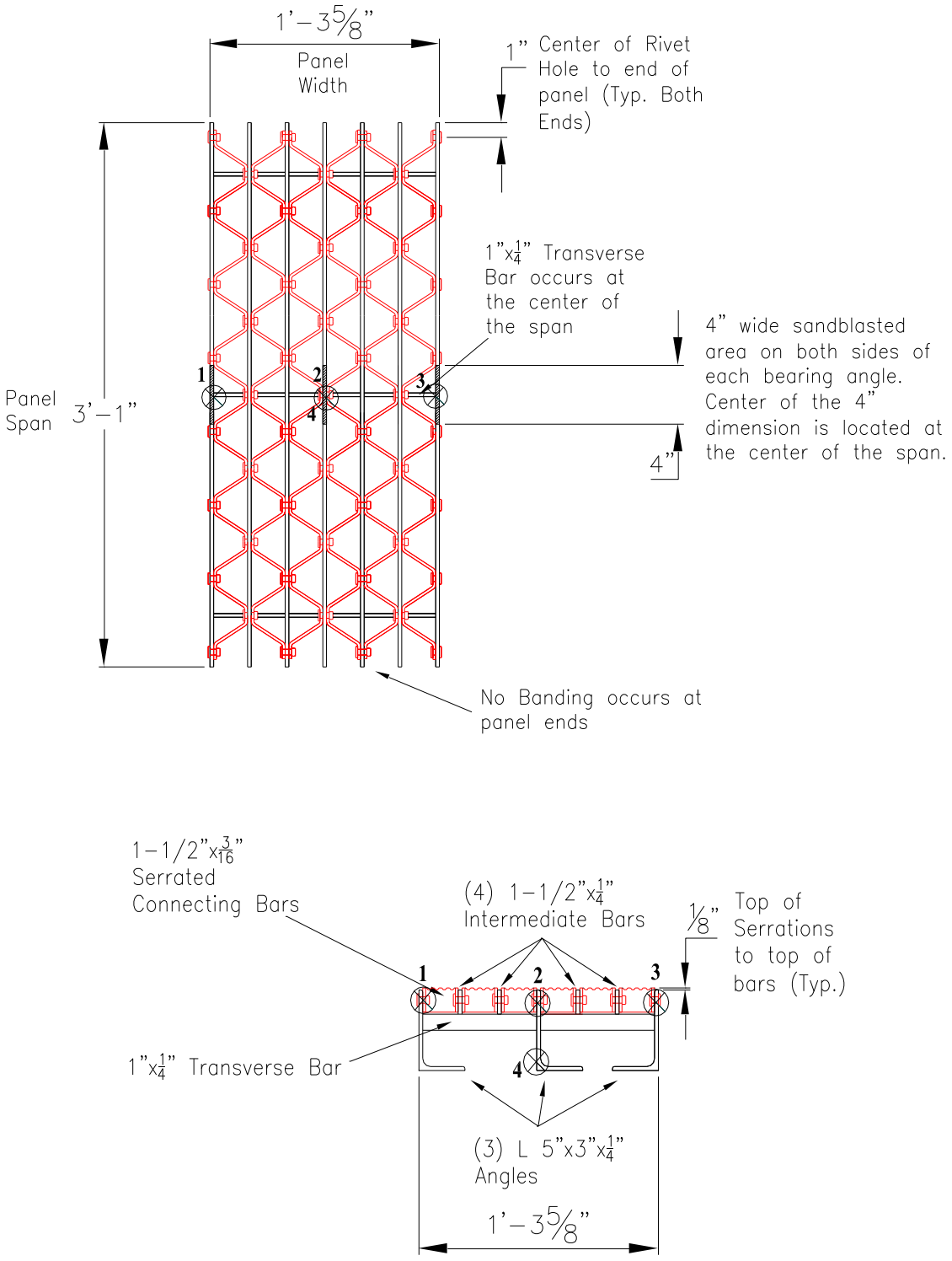

Figure 4.11 – Sample F of a 37R5 L-Series

4.3.4 Instrumentation

A total of four strain gages were attached to each sample in the set. Three gages were placed on each of the main bearing bars 0.25in from the top of the panel. A fourth gage is placed 0.25in from the bottom of the middle bearing bar under loading. Gages used were of type type CEA-06-125UW-120 manufactured by Vishay measurements with a resistance of 120 ohms and a gage factor of 2.11 ± 0.5%. There was an initial static loading of the test panels. Recorded strains were used to establish the target strain range. Strain data is captured using the micro measurements system 5000 using strain smart software. Loading was applied with an MTS actuator that has a capacity of 55kips and was controlled electronically by TESTAR Software.

4.3.5 Test Layout

Observations from the results of the large panel tests served as a basis for the design of the test set up of the smaller samples. Fatigue cracks in riveted gratings predominantly occur within the tension regions over the continuous support stringers. Component details at the section in the tension zone above the neutral axis are thus critical in the fatigue evaluation. This includes the riveted details of the bearing bars and angles, intermediate bars and connecting bars. Smaller sample testing involved loading of a simply supported panel with the top of the panel inverted, to create that tension region where the critical details exist.

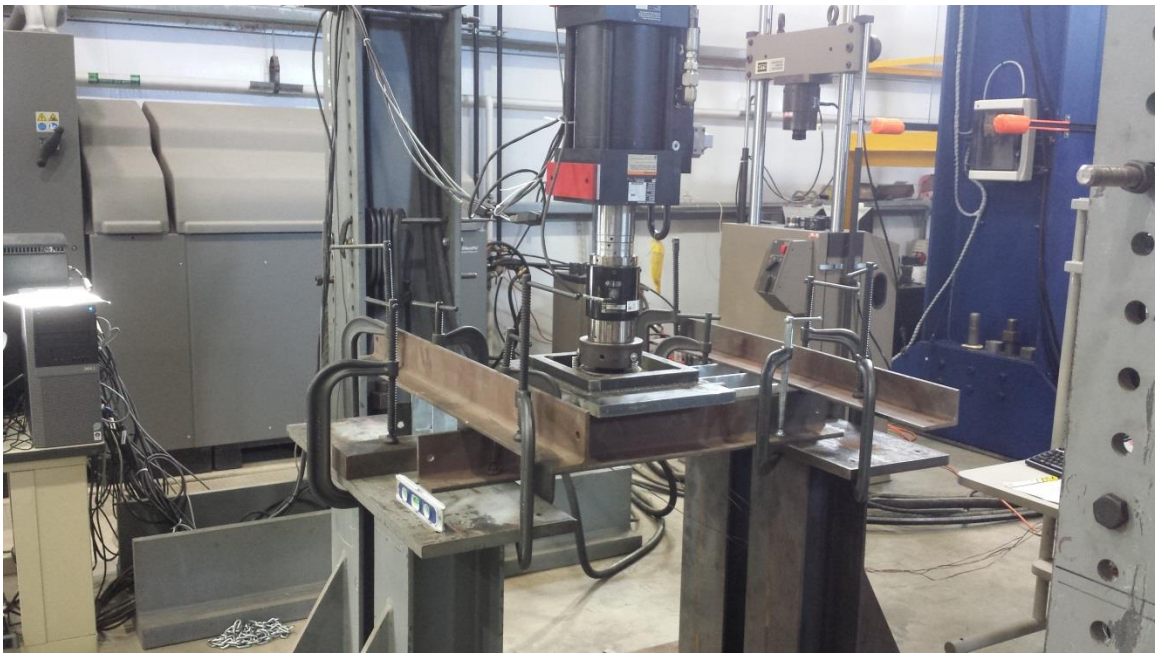

Figure 4.12 - Test set-up for smaller size heavy duty riveted panels

4.3.6 Test Procedure

An initial static loading test was performed to establish a minimum and maximum load at which the targeted stress range could be reached. Stress ranges considered for all panels included 25ksi, 30ksi and 35ksi .Further testing occurred for samples A and F at 20ksi. All sample types available were subjected to loads for a particular stress range. Individual samples of the various types were identified by the target stress ranges. After an acceptable load range was established, the sample was then loaded at a frequency of 1Hz until failure occurred. Failure is said to have occurred under the following conditions:

- Crack develops and propagates to about half the size of one bearing bar in the sample.

- Cracks develop in at least two of the sub- components of the grating and have propagated to a dominant size.

4.4 Summary

During large panel testing, two different grating panels were connected together by high strength bolts as would occur in practice and loaded at different positions along the span. Test 1 involved loading at mid span across the width of panel 37R5-A1, with the second panel, 37R5-A2, loaded at the edge of the connected section in Test 2. After no failure had occurred after 2 million cycles of loading, the magnitude of the maximum load was increased by 10kips resulting in Test 3 and 4. Test 5, 6 and 7 were conducted on panels 37R5-B1 and B2 which had larger stringer spacing than earlier tests. Gages were positioned to capture the strains in the bearing bars and angles to allow estimation of stresses across the gratings. The panels were supported at the ends and mid span by W 8 x 24 beams acting as stringers, firmly held to prevent movement of the gratings under load.

The loading used simulated that of the design truck axle given in the AASHTO LRFD bridge design specifications (3.6.1.2-2). A total axle load of 32kips was used for maximum force effects on the panel. An impact factor of 30% of design loads was applied (much higher than AASHTO 15% for fatigue loading) to account for dynamic effects on the panels. A rectangular tire patch measuring 20in by 10in was used as the tire contact area with the pressure considered to be uniformly distributed. In order to maximize the effect of the stress at the critical detail under consideration, a single design truck was positioned on the structural panel based on an influence line analysis of the

loading. The loading pads were placed 3ft each way from the center of the mid span support. The grating was then cyclically loaded. A total of 2 million cycles was applied with a frequency of 1 Hz. Tests were stopped if the sample developed cracks in at least 2 of the components before the two million cycle mark was reached. In cases where no signs of damage occurred after the required number of cycles, the maximum load was increased and the test restarted. With H-20 loading applied to the panels, failure occurred as a result of a definite stress range corresponding to the extent of loading.

To better characterize the general fatigue behavior of the heavy duty riveted gratings, another set of tests on smaller panels was conducted and calibrated to initial large panel tests. Smaller panels were made up of four configurations of the 37R5 lite and two of the 37R5 L-series. Panels were tested at different stress ranges of 25ksi, 30ksi and 35ksi with further testing at 20ksi for samples A and F.

CHAPTER V

PROPOSED S-N CURVE AND TEST RESULTS FOR RIVETED GRATINGS

5. 1 Overview

A preliminary test was conducted on a panel under static loading to study its behavior and also provide information for fatigue testing of the heavy duty riveted gratings. Six large panels were tested in fatigue using AASHTO H-20 design truck loading. Additional smaller size panels with varying geometrical properties were also tested under different stress ranges. Initial results of the various tests are reported herein and highlights how variations in load, geometry, main bar spacing, position of rivets and geometry of main bearing bar affects the behavior of heavy duty riveted gratings. Results of both large and small panel testing are used to develop an S-N curve for the fatigue life estimation of riveted gratings.

5.2 Large panel test results

Test 1 involved mid span loading of a 37R5 lite panel with a stringer spacing of 49in. The panel was loaded to 2million cycles at mid span (37R5-A1) with a maximum load of 42.6kips and a minimum of 1000lbs. Maximum strains in the negative region over the central support were about 550 micro- strain. There were no signs of fatigue damage to the panels. No cracks were observed in the panel after loading.

Test 2, which involved edge loading of the 37R5 lite panel, did not develop any visible cracks or damage after 2 million cycles of repetitive loading with the AASHTO H-20 axle loading with an impact factor of 30%. Based on these results, the magnitude of the load was increased in both Test 1 and 2 by 10kips to investigate the behavior under much elevated stress ranges and are referred to as Test 3 and 4 respectively. Fatigue damage was observed in the 37R5-A1 panel when load was increased in Test 3. There were cracks in the negative region over the central support at about 1.8million cycles of loading. Shear (diagonal tension) cracks emanated from the weld of the attachment plate to the bearing bars around 800,000 cycles. Cracks developed normal to the direction of loading and is believed to be the result of the dishing effect in that direction. In Test 4, initial cracks started at about 450,000 cycles of loading with the development of shear cracks at about 650,000 cycles of loading. Figure 5.3 and 5.4 shows the crack maps for test #3 and #4 respectively.

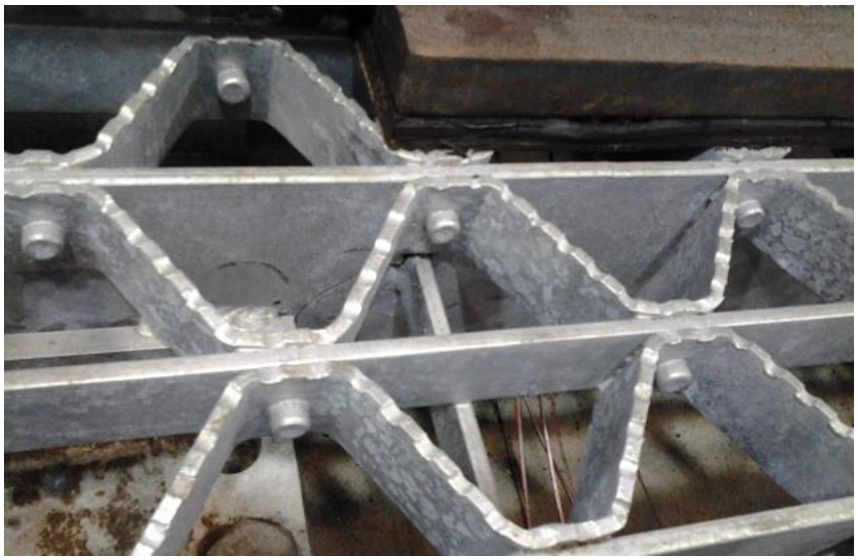

Figure 5.1 - Shear (diagonal tension) cracks at weldment of 37R5-A1 (Test 3)

The span of the panels was increased from 49in to 65in in subsequent tests and resulted in much higher stresses than in previous tests. Test 5 involved loading at the midspan of the 37R5-B1 panel which resulted in the development of an initial crack at about 100,000 cycles. Loading continued till the next crack was observed at about 400,000 cycles. Edge loading of the adjacent span in test 6 resulted in fatigue cracking at about 100,000 cycles, followed by a second crack at about 200,000 cycles in an adjacent bearing bar. Figure 5.5 and 5.6 shows the crack map for Test #5 and #6 respectively.

Figure 5.2 - Tension crack developed at edge of panel during Test 6

In Test 7 which involved loading at the free edge of the sample, failure occurred at about 130,000 cycles with the development of two cracks in the bearing bars supporting the load over the central support. Figure 5.7 shows the crack map for Test #7

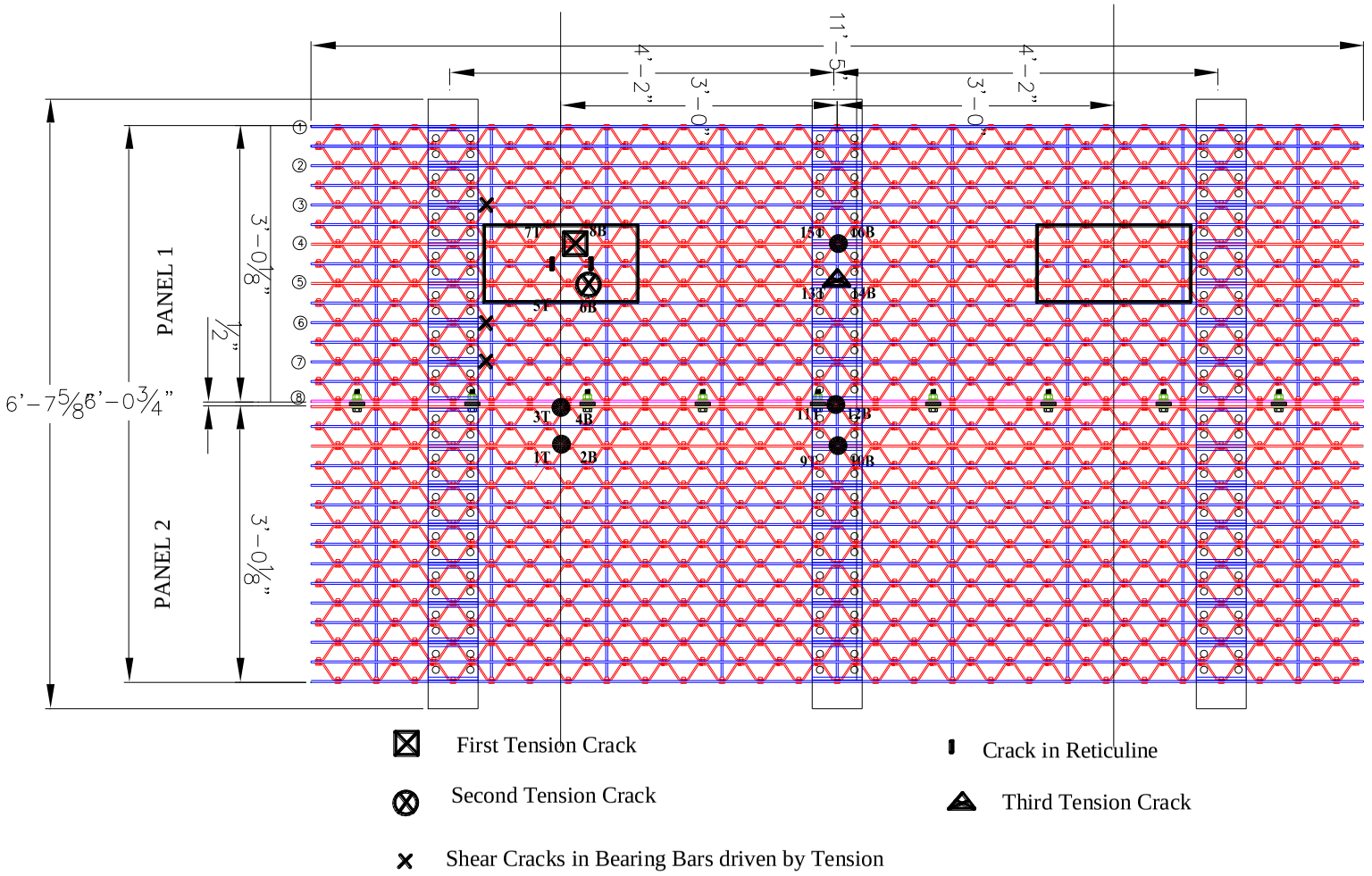

Figure 5.3 - Crack map for Test #3 (midspan loading)

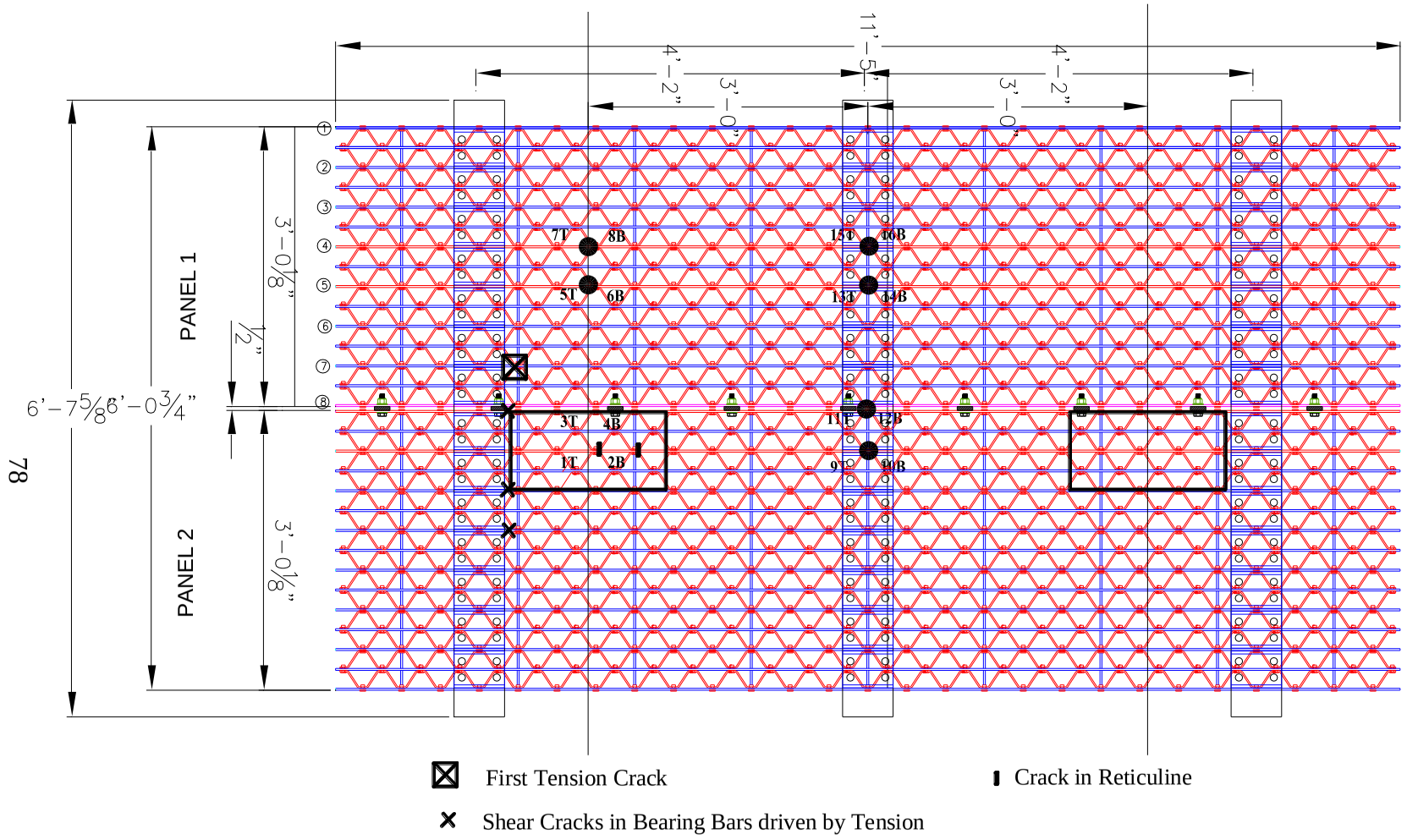

Figure 5.4 - Crack map for Test #4 (edge loading)

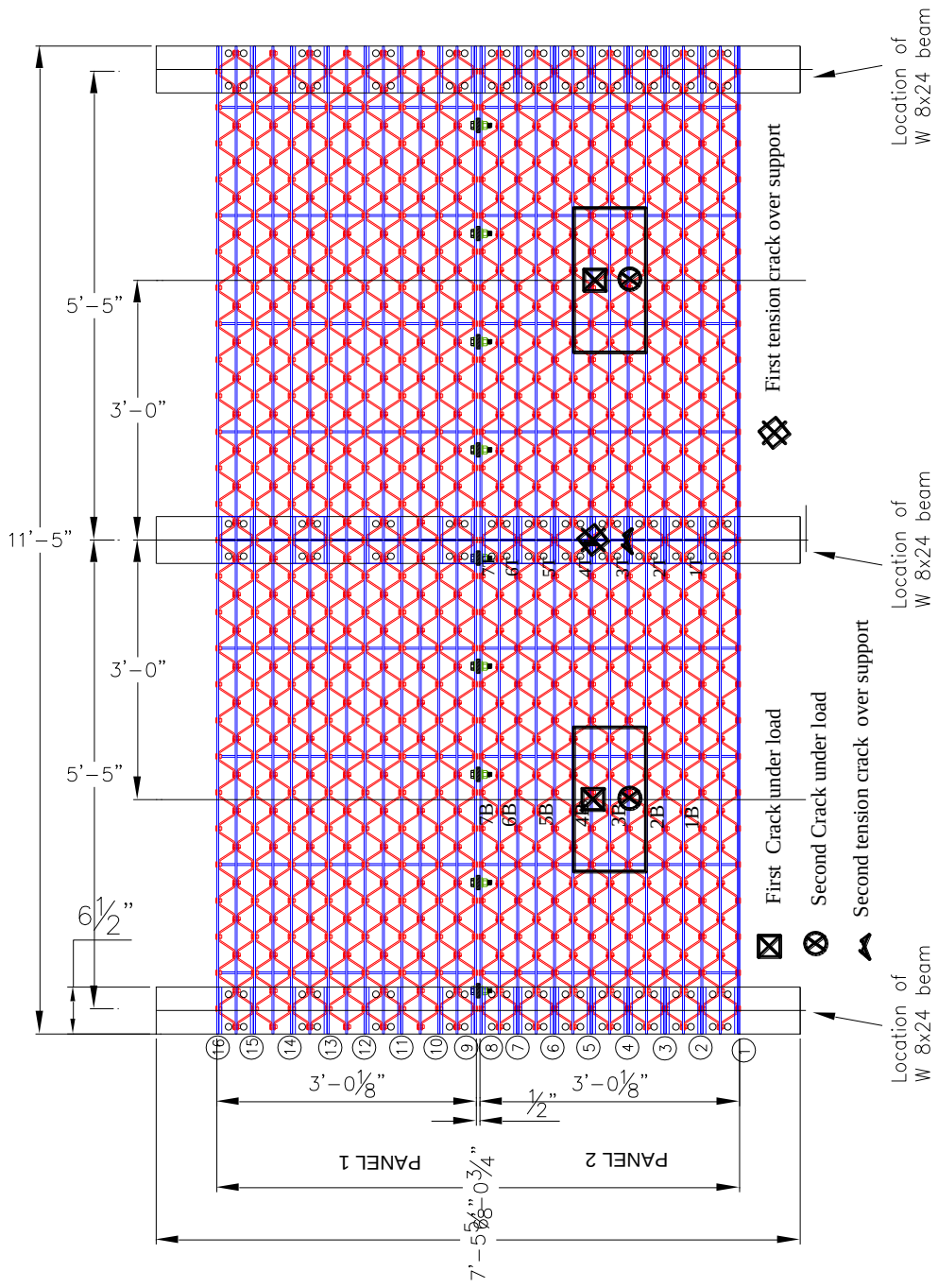

Figure 5.5 - Crack map for Test #5 (midspan loading)

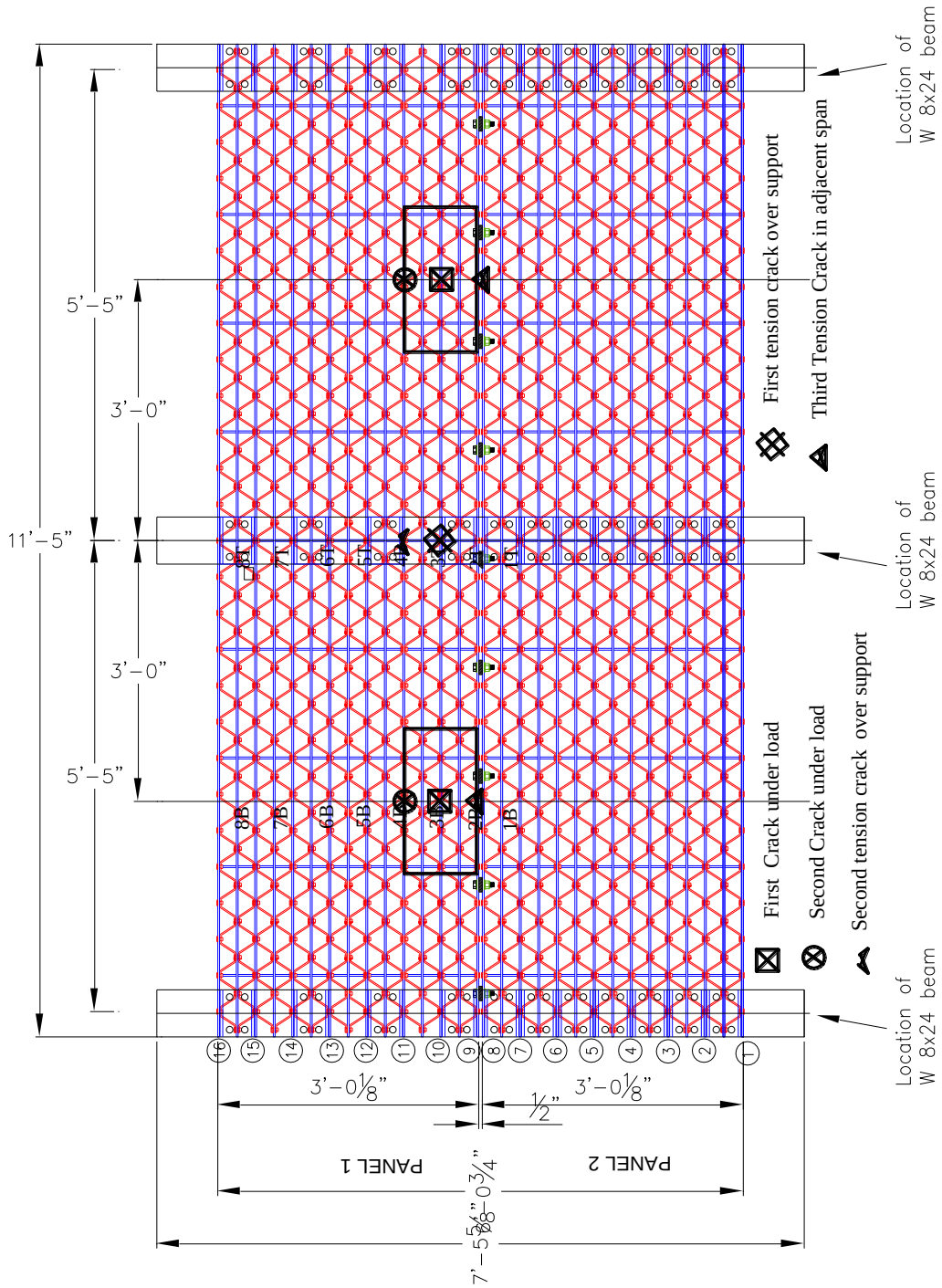

Figure 5.6 - Crack map for Test #6 (edge loading)

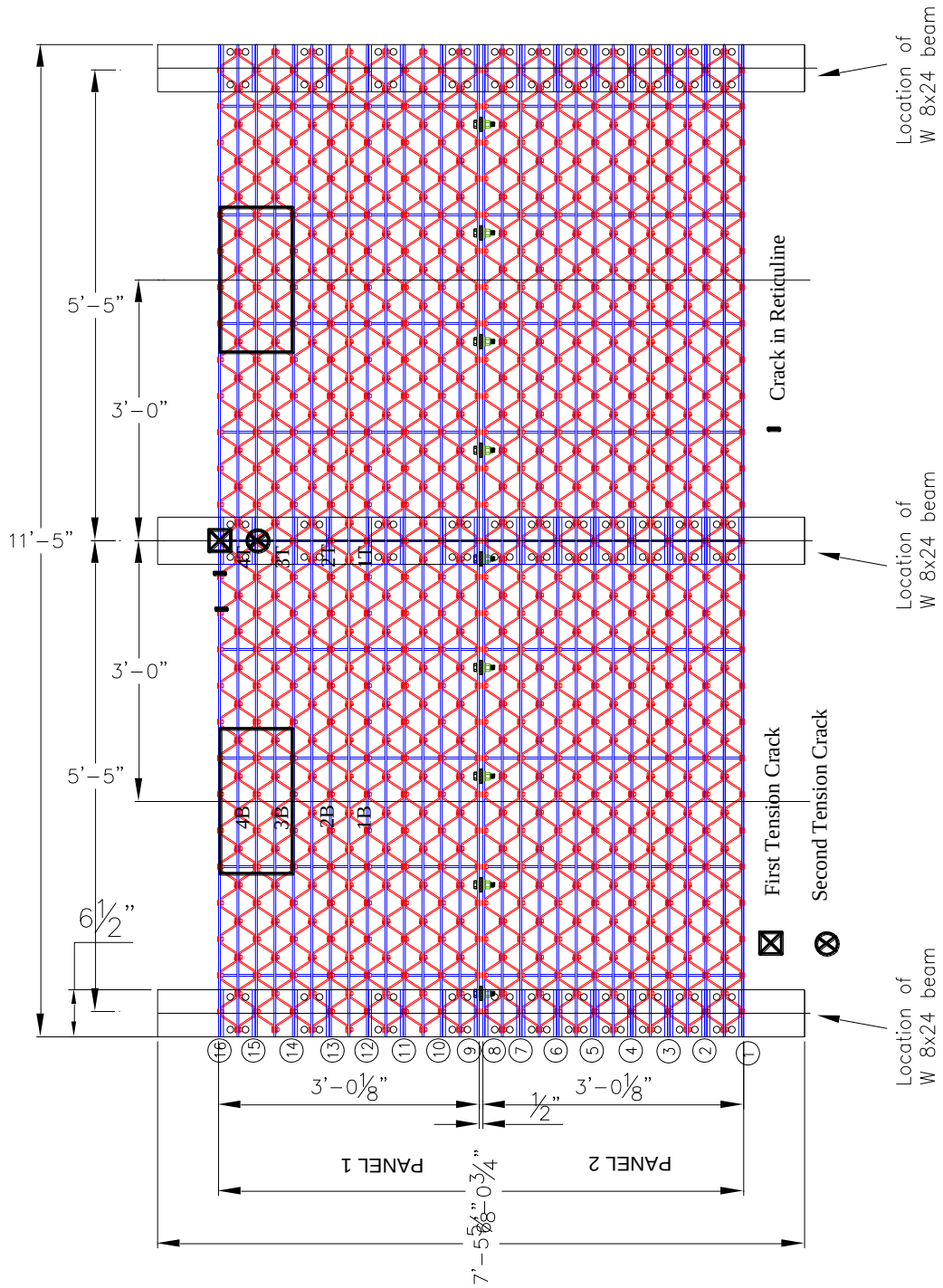

Figure 5.7 - Crack map for Test #7

Test 8 and 9 involved loading on the 37R5 L- series. Mid span loading of the grating was characterized by the development of cracks at the riveted detail in the panel at about 250,000 cycles. There was stable crack growth till the next crack was observed in the adjacent bar at about 400,000 cycles. With the adjacent span loaded at the edge (test 9), the first crack was observed at about 400,000 cycles and then propagated steadily until a second crack formed in an adjacent bar at about 1.2 million cycles. Below is a summary of test results from testing of the large panels. Crack maps are shown in Figure 5.8 and 5.9 for Test #8 and #9 respectively.

Table 5.1 – Summary of fatigue test results for full size panels

Panel (Test #)	Stress Range (ksi)	Number of cycles	Failure Locations
37R5-A1 (T1)	15.2	> 2,000,000	No failure observed
37R5 –A2(T2)	13.2	> 2,000,000	No failure observed
37R5- A1(T3)	34.6	1,060,000	Figure 5.3
37R5-A2 (T4)	32.0	650,000	Figure 5.4
37R5-B1(T5)	32.4	400,000	Figure 5.5
37R5- B2(T6)	33.26	200,000	Figure 5.6
37R5- B2(T7)	36.51	150,000	Figure 5.7
37R5-L1 (T8)	37.5	400,000	Figure 5.8
37R5-L2 (T9)	28.2	1,200,000	Figure 5.9

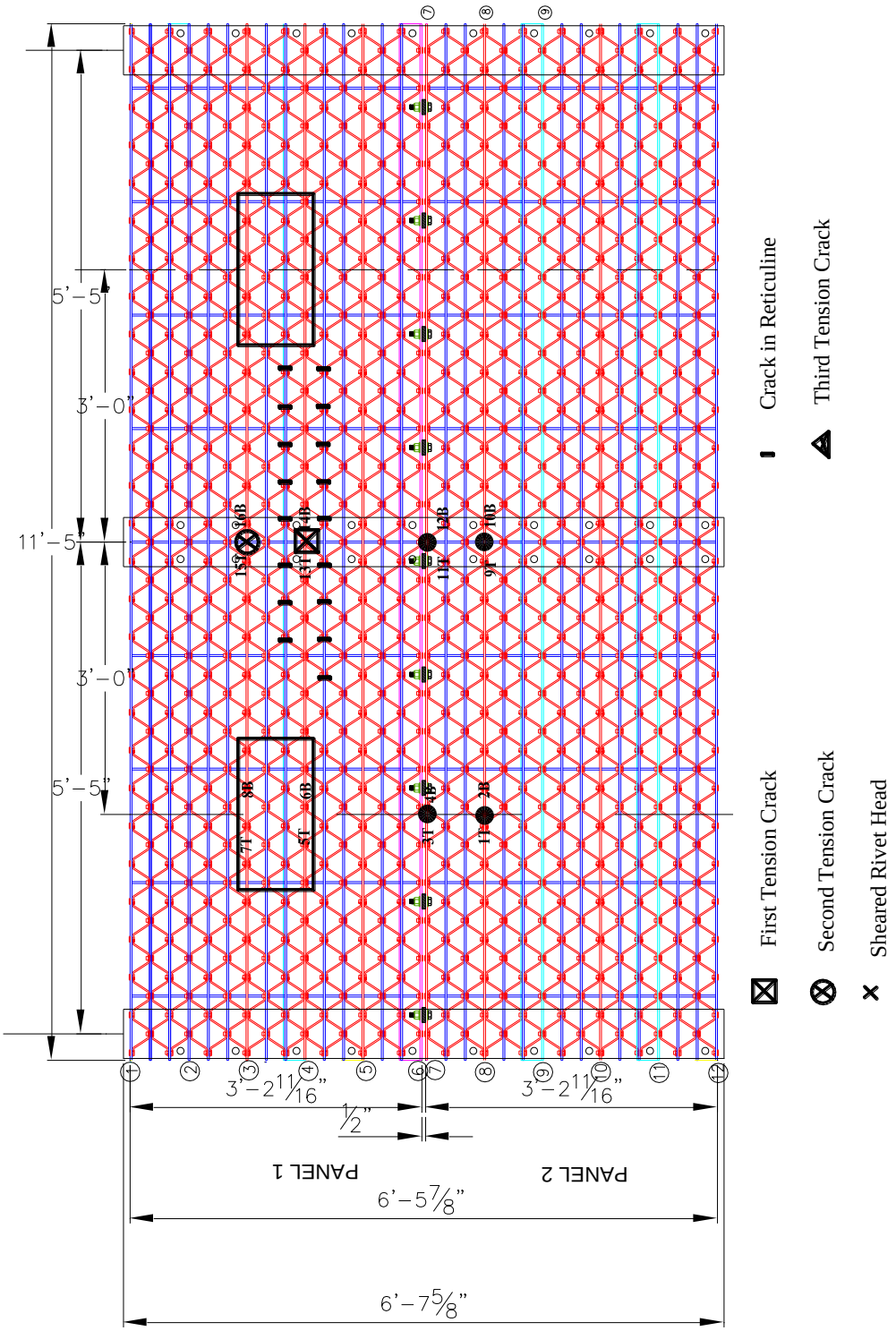

Figure 5.8 - Crack map of the 37R5 L-series for Test #8

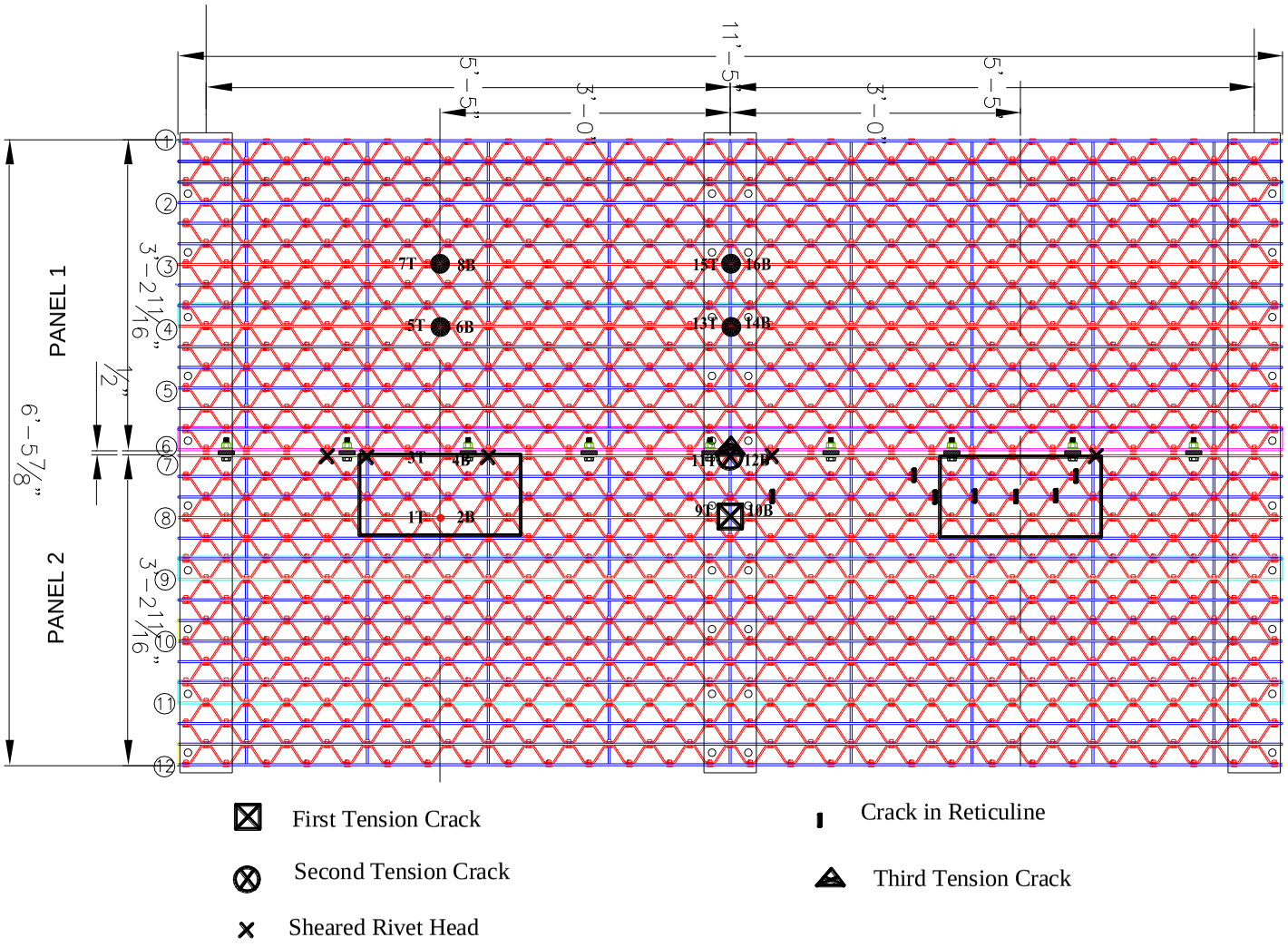

Figure 5.9 - Crack map of the 37R5 L-series for Test #9

No fatigue cracks were observed in both test 1 and 2 at stress ranges of 15.2ksi and 13.2ksi respectively after 2 million cycles of loading. . An increase in load did not result in a linear increase in the magnitude of the stresses after 2 million cycles of loading, with the grating exhibiting non-linear behavior since microstructural damage might have occurred but not have led to the development of a crack. A 10kip increase in the maximum load to 52.6kips resulted in stress ranges of 34.6ksi and 32ksi fort test 3 and 4 respectively. Loading at the new stress ranges developed cracks in the panels during test 3 and test 4 under 2million cycles. Conservative estimates of the fatigue life is determined considering damage caused by previous and current test on the panels. By cumulative damage, an equivalent stress range is calculated for the respective cases using equation (5-1).

$$S_{re} = \left[\sum_i \gamma_i S_{ri}^3 \right]^{1/3} \qquad (5\text{-}1)$$

Where S_{re} is the equivalent stress range,

γ_i is the fraction that any particular portion of the stress range

S_{ri} is of the total number of cycles

Table 5.2 Equivalent stress range for 37R5 Lite panel A1

Panel	Equivalent Stress range	Number of cycles to failure
37R5-A1	25.6	>3,060,000
37R5-A2	21.5	>2,650,000

Results from the fatigue testing of the large panels are plotted together in figure 5.10 with the detail categories A, B and C of the AASHTO S-N curves in the bridge specifications.

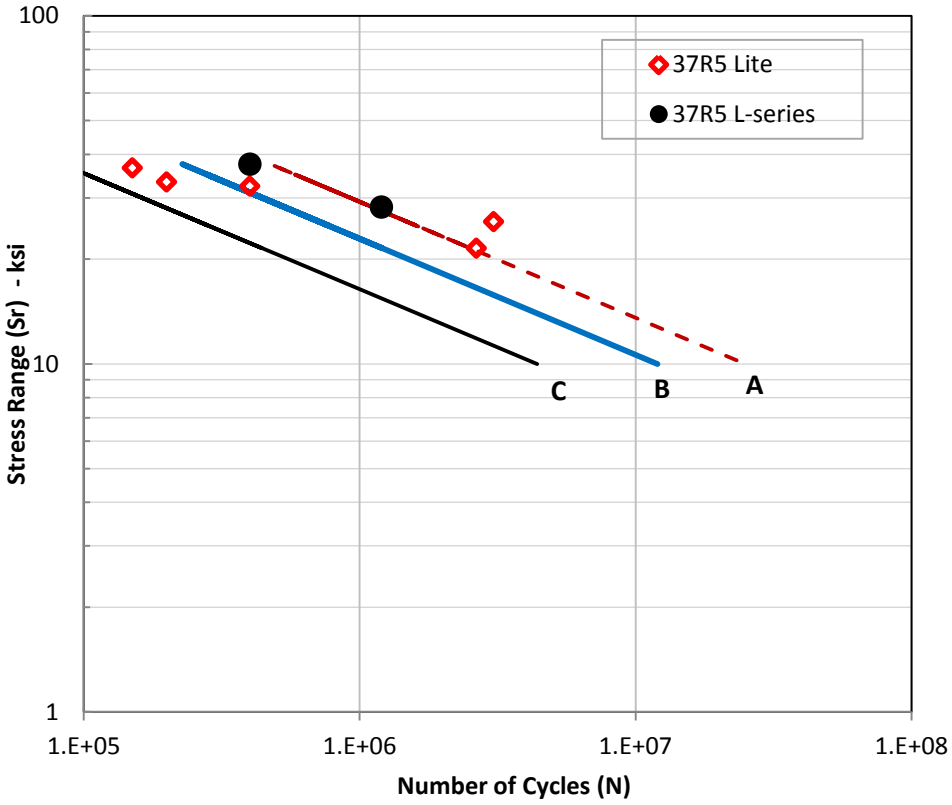

Figure 5.10 – Laboratory results for large panels of the heavy duty riveted gratings

5.3 Smaller panel results

Results from the fatigue loading of the smaller samples made of different types of the 37R5 Lite or 37R5-L-series panels are presented. Fatigue testing of the various samples occurred at stress ranges of 25ksi, 30ksi and 35ksi for all panels. Samples A and F which are representative of one of each type of the 37R5 lite and L-series panels were further

tested at a stress range of 20ksi. Fatigue failures occurred when cracks had developed in the samples during different stages of loading as shown in figure 5.11.

Figure 5.11 – 37R5 Lite Small Panel with fatigue cracks

Results from large panel testing showed that no fatigue failures at the negative moment region were expected in the panels tested at a stress range of 15ksi. When sample A which is a 37R5 lite panel was tested under a stress range of 20ksi, no fatigue damage was observed after 2 million cycles of loading but sample F developed cracks at about 1.1million cycles. A total of 26 samples were tested and the results are plotted in Figure 5.12

Table 5.3 – Summary of fatigue test data for smaller samples

S_r	N	Sample A	Sample B	Sample C	Sample D	Sample E	Sample F
20	N_{20}	> 2000000	x	x	x	x	1102968
25	N_{25}	524000	713031	588450	496584	783673	468225
30	N_{30}	345200	342737	360073	443051	662900	343327
30	N_{30}	323000	263000	256996	263409		254753
35	N_{35}	257200	475300	216348	258500	420534	217865
35	N_{35}	x	x	x	x	263300	x

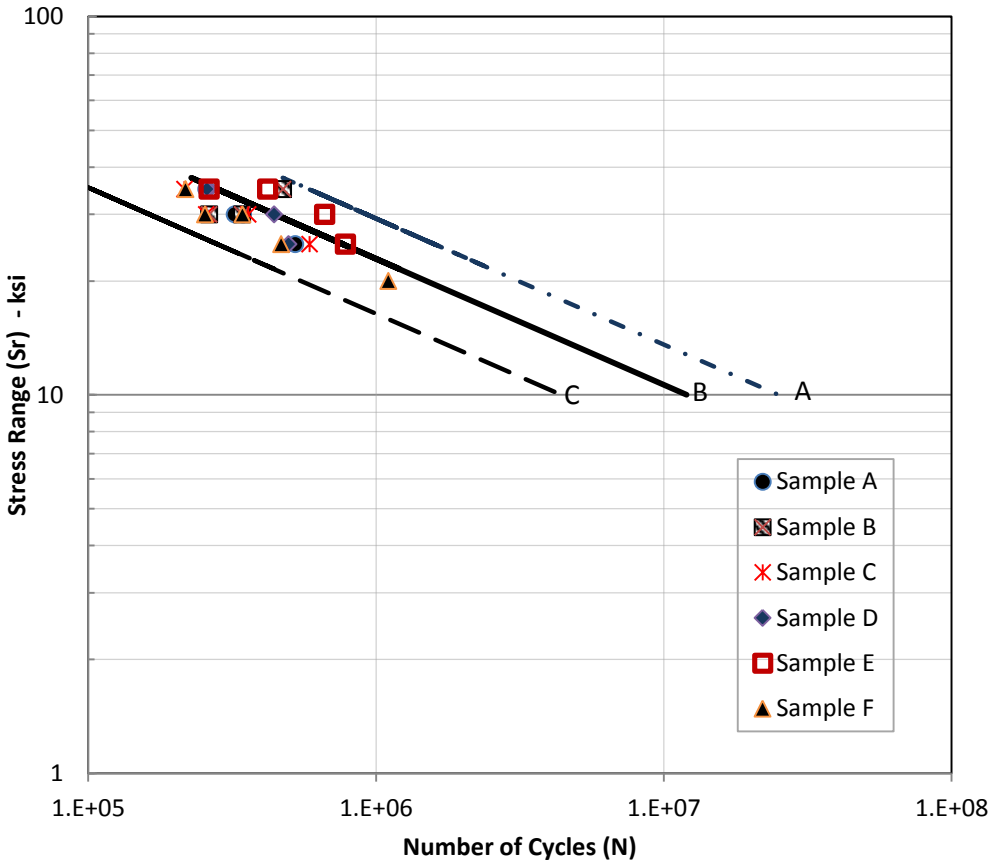

Figure 5.12 – Laboratory results for smaller samples of the heavy duty riveted grating.

5.4 Discussion of Results

After 2 million cycles of loading in test 1 and 2, the 37R5 lite panels did not develop any cracks or show signs of fatigue damage. Maximum negative bending stresses were recorded directly under the load but the section below the neutral axis was only base metal with no structural details or attachment behaving more like a category A detail. With a stress range of about 35ksi, lower bound fatigue life prediction for a Category A is about 600,000 cycles making the heavy duty riveted gratings perform better than predicted. The critical detail for the heavy duty riveted grating occurs in the tension region over the central supports with the riveted detail. The stress range at those positions was in the order of 15ksi and 13.2ksi respectively with no sign of fatigue damage. This is a result of the stress range being under the constant amplitude fatigue limit. In order to investigate the constant amplitude fatigue limit for the gratings, further testing involving smaller panels of the 37R5 lite and the 37R5 L-series was performed. At 20ksi and after 2.3 million cycles of loading, the 37R5 lite sample did not show any signs of fatigue failure but the 37R5 L-series failed at about 1.1 million cycles. It can therefore be inferred that the constant amplitude fatigue limit of the heavy duty riveted grating is between 15ksi and 20ksi. With the spread of the fatigue data around the category B line, a conservative value of the constant amplitude fatigue limit of a Category C', which is 12ksi, can nominally be adopted in the design of the heavy duty riveted grating for fatigue.

When the magnitude of the load was increased by 10 kips in Test 3 and 4, resulting stresses increased at the critical details to about 34.6ksi and 32ksi respectively

resulting in the development of cracks. An equivalent stress range therefore was used to represent the behavior of the panels based on the Miner's cumulative damage approach. An increase in the stringer spacing from 49in to 65in resulted in a corresponding increase in the stress range in the critical detail region for Test 5 and 6. Cracks developed at various stages of loading and there was considerable fatigue damage before 2 million cycles. A similar behavior was observed in the case of Test 7 at the free edge.

Considering the fatigue behavior of the 37R5 L-series, predicted fatigue life for a category E detail at the tested stress range would be about 25,000 cycles. Actual cracks were observed at the riveted detail in the panel with a much higher stress at about 200,000 cycles making the detail behave more like a category C. The assumption for fatigue life estimation of this heavy duty riveted gratings as a Category E detail will therefore be overly conservative. Visible cracks developed in the 37R5 L-series panel during testing at about 200,000 cycles with stable propagation until 400,000 cycles, when a second crack was detected. The redistribution of stress was clearly seen based on the subsequent areas of damage within the grates. There was cracking of the reticuline bars spreading from the areas of the critical detail towards the load positions around the midspan. Much of the stress was transmitted to the reticuline bars and rivets along the span of the bearing bars.

The effect of loading on one panel with respect to adjacent panels was captured through the edge loading of the 37R5 panel in Test 4 and Test 6. Cracks initiated beneath the supporting bearing bars and then propagated to a dominant size before the next crack was seen in the adjacent panel. After failure had occurred in the sample based on the

failure criteria, the sample was loaded to 2million cycles to investigate the extent of damage in the panel. After stable crack propagation and the subsequent loading of the 37R5 L- series panels to 2 million cycles under edge loading, a significant amount of structural damage occurred. This included yielding of the bearing angles and reticuline bars and failure of some of the rivets. This clearly demonstrated how an increased stress range affected the fatigue behavior of the panel after the main load carrying members had yielded. For consistency, the same level of maximum strain was chosen for all cases with variations in the minimum strain for a desired stress range during small panel testing. This confirmed that stress range is the key factor to consider in crack propagation and not the magnitude of maximum stress. Results from testing of the smaller size panels were consistent with findings from actual panel testing.

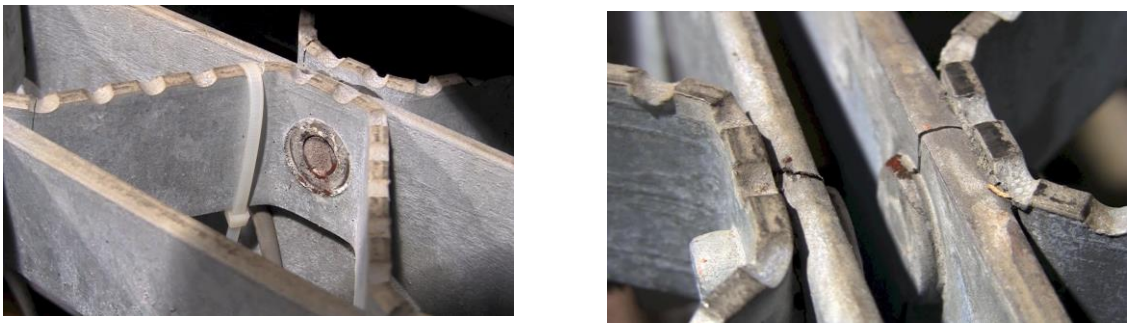

Figure 5.13 – Fatigue failure of components of the 37R5 L-series at 2 million cycles

5.5 Proposed S-N curve for heavy duty riveted gratings

In determining the fatigue life of the heavy duty riveted gratings, initiation is said to have occurred and thus, the fatigue life is based on the fatigue crack propagation properties and then the time to fracture. Typical S-N curves relate the behavior of a

component at an allowable stress to the number of cycles needed to cause failure under fatigue loading. The complicated stress patterns of the heavy duty riveted gratings due to the assemblies of the components make analytical prediction of the fatigue life challenging. Empirical relationships based on experimental data will therefore provide a good basis for the determination of the fatigue life. Laboratory work involved 9 tests on 6 full size panels and 26 smaller samples of two types of the heavy duty riveted gratings. The pattern of failures was localized around the areas of loading and in the negative moment regions over the midspan supports. When samples were tested under low stress ranges, no fatigue damage occurred. Figure 5.14 shows laboratory fatigue data plotted with S-N curves from the AASHTO bridge manuals for both full and smaller size panels

The fatigue design requirements of the AASHTO LRFD manuals do not assign a design category for heavy duty riveted gratings. Laboratory data from this research is been used as the basis in the establishment of an S-N curve for heavy duty riveted gratings. The current S-N curves used in design manuals were based on a best fit line through regression analysis of fatigue data. Results of both full and smaller size panel testing of the 37R5 Lite and 37R5 L-series were used to establish a relationship between stress range and the number of cycles to failure of a heavy duty riveted grating. A log-log transformation of test data represents a normal distribution of test data and establishes the relationship between number of cycles to failure, N and stress range, Sr as

$$\log N = \log A - B \log S_r \qquad (5\text{-}2)$$

Where Log A is the log-N axis intercept and B is the slope. Values of B range from 3.07 to 3.37 though a value of 3 has been adopted in design manuals.

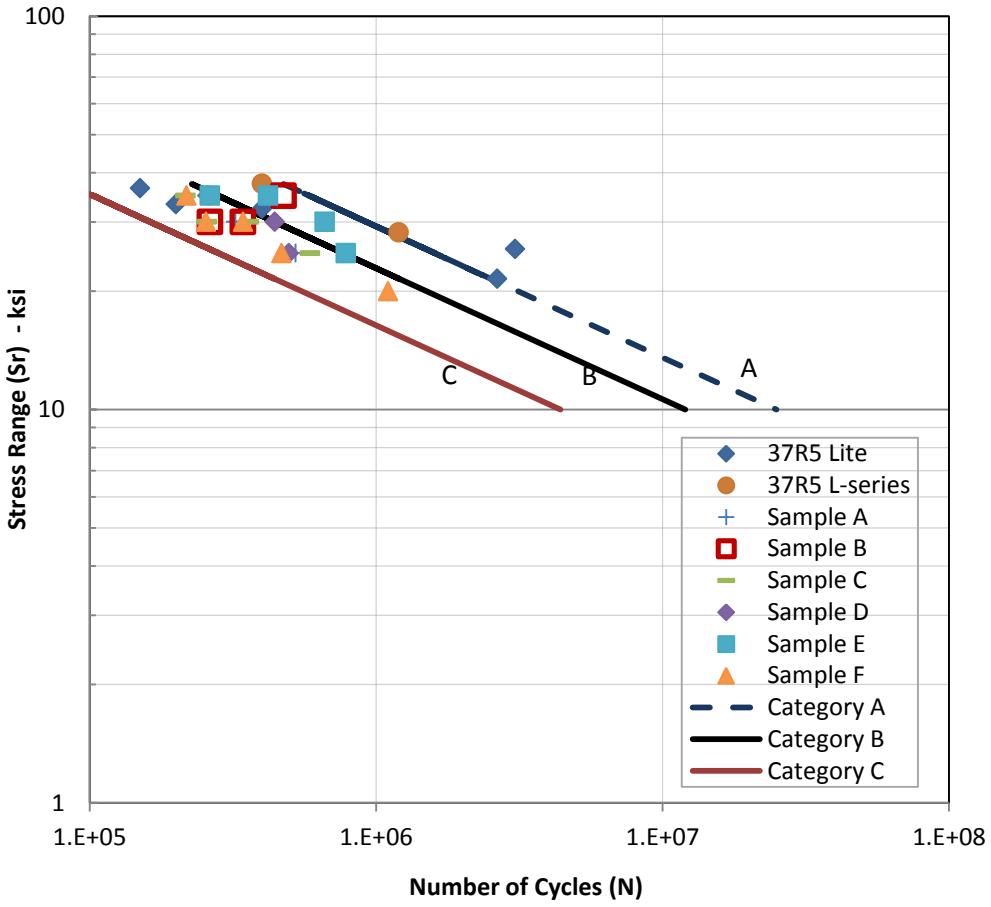

Figure 5.14 – Laboratory data of the heavy duty riveted gratings with AASHTO curves

Based on a regression analysis of fatigue data of the heavy duty riveted grating, the equation 5-3 was obtained as the equation of the line of best fit.

$$\log N = 10.301 - 3.164 \log S_r \qquad (5\text{-}3)$$

When the slope is transformed to 3.0 in order to compare test data with the fatigue requirements of the AASHTO manual, the mean line is given by equation 5-4.

$$\log N = 10.02 - 3 \log S_r \qquad (5\text{-}4)$$

Figure 5.15 shows a graph of the line of best fit, with the line of the transformed equation. A lower bound design curve was obtained from the mean curve by shifting the curve 2 standard deviations, sd, down the Log N axis as shown in equation 5-5

$$\text{Log } A_{\text{lower bound}} = \text{log}A_{\text{mean}} - 2\text{sd} \qquad (5\text{-}5)$$

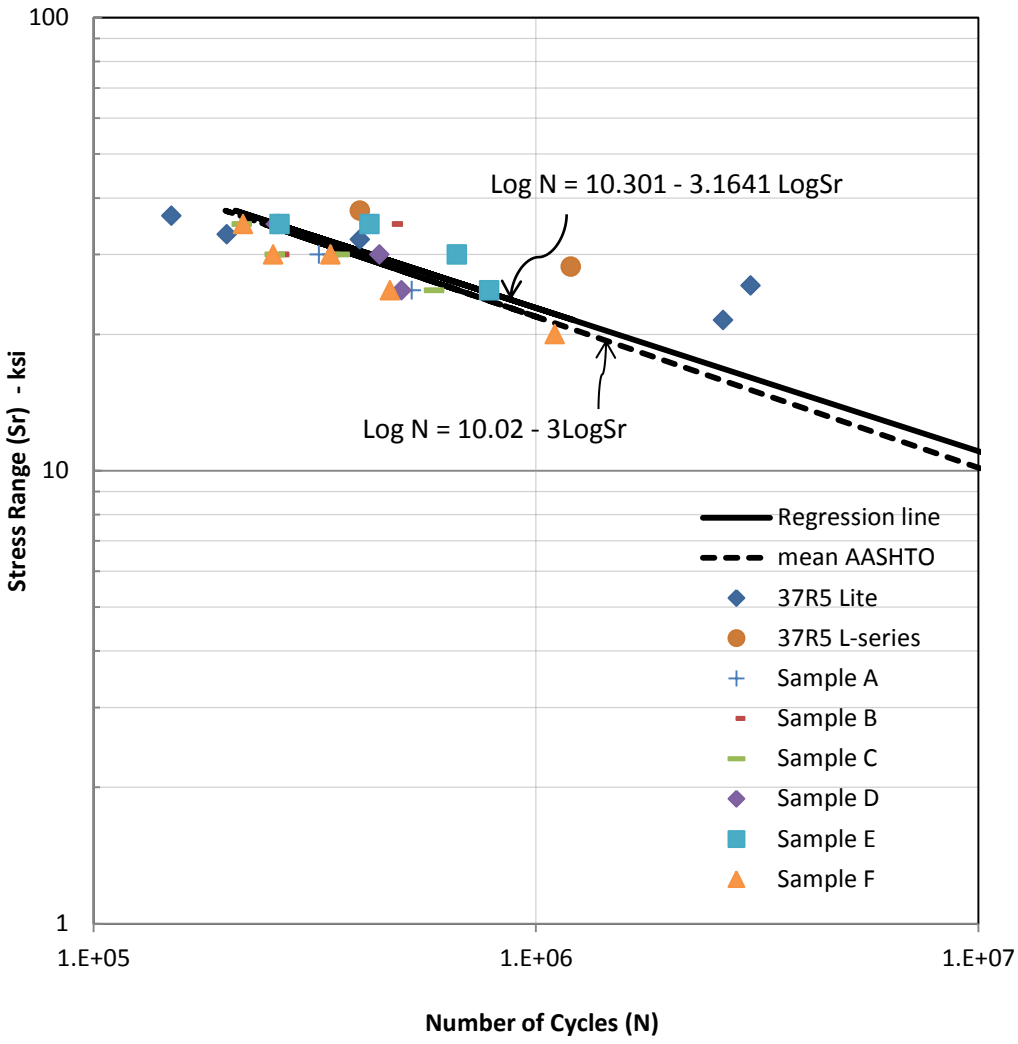

Figure 5.15- Regression analysis of laboratory data for heavy duty riveted gratings

Regression analysis data from the laboratory test is compared with that used in the establishment of the current AASHTO design curves as shown in Table 5.3. AASHTO curves used a shift of 1.96 of standard deviation for a 95% confidence level

Table 5.4 – Comparison of regression analysis coefficients with AASHTO

Category/ Detail	Slope, B	Intercept, (mean)	Standard Deviation	Intercept (lower)
A	3.178	11.121	0.221	10.688
B	3.372	10.870	0.147	10.582
C	3.25	10.038	0.063	9.915
D	3.071	9.664	0.108	9.453
Riveted Grating	3.1	10.301	0.302	9.697

The equation of the lower bound which is the design curve for a 97.5% survival of fatigue test data of heavy duty riveted gratings is given as:

$$\text{Log } N = 9.416 - 3\log Sr \qquad (5\text{-}6)$$

When compared with the AASHTO design category curve, it is in close proximity to a category D detail. However, experimental results show that a constant amplitude fatigue limit of a category D detail, which is 7ksi when used in the design of heavy duty riveted gratings, will be overly conservative. Mean value of the test data is close to a category B with the constant amplitude fatigue limit of the heavy duty riveted grating behaving like a category B. No fatigue failures occurred for samples tested at stress ranges of both

13.2ksi and 15.2ksi. A reasonable estimate for the constant amplitude fatigue limit is therefore chosen as 12ksi (category C') which occurs between C and D.

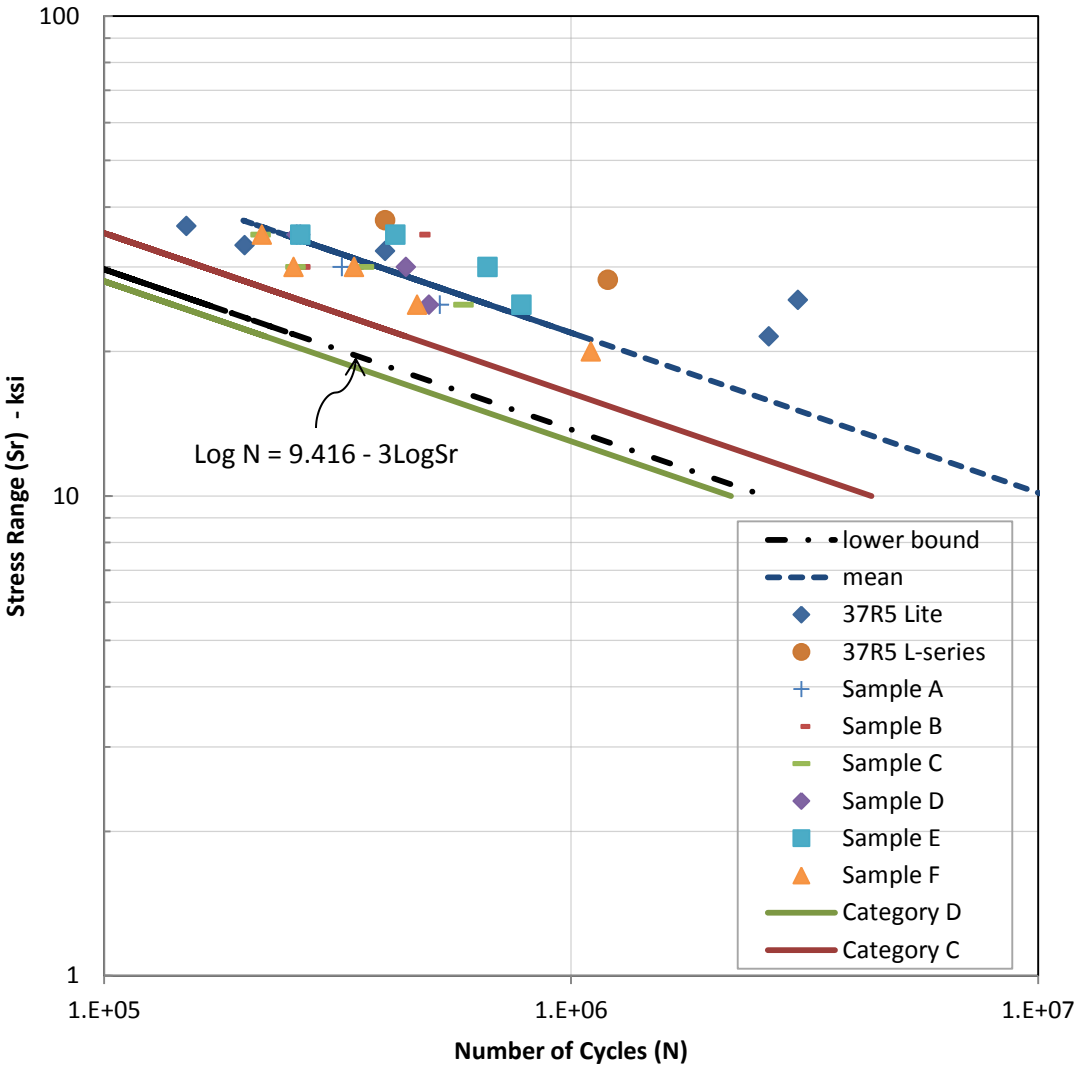

Figure 5.16 – Graph of lower bound curve for heavy duty riveted gratings

5.6 Fatigue Design Criteria

The results of the fatigue data are applicable to all forms of the 37R5 heavy duty riveted gratings. For finite fatigue life predictions, the category D design curve of the AASHTO LRFD manual is recommended. The mean values of the test data fits the category B data reasonably well and thus a constant amplitude fatigue limit of 12ksi which is between that of category B and C' is adopted. The fatigue design equation for a heavy duty riveted steel grating is given equation 5-7 and a summary of the fatigue design is shown in figure 5.17.

$$N = 2.6 \times 10^{9} S_r^{-3} \qquad (5\text{-}7)$$

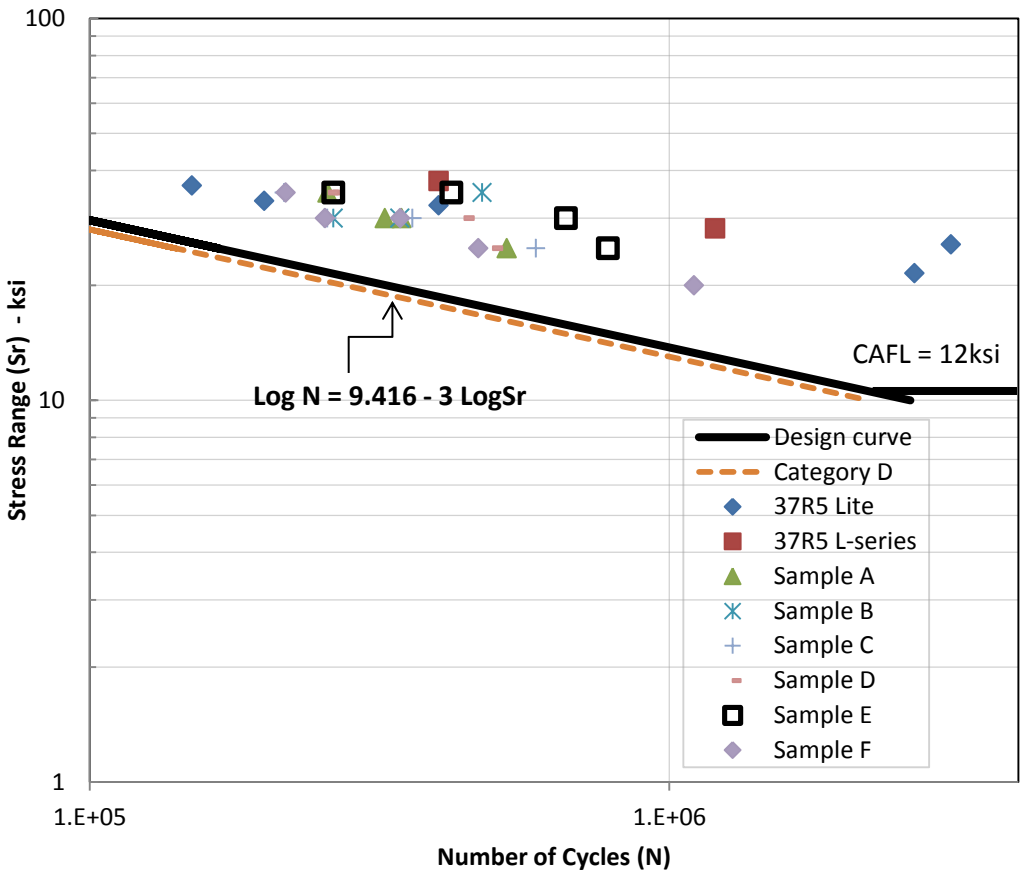

Figure 5.17- Fatigue Design criteria for heavy duty riveted gratings

CHAPTER VI

FATIGUE BEHAVIOR PREDICTION USING FRACTURE MECHANICS

6.1 Overview

Fatigue cracking of gratings occurs as a result of the repeated application of stresses on load carrying members. Riveted gratings occur as an assemblage of sub-components riveted to bearing bars. The presence of these subcomponents and how they are connected to the main bearing bars affects the overall fatigue life. The severity of the presence of a crack depends on a number of factors not limited to the:

i. The type of sub-component in the grating

ii. Location of the crack

iii. Effect of bending stresses which dictate the stress range due to applied loads

iv. Presence of stress raisers

When a remote stress is applied after a crack develops, the crack opens and the amount of stress that has to be supported is carried by the uncracked section. The crack tip represents a severe stress concentration. The collective process of crack opening and the cyclic plastic straining of the material around the crack tip is the fundamental mechanism that further drives developed cracks. A fracture mechanics approach has been used to predict the fatigue life of heavy duty riveted steel gratings by considering two failure

patterns of bearing bars of the 37R5 lite panel during fatigue testing of the riveted grating.

6.2 Fracture Mechanics approach

The total fatigue life of a structure is made up of the time for crack initiation, propagation and then fracture. Crack initiation is characterized by the formation of micro cracks merging to form small cracks. During crack propagation, the effect of the stress range in the vicinity of the small cracks drives it into a dominant size. Most structures contain pre-existing discontinuities either in the material or in the geometry that limits the crack initiation period. Flaws occur due to manufacturing and fabrication processes. The discontinuities act as points of stress concentration and the stresses can be estimated if they have well defined geometries. In the case of very small sharp cracks, the use of the stress concentration approach becomes meaningless and thus the concept of fracture mechanics is applied. The number of defects and how the behavior of the structure is affected is also dictated by the physical size. Larger volumes of material or components contain more defects than smaller ones.

Fracture mechanics is used in evaluating the strength of a component or structure in the presence of a crack or flaw. It is used in structural design to determine an acceptable stress level and defect size based on material properties for specific conditions under repetitive loads. During the fatigue process, where material conditions are primarily linearly elastic, linear elastic fracture mechanics (LEFM) concepts are applied. LEFM is an analytical procedure which relates the stress field magnitude and

distribution in the vicinity of the crack tip, that is, the nominal stress applied to a test specimen, the size, shape and orientation of a crack or crack-like discontinuity.

The predominant principle is to have the nature of the stress field ahead of the crack to be characterized by the stress intensity factor, K. The stress intensity factor relates the nominal stress level and the size of the crack, a. The local deformation of cracks occurs in three modes based on the relative movement of the two cracked surfaces.

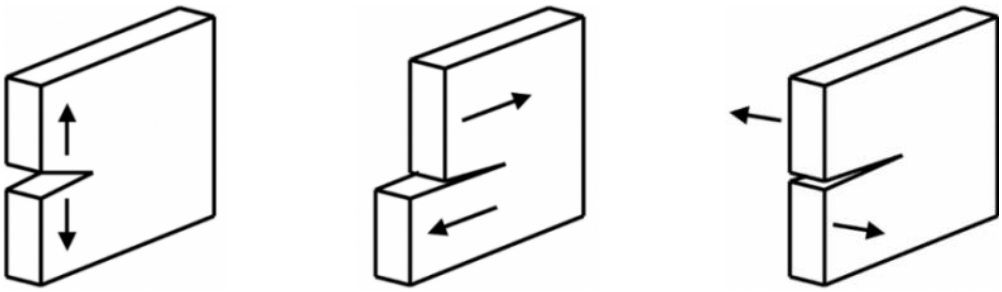

I (Tension) **II** (Shear) **III** (Torsion)

Figure 6.1 - Modes of local deformation (a) Mode I (b) Mode II (c) Mode III

The stress intensity factor has different values for each mode but most cracks that develop in structures occur as Mode I or a combination of Mode I and another mode. The general form of the stress intensity factor is given by equation 6-1

$$k = \sigma_{nom} F(g)\sqrt{\pi a} \quad \text{where a = crack length} \tag{6-1}$$

F (g) = F_g. F_e. F_s. F_w – corrections to wide plate solution and depends on the geometry of the particular detail and nature of the crack. F_g is the stress gradient correction factor, Fe is the crack shape correction factor, F_s is the free surface correction factor and F_w is the finite width correction factor. Different values of k have been established and are found

in literature for various geometries and modes of loading. The stress intensity factor can be modified and applied towards predicting fatigue life by writing the change in the remote stress for repeated loading as equation (6-3)

Change in the remote stress, $\Delta\sigma_{nom} = \sigma_{max} - \sigma_{min}$ (6-2)

Change in stress intensity, $\Delta k = \sigma_{nom} F(g)\sqrt{\pi a}$ (6-3)

6.3 Crack initiation and Propagation as applied to gratings

A critical consideration made during the design of structural components is to accept that some level of cracks or discontinuities already exist in the sample. Of importance is the need to investigate the length of time it takes a crack to grow from an initial size to a permissible dominant size. This is dictated by the initial crack size, a_i, the maximum permissible or critical size, a_{cr} and the crack growth rate between a_i and $a_{cr.}$ The initial crack size, a_i is considered as the minimum size that can be detected using non-destructive inspection techniques. It is often considered as a grain size of the material. The critical length length, a_{cr} is determined if the fracture toughness of the material is known.

As applied to heavy duty riveted gratings, the maximum stress level for unstable crack growth is below the yield and thus linear elastic fracture mechanics is applied. The fatigue crack propagation rate is defined as the crack extension, Δa, during a small number of cycles, ΔN. Three stages are involved in the crack growth process namely the fatigue crack initiation, propagation and fracture. The process involved in the formation of the first crack is preceded by the movement of dislocations within the material leading

to the formation of intrusions and extrusions. The presence of inclusions acts as relative sites for crack initiation with increased stresses. Geometrical discontinuities in a structure increase the magnitude of the nominal stress intensity in its vicinity, and significantly reduce the crack initiation period. When a material is cyclically loaded under a lower stress, some level of plastic deformation occurs around the crack tip which can subsequently lead to failure through damage accumulation. The presence of these flaws and how they affect the crack initiation and propagation properties provide basis for a fracture control design.

In the current study, it is considered that initiation of the crack has already occurred and thus the fatigue life is based solely on propagation life. The fatigue crack propagation behavior can be divided into three regions (Figure 6.2). Region I characterize the existence of a fatigue threshold under which cracks do not propagate under cyclic fluctuations. Crack growth in this region is mainly controlled by microstructure, mean stress and environmental factors. Region II (Paris region) represents the behavior after the fatigue threshold stress intensity and shows the relation between the crack growth rate and stress intensity factor. There is stable macroscopic crack growth with less effect from microstructure and mean stress. Region III has very high crack growth rates and is controlled by the fracture toughness of the material. The fracture mechanics approach provides a method where the approximate number of cycles to failure can be estimated in the Paris region as shown in Region II. The form of a commonly used relationship was suggested by Paris and Erdogan as equation (6-4)

$$\frac{da}{dN} = C\left(\Delta k\right)^m \tag{6-4}$$

a = length of the crack

N= number of cycles to failure

ΔK = stress intensity factor range

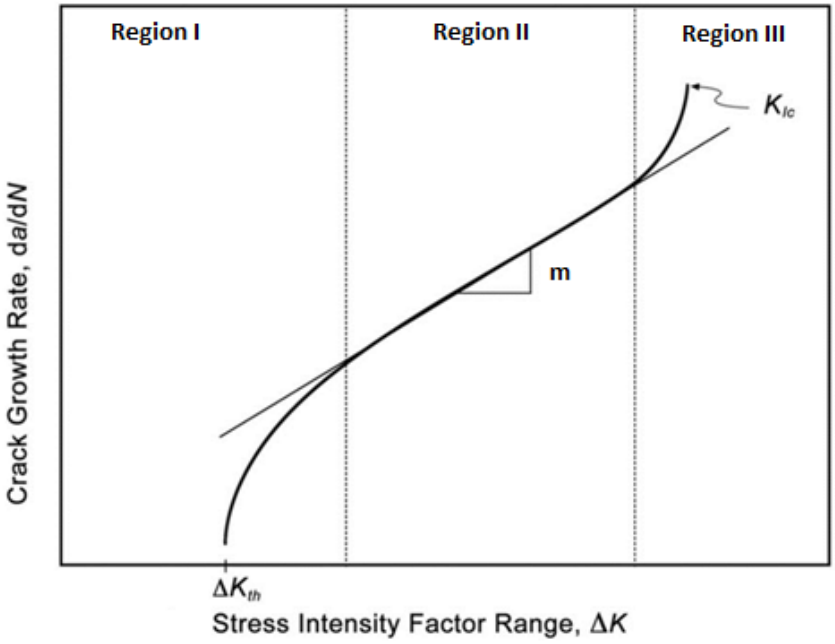

Figure 6.2 - Crack growth rate vs stress intensity factor.

C and m are constants with m determined by regression analysis of experimental data. The fatigue life, N can be estimated from the Paris relation if all the other parameters are known through integration as:

$$N = \frac{1}{C}\int_{a_i}^{a_f} \frac{1}{(\Delta k)^m} da \qquad (6\text{-}5)$$

Where a_i and a_f represents initial crack size and the critical crack length respectively

A crack growth rate relation proposed by Barsom and Rolfe (1999) for the ferrite-pearlite steel will be used in the prediction of fatigue. The expression is given equation (6-6)

$$\frac{da}{dN} = 3.6 \times 10^{-10} \Delta K^3 \quad \text{in/cycle} \qquad (6\text{-}6)$$

Fracture mechanics can be used in structural design to determine acceptable stress levels, defect sizes and material properties for certain working conditions. In estimating the fatigue life of a structure, the designer needs information about the type of structure, overall and member dimensions, stress fluctuations, potential crack growth locations in the structure and the material properties which affect crack growth. It is also affected by the type of loading, specimen size, shape and surface roughness, the load waveform and the presence of chemically active agents. Fatigue testing of specimens under similar conditions can produce different results due to the varied distribution of material microstructural properties, initial defect conditions, etc.

6.4 Design philosophies

A number of design philosophies exist for the fatigue design of structures. The criteria of unlimited safety are aimed at design for infinite fatigue life and local stresses and strains occur below the fatigue limit. This leads to structures which are not always economical and in some cases, impractical. Safe life design principles involve designing for a finite life with a margin of safety for scatter of fatigue data and other unknown factors. It finds usage in a number of applications in the automotive and aerospace industries. The Fail safe design approach allows for failure in an area which should be localized and must not lead to the failure of the system. Some acceptable level of cracking is allowed but should

be so distributed that no failure occurs before detection and repair. The damage tolerant design approach is a refinement of the fail safe approach and assumes that cracks do exist due to processes in fabrication, manufacturing or fatigue and uses fracture mechanics principles and tests to check whether such cracks will grow large enough to produce failures before they are detected by periodic inspection.

6.5 Fatigue Life Estimation methods

During estimation of the fatigue life of structures, different methods are exists. In specific cases one or a combination of any of the methods are employed

1. The nominal stress life (S-N) method involves the use of already established S-N curve of materials for notched and unmatched samples. Corrections are made for specific cases of loading and environment.
2. The local strain life (ε-N) method is usually applied in cases of low cycle fatigue. The local strain at a notch is related to smooth specimen strain- controlled fatigue behavior.
3. Fatigue crack growth (da/dN - ΔK) method requires fracture mechanics to obtain the number of cycles to grow a crack from a given length to another length and to fracture

6.6 Fracture mechanics of Riveted Gratings

Experimental testing of the samples resulted in the formation and propagation of cracks under fatigue loading. Failure is said to have occurred if a second crack developed in an adjacent main bearing bar from the first crack. It was observed that heavy duty riveted steel gratings had enough residual strength after the development of the first crack till the second crack formed. The panels were still able to support loads even after several localized failures had occurred. This indicates the level of redundancy in heavy duty riveted gratings and is thus classified as structurally redundant. A fracture control plan for heavy duty riveted gratings involves a damage tolerant approach where a crack is initially considered to be present and is allowed to propagate to a critical size before detection and subsequent repair.

6.6.1 Description of Test Sample

The sample considered for the evaluation of the fatigue life using LEFM was tested at the Gas Turbine Facility of the University of Akron. This involved a 37R5 Lite heavy duty riveted grating panel described in the experimental set-up as sample A. It has three bearing bars and a number of reticuline bars riveted at 5in centers. Stress ranges of 20ksi, 25ksi, 30ksi and 35ksi were applied. Laboratory results from the testing of both full size and smaller size samples resulted in crack formation in

(a) The main bars with holes made for the attachment of the other components with rivets

(b) The main bar sections without holes but with much higher stresses

(c) The reticuline and the intermediate bars after main bars had failed.

The results from the fracture mechanics approach are compared with laboratory data and thus parameters used are calibrated to laboratory data. All section and material properties used in subsequent equations and analysis are based on sample A.

(a) 37R5 Lite (b) 37R5 L-series

Figure 6.3 – Failure of a main bar with hole for rivets in the 37R5 grating

6.6.2 Fracture toughness requirements

The fracture toughness of a material represents the inherent ability of a material to withstand a given stress field intensity at the tip of a crack. Unstable crack growth occurs when the stress field intensity reaches a critical value, K_C. In plane strain conditions and in mode 1 deformation, it is designated as K_{IC}. In order to use fracture mechanics as a basis for a fracture control plan for structural components, K_{IC} or K_C values of the material must be determined at the temperature and loading rate for the intended use. Barsom and Rolfe suggested relationships between K_{IC} and CVN test results on the basis of the results of various investigations. It was established that the relationship between

slow-bend K_{IC} and slow bend CVN test results is the same as the relationship between impact K_{IC} (K_{ID}) and impact CVN. The loading rate for bridges are closer to slow bend loading than to impact loading. Conservative engineering estimates of K_{IC} is predicted using an empirical relation for bridges involving slow loading.

$$K_{IC} = \sqrt{5E(CVN)} \tag{6-7}$$

Where E = elastic modulus

K_{Ic} and CVN are tested at the same temperature and strain rate.

CVN values for the evaluation of the fracture toughness according to the LRFD specifications of the AASHTO is that for mechanically fastened fracture critical connections for A36 steel of thickness less than 4 in, the minimum test value energy is 20ft-lbs. Non-fracture critical connections of thickness less than 4in have a minimum test value of 15ft-lbs

The various details considered in the sample can be described as non-critical since there is an adequate level of redundancy in the structure (in bending). A CVN value of 15ft-lbs has been used in the evaluation of the fracture toughness yielding a value for K_{IC} of $46.6\, ksi\sqrt{in}$. If the plane strain fracture toughness, K_{IC} of the material used for the bearing bars are known, then the critical crack size, a_c can be determined by equation 6-8.

$$a_c = \frac{1}{\pi}\left(\frac{K_{IC}}{f(g)\Delta\sigma}\right)^2 \tag{6-8}$$

Table 6.1 shows critical lengths for the various stress ranges based on a wide plate with an edge crack for a bearing bar of the 37R5 lite

Table 6.1 – Critical crack lengths for various stress ranges for gratings

$S_{r,}$ ksi	15	20	25	30	35
$a_{cr,}$ in	2.45	1.38	0.88	0.61	0.45

6.6.3 Stress Intensity factors for details

The crack growth rate is a function of the stress intensity factor range. Observations based on fatigue testing of the heavy duty riveted gratings lead to the consideration of two failure patterns. Stress intensity factor solutions that are already published in literature which applies to these failure patterns are described below.

(a) Plate with an edge crack in bending

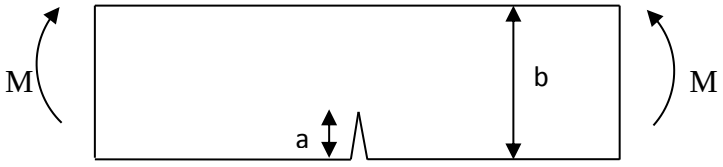

Figure 6.4- plate with an edge crack in bending

$$K_I = \sigma\sqrt{\pi a}F\left(\frac{a}{b}\right) \qquad \sigma = \frac{6M}{b^2}$$

Brown least square fitting method - (Paris, Tada & Irwin, 2000)

Accuracy: 0.2% for a/b

$$F\left(\frac{a}{b}\right) = 1.122 - 1.40\left(\frac{a}{b}\right) + 7.33\left(\frac{a}{b}\right)^2 - 13.08\left(\frac{a}{b}\right)^3 + 14\left(\frac{a}{b}\right)^4$$

(b) Plate with cracks emanating from a notch - (Barsom & Rolfe, 1999)

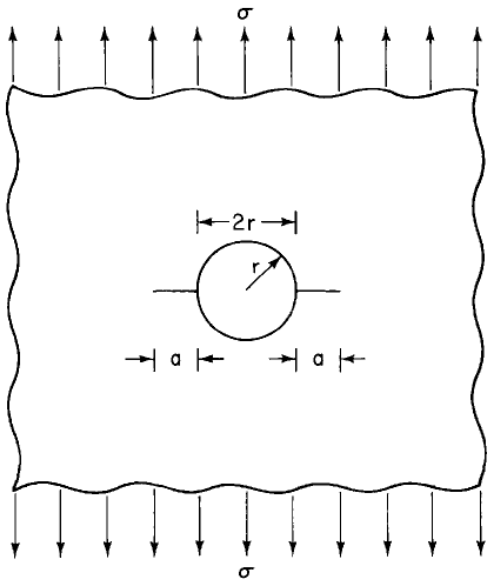

$$K_I = F\left(\frac{a}{r}\right)\sigma\sqrt{\pi a}$$

r = radius of hole

a = crack length from the side of hole

For short cracks, $K_I = K_t.\sigma\sqrt{\pi a}$

Figure 6.5- plate with crack emanating from notch

Table 6.2 – Values of F(a/r) for plate with crack from notch

a/r	F(a/r), One crack	F(a/r), Two cracks
0.00	3.39	3.39
0.10	2.73	2.73
0.20	2.30	2.41

6.7 Fatigue life predictions

A fracture mechanics approach is used to predict the fatigue life of the heavy duty riveted gratings. Two cases of crack growth behavior are investigated based on observations from fatigue testing.

Case 1: A main bearing bar with crack from the edge in bending.

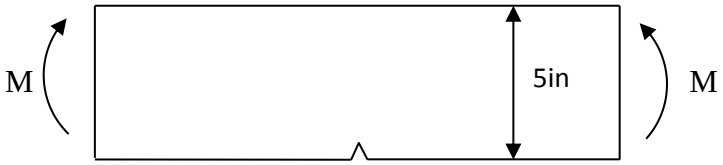

An initial crack size of 0.03in was used for a more conservative estimate of the fatigue life with the stress intensity factor based on the solution of a plate with an edge crack under bending (Figure 6.4). The crack growth rate relation proposed by Barsom and Rolfe for the Ferrite pearlite steel is used.

$$\frac{da}{dN} = 3.6\times10^{-10}\Delta K^{3} \quad \text{in/cycle}$$

Final crack sizes, a, were determined from the fracture toughness properties of steel and depend on the stress range. Applied stress range used includes 15ksi, 20ksi, 25ksi, 30ksi, 35ksi. Fatigue life is calculated as

$$N = \int_{0.03}^{a} \left(\frac{da}{3.6\times10^{-10}\Delta K^{3}} \right) \tag{6-9}$$

Case 2: A main bearing bar with a notch with crack from the edge in bending

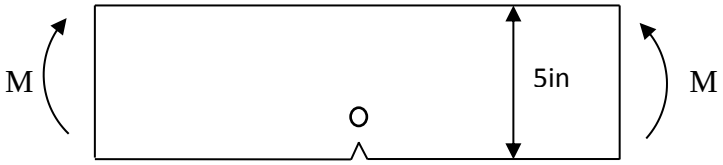

The total fatigue life for the main bearing bar with a notch involves a combination of estimates for a bar with an edge crack and from a crack emanating from a notch. Estimates for a bar with an edge crack occur similar to case 1. An initial crack size of

0.03in is used. The rivet hole is placed 0.75in from the edge of the bar and has diameter 0.375in. When the critical crack size based on fracture toughness requirements and stress range is greater than 0.9375in, the second phase of crack emanating from a notch results. This applies to the stress range of 15ksi and 20ksi for a critical crack size of 2.45in and 1.38in respectively.

$$N_{total} = N_{edge} + N_{hole}$$

The stress intensity factor solution for a plate with an edge crack under bending from an initial crack size to the opening of the rivet hole (Figure 6.4) is used for estimates in the first case, N_{edge}. The critical crack size used in this case for stress ranges of 25ksi and 30ksi was 0.5625in but a value of 0.45in was used for 35ksi.

The second, N_{hole} uses an approximate solution for the stress intensity factor of a plate with crack emanating from a notch in tension. This involves estimates of the number of cycles needed to advance the crack from the edge of the hole to its critical size. An approximate equation for the worst case scenario is employed. A conservative value of F(a/r) of 3.39 is used. As a/r approaches zero, F(a/r) for either one or two cracks approaches the stress concentration for a round hole, K_t of 3.

$$K_I = 3\sigma\sqrt{\pi a}$$

The results for fatigue life estimates is summarized in Table 6.3 and is plotted along with the lower bound curve based on experimental data and the AASHTO curves (Figure 6.6)

Table 6.3 – Fatigue life estimates for the 37R5 using fracture mechanics approach

Stress Range	Case 1	Case 2
15	1097752	934807.8
20	443936.4	400987.2
25	217379	205034.5
30	137219	118654.23
35	86411.97	72072.6

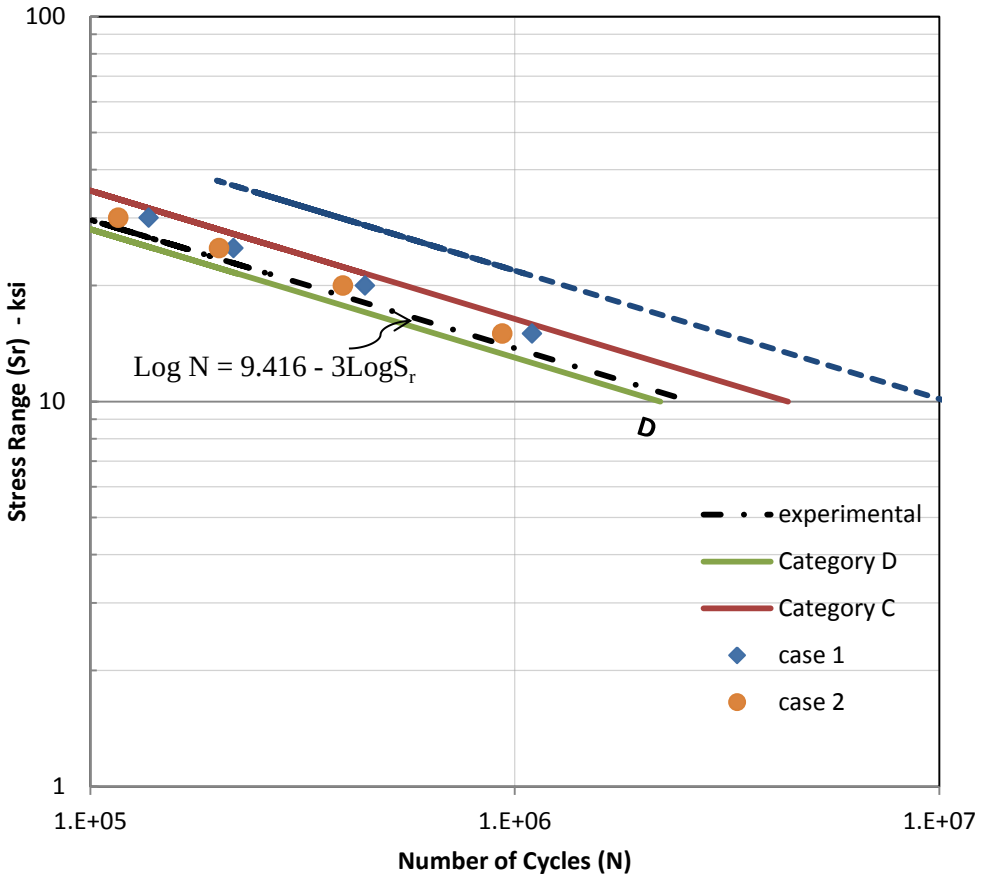

Figure 6.6 – Fatigue life results of gratings compared.

From the results, the controlling detail for the fatigue estimates of heavy duty riveted gratings is a bearing bar with a notch. The results from the fracture mechanics approach compares well with that of laboratory data. The fatigue behavior of the gratings based on the fracture mechanics estimates is between that of a category C and D and lies above the lower bound estimates from experimental results. If the stress range is known, the fatigue life of the heavy duty riveted grating can be estimated based on the length of a crack from figure 6.7 and be used to estimate the remaining fatigue life of existing heavy duty riveted gratings on bridges.

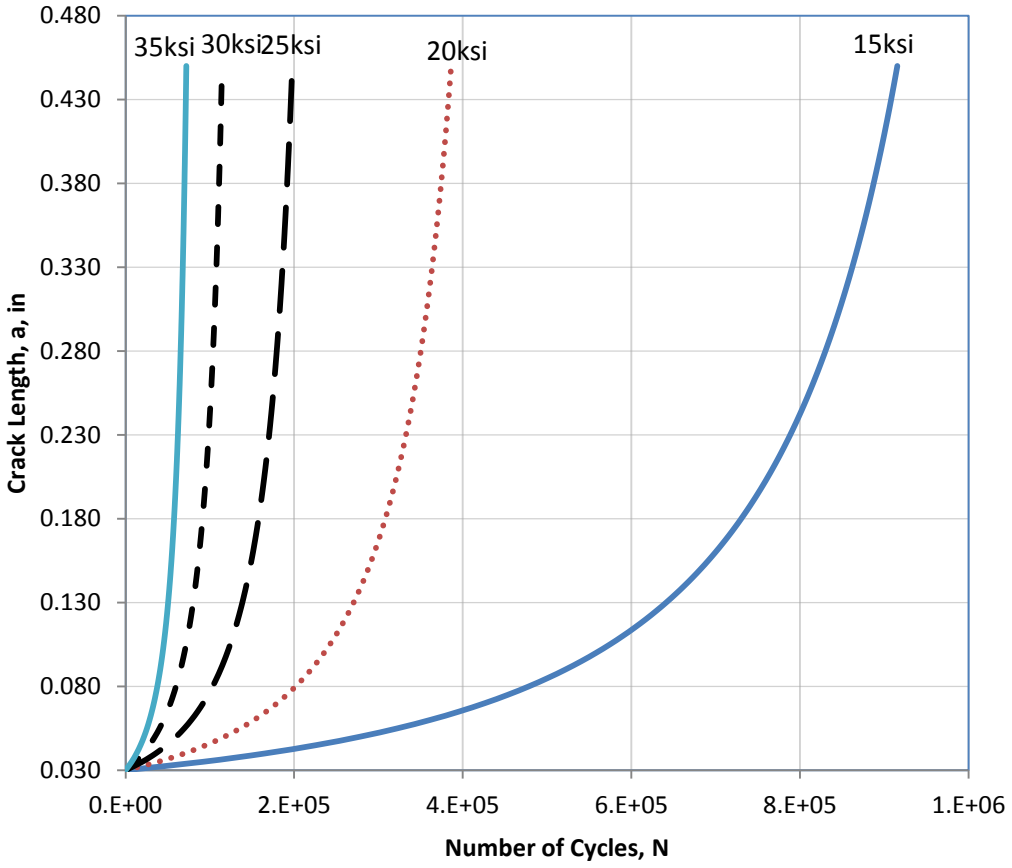

Figure 6.7 - Fatigue life estimates based on crack length and stress range

CHAPTER VIII

PROPOSED DESIGN GUIDE FOR HEAVY DUTY RIVETED STEEL GRATINGS

7.1 Introduction

The current design method for heavy duty riveted steel gratings is explored as provided by the NAAMM Manual. In as much as this has been in use for years, it is based on allowable stress design principles where design inconsistencies exist. A limit state design analysis is explored for design of the heavy duty riveted gratings by examining various limit states. Design approaches are based on static and fatigue testing of these gratings at the Gas turbine facility of the University of Akron. The proposed method will be based on load and resistance factor design (LRFD) concepts

7.2 Philosophy of Design

Two philosophies of design exists namely allowable stress design and limit state design methods. A major consideration in the design of a structure is for the capacity of the structure to be greater than or equal to the applied loading. This is a key requirement for both design philosophies.

7.2.1 Allowable Stress Design

The allowable stress design method was preferred by engineers till the advent of load and resistance factor design. Uncertainties in the variation of material properties and loading are incorporated in a factor of safety. The factor of safety which was empirical and chosen based on experience, introduces inconsistencies in the design process. The allowable stress design method has a number of shortcomings. The variability of load and resistance was not well accounted for based on occurrence and importance. The fundamental measure of resistance was allowable stress instead of strength. There are reliability issues with its use since it does not provide a consistent measure of probability of failure. The design equation for allowable stress design is given as

$$\frac{R_n}{F.S} > \sum Q \tag{7-1}$$

R_n = nominal or ultimate resistance

F.S = factor of safety

$\sum Q$ = summation of force effects

7.2.2 Limit State Design

A limit state is the point at which a structure fails to perform the function for which it was designed. Limit states are divided into strength limit states and serviceability limit states. Strength limit states are behavioral phenomena as achieving ductile maximum strength, buckling, fatigue and fracture, overturning and sliding. Serviceability limit states are those concerned with occupancy of a building such as deflection, vibration, permanent deformation, etc. Limit states considered in the AASHTO Load and Resistance Factor

Design specifications includes service limit states, strength limit states, extreme events limit states and the fatigue limit state

7.2.3 Load and Resistance Factor Design

Load and resistance factor design is a probability based approach where uncertainties in the loading and that of the resistance are considered. In LRFD, a statistically based resistance factor, ϕ, whose value is usually less than one, is applied to the resistance provided by the system. The load side is multiplied by a statistically based load factor for the various load conditions involved. Load factors, γ_i differ depending on the degree of predictability and occurrence. Given the nominal resistance, the safety criterion can be written as

$$\phi R_n \geq \sum n_i \gamma_i Q_i \qquad (7\text{-}2)$$

ϕ = statistically based resistance factor

R_n = nominal resistance

n_i = load modifier to account for effects of ductility , redundancy and operational importance

γ_i = statistically determined load factor

Q_i = load effect

When applied to heavy duty riveted steel gratings, the value of ϕ for a particular limit state will depend on a number of factors. LRFD accounts for variability in both resistance and load and achieves relatively uniform levels of safety providing more consistency. Limitations towards the development of LRFD are that the procedure involves a rigorous

approach requiring large volumes of data which cannot be obtained without testing. When applied to heavy duty riveted gratings, the value of ϕ for a particular limit state can take into account the nature of the material properties for the bearing bars and quality of fabrication and control programs.

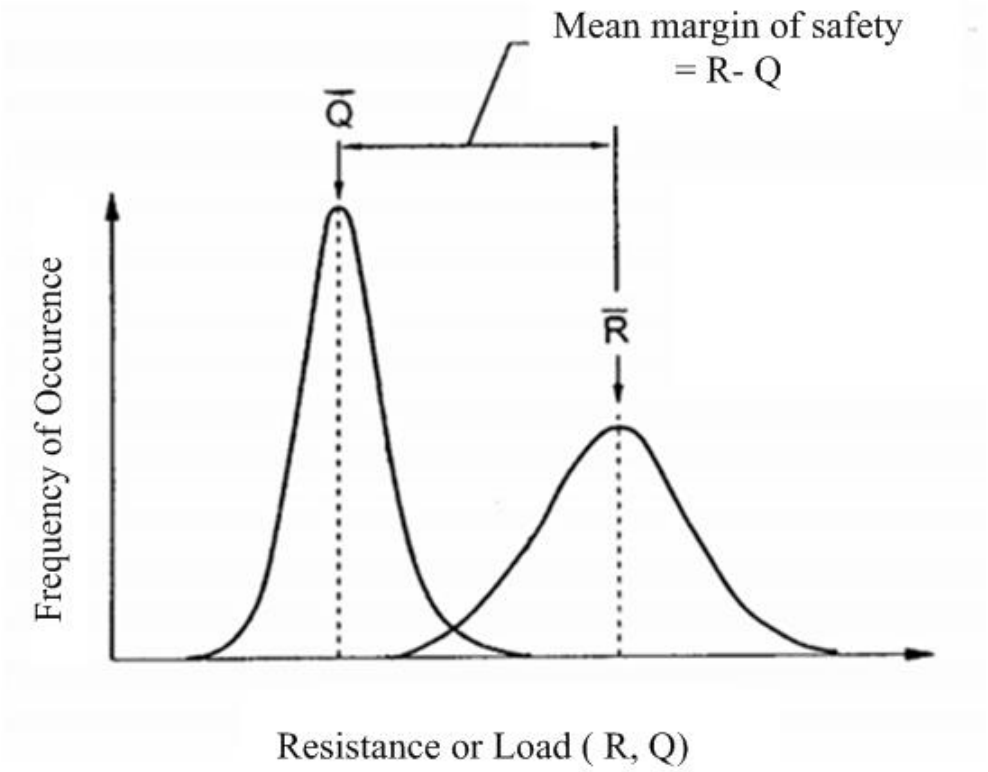

Figure 7.1 Variations of Resistance and Load

The process of assigning values to both resistance and load factors is called calibration. It can be achieved by judgment, fitting to other codes, reliability theory or a combination of the approaches. The factors developed by AASHTO for steel structures will be applied towards the design of the heavy duty riveted steel gratings.

7.3 Design Methods

A number of analysis methods exist for the design of open grid decks and are described below. The yield line analysis method which takes advantage of the reserve strength after yield was used by Cannon (1969) and Vukov (1986) to analyze square and rectangular grid systems. A review of the various design methods is presented below.

7.3.1 NAAMM Approach

The National Association of Architectural Metal Manufacturers (NAAMM) uses an allowable stress design approach in the design of the heavy duty riveted gratings. Bearing bars are so designed to ensure that the maximum stresses do not exceed allowable stresses. This limits bending stresses to $0.6F_y$ on the bearing bars. The moment capacity of a heavy duty riveted gratings is estimated on a simply supported span of the grating and applied to all other spans with either a concentrated load or a uniformly distributed load. The load distribution criteria conform to the AASHTO Standard Specifications for Highway Bridges, 16th Edition with a tire contact area of 20 in x 20in. Maximum deflection for gratings subject to vehicular loads are restricted to 0.125 inches or L/400.

7.3.2 Orthotropic plate theory

Orthotropic plate theory has been utilized in the design of both open and filled grid decks. Timoshenko et al (1959) describes the behavior of plate as having different elastic properties with the following assumptions:

- No deformation occurs in the middle plane of the plate and thus remains neutral during bending
- Points of the plate lying initially on a normal to the middle plane of the plate remain on the normal to the middle surface of the plate after bending.
- The normal stresses in the direction transverse to the plate can be disregarded.

A general differential equation for bending and twisting moments of an orthotropic plate can be written as:

$$D_x\left(\frac{\partial^4 w}{\partial x^4}\right)+2H\left(\frac{\partial^4 w}{\partial x^2\partial y^2}\right)+D_y\left(\frac{\partial^4 w}{\partial y^4}\right)=q(x,y) \qquad (7\text{-}3)$$

$$H=D_1+2D_{xy}$$

Where D_x = flexural rigidity in the strong direction

D_y = flexural rigidity in the weak direction

D_1 = torsional rigidity contribution from the strong and weak direction rigidities

D_{xy} = torsional rigidity

H = sum of the torsional rigidity contribution from the strong and weak direction rigidities (D_1) and torsional rigidity (D_{xy});

$w(x,y)$= vertical plate deflection in the Cartesian coordinate system;

$q(x,y)$ = applied transverse load in the Cartesian coordinate system. Corresponding moment equations include:

$$M_x=D_x\frac{\partial^2 w}{\partial x^2}+D_1\frac{\partial^2 w}{\partial y^2} \qquad (7\text{-}4)$$

$$M_y=D_y\frac{\partial^2 w}{\partial y^2}+D_1\frac{\partial^2 w}{\partial x^2} \qquad (7\text{-}5)$$

$$M_{xy} = 2D_{xy}\frac{\partial^2 w}{\partial x \partial y} \tag{7-6}$$

Results from moment capacity predictions for grid decks showed that orthotropic plate theory was good for filled grid decks but not open grid decks (Huang, 2001)

7.3.3 Unified Method by Higgins

Higgins et al (2001) reviewed current procedures for the analysis of bridge decks and established that in as much as the classical orthotropic theory proved useful in the design of a number of decks; it could not be applied to all decks. New analytical expressions were developed based on the torsional rigidities, H, of grid decks for the three possibilities that exist. (Timoshenko and Woinowski-Kreiger, 1959)

Case1. $H > \sqrt{D_x D_y}$

The solution has real and unequal roots that correspond to relatively torsionally stiff, flexurally soft deck, which correspond to partially and fully filled grid decks.

Case 2 $H = \sqrt{D_x D_y}$

The solution has equal and real roots that correspond to relatively thick plate or typical reinforced concrete slab.

Case 3 $H < \sqrt{D_x D_y}$

The solution has imaginary roots that correspond to relatively torsionally soft, flexurally stiff decks, which correspond to open steel grid decks.

The design equations developed could be used to estimate the maximum strong direction live load moments without cumbersome moving load analysis and can thus be applied to a number of deck types.

7.4 Proposed Design Approach for Heavy Duty Riveted Gratings.

The proposed design method is based on requirements of the AASHTO Bridge Design Specifications and results of static, finite element and fatigue testing of heavy duty riveted steel gratings. It is a limit state design method using load and resistance factors. Limit states considered include strength, service and fatigue. A number of assumptions are made during the implementation of the procedure and includes the following:

- Load distribution criteria conform to the AASHTO LRFD Bridge Design Specification with a tire contact area of 20in x 10in.
- The number of bars within the effective width of the grating provides the same level of resistance to applied loads. Intermediate bar contribution should be considered when estimating the structural capacity of the grating within the effective width but not connecting bars.
- Fatigue evaluation is based on a reduced effective width and occurs only for details over interior supports.
- All limit states considered are of the same importance
- Deflection limit for the design of heavy duty riveted grating is same as stated in the NAAMM manual

7.4.1 Effective width

The effective width to be considered for the design of the heavy duty riveted gratings is based on laboratory results for the static loading and finite element analysis of the gratings for H20 loading. Existing primary strip widths in AASHTO are not applicable for heavy duty riveted gratings. The proposed effective primary width to be considered for the design of heavy duty riveted gratings for strength is given by:

$$\text{Width of Primary Strip} = N + 2S_b \ \text{(in)} \tag{7-7}$$

N = width of the tire patch perpendicular to the bearing bars

S_b = spacing of bearing bars in the grid

The value of N is 10in when the direction of loading is perpendicular to the main bearing bars and 20in when loading direction is parallel. There is a marginal increase in the primary strip width when the magnitude of load increases but its effect is negligible in the heavy duty riveted steel grating. Figure 7.2 shows a graph of the strain distribution across the width of the 37R5 lite with increasing loading. The effective width is calculated after the number of bearing bars within the primary strip width is known and is given by equation (7-8).

$$\text{Effective width} = S_b\,(n_{bb}-1) + t_b \tag{7-8}$$

n_{bb} = number of bearing bars within the primary strip width

t_b = thickness of bearing bar

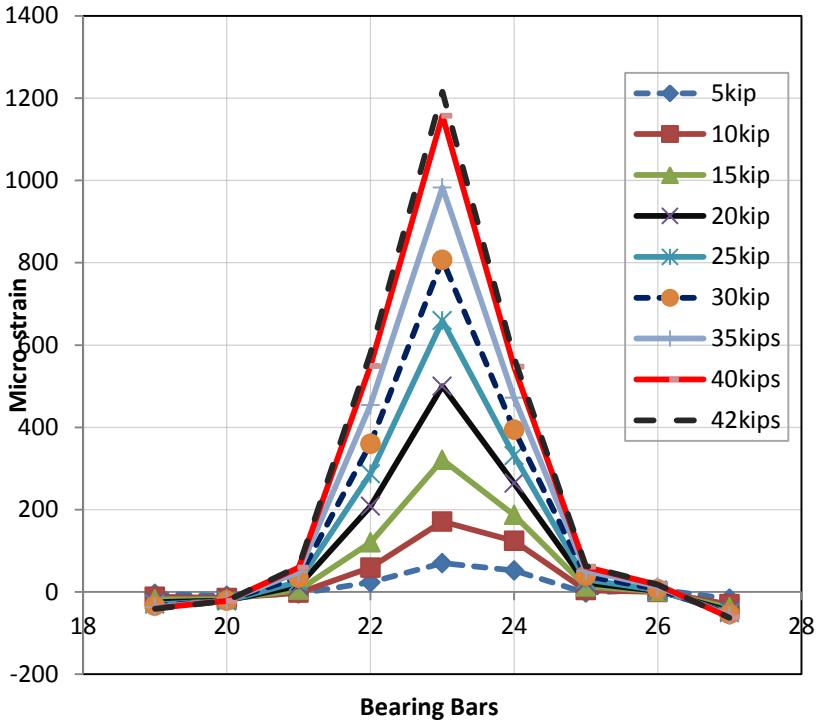

Figure 7.2 – Strain distribution across width of grating with increasing load

A summary is provided in Table 7.1 for the effective width for different forms of the 37R5 heavy duty riveted steel grating when traffic flows in both the perpendicular and parallel directions to bearing bars. The effective width values are compared with that based on a prediction using the primary strip width of the AASHTO which is given by:

$$\text{Width of Primary Strip} = 1.25P + 4.0S_b \text{ (in)} \quad (7\text{-}9)$$

P = axle load (kips)

S_b = spacing of grid bars (in)

For serviceability and fatigue limit states, a reduced strip width is proposed. This should be taken as 75% of the effective width calculated for strength

Table 7.1 – Width of primary strip for the design of heavy duty riveted gratings

Panel Type	Bearing bar (BB) Size (in)	Intermediate Bar (IB) Size (in)	Effective width (in)		
			Perpendicular	Parallel	AASHTO
37R5	5 x 1/4	*	13.075	23.335	29.25
	5 x 3/8	*	13.2	23.46	29.25
37R5 Lite	5 x 1/4	1-1/2 x 1/4	15.64	25.9	38.5
	5 x 3/8	1-1/2 x 1/4	15.765	26.025	38.5
37R5 L-Series	5 x3 x 1/4	1-1/2 x 1/4	23.335	31.03	47.75

7.4.2 Strength Limit State

Design for strength is based on an elastic analysis. The strength limit state of the heavy duty riveted grating includes the determination of the flexural and shear capacities. In order to determine the applied moment and shear, a conservative approach can be used. It involves considering a partially distributed load placed on a simply supported span of the heavy duty riveted grating for maximum force effects.

(a) Flexure

The moment capacity of the heavy duty riveted grating is taken as a sum of the individual moment capacities of the bearing and intermediate bars within the effective width. The

LRFD condition governing the design of the heavy duty riveted grating for flexure is given by:

$$\gamma_i M_u \leq \phi_f M_n \qquad (7\text{-}10)$$

Where γi = load factors

M_u = Applied Moment

M_n = nominal moment resistance

ϕ_f = resistance factor for flexure

The nominal moment resistance per foot of grating is given by

$$M_n = F_y S_x R_h R_b \qquad (7\text{-}11)$$

Where F_y = yield strength of the steel

S_x = section modulus for the grating within the effective width expressed per foot of grating

R_h = hybrid factor = 1.0 for heavy duty riveted steel gratings

R_b = web load shedding factor = 1.0 for heavy duty riveted gratings

The resistance factor for flexure, ϕ_f is taken as 1.0 in bridges and 0.9 in other applications. Bearing bar sections are considered compact with no lateral torsional buckling because connecting bars riveted 5in along main bars provide enough lateral stability to prevent buckling.

(b) Shear

No shear failures were observed in heavy duty riveted grating both during service and in experimental testing even at high loads and is not the controlling limit state for design. The shear capacity of the heavy duty riveted gratings is taken as the individual capacities

of the bearing bars within the effective width. The LRFD condition governing the shear design of the heavy duty riveted grating is given by:

$$\gamma_i V_u \leq \phi_v V_n \tag{7-12}$$

Where V_u = applied shear

V_n = nominal shear resistance

The nominal shear capacity of the heavy duty riveted grating is given by

$$V_n = n_{bb} C V_p = 0.58 n_{bb} F_y D t_w \tag{7-13}$$

Where D = depth of bearing bar

t_w = thickness of bearing bar

C= ratio of the shear buckling resistance to the shear yield strength and is taken as 1.0 for heavy duty riveted gratings.

The resistance factor for shear, ϕ_v is taken as 1.0 for bridges and 0.9 for other applications

7.4.3 Serviceability Limit State

Deflection requirements need to be met during the design of heavy duty riveted gratings. The AASHTO manual sets a limit for excessive deck deformation as live load and the dynamic load allowance not to exceed L/800. In estimating the deflection on a heavy duty riveted grating, a conservative approach can be used and involves estimating deflection of the wheel load on a simply supported span of the grating. If continuous spans exist, a continuity factor less than 1.0 can be applied. A deflection limit of L/400 is recommended for the design of heavy duty riveted gratings as provided in the NAAMM manual

7.4.4 Fatigue Limit State

Heavy duty riveted gratings should be conservatively designed for fatigue as a category D but with a constant amplitude fatigue limit of 12ksi. The LRFD expression for the investigation of the fatigue limit state is given by:

$$\gamma(\Delta f) \leq (\Delta F)_n$$

Where γ = load factor

Δf = live load force effects with dynamic allowance

ΔF = nominal fatigue resistance

For infinite fatigue life

$$\gamma(\Delta f) \leq \Delta F_{TH}$$

Where ΔF_{TH} = constant amplitude fatigue limit =12ksi

Fatigue Resistance is taken as

$$(\Delta F)_n = \left(\frac{A}{N}\right)^{1/3} \geq \frac{1}{2}(\Delta F_{TH})$$

$N = (365)\ (75)\ n\ (ADTT)_{sl}$

$A = 2.9 \times 10^9$ or category D

n= design life of 75 years

N= number of stress range cycles per truck passage.

7.5 Design Example

Check the suitability of the 37R5 L-series riveted deck to be used to replace a welded deck on a 4-span movable bridge with stringer spacing of 5ft for strength, service and

fatigue limit states. Grade 36 steel is used for both bearing angles and intermediate bars. The main bars are to be oriented perpendicularly to the direction of traffic flow.

(a) Design Information

The 37R5 L-series to be supplied by XC Gratings Inc has the following properties:

1. Grating Properties

Bearing angle size: 5in x 3in x ¼in

Intermediate bars: 1-1/2in x ¼in

Reticuline bars: 1-1/2in x ¼in

Spacing of grid bars, S = 2.5625in

Spacing of main bars, Sb = 7.695in

Stringer Spacing, L = 5ft

2. Steel Properties and Nature of Loading

Yield Strength of Steel, F_y = 36ksi

Elastic Modulus, E = 29000ksi

Wheel Live Load, P = 16kips

Dynamic Load Allowance Strength, IM_{str} = 33% Fatigue = IM_{fat} = 15%

W_{deck} = 24.61lb/ft

3. Effective width

Assumed Primary width, $P_w = 10 + 2S_b$ = 25.376in

Total Number of bars, $N = P_w/S = 10$ (approximate)

Number of bearing bars, $n_{bb} = P_w/Sb = 4$ (approximate)

Number of intermediate bars = $N - n_{bb} = 10 - 4 = 6$

Effective width for strength, $W_{str} = S_b (n_{bb}-1)$ + Thickness of bearing bar

$= 7.695(4 - 1) + 0.25 = 23.335$in

Effective width for Serviceability, $W_{ser} = 0.75 \times W_{str} = 17.5$in

Effective width for Fatigue, $W_{fat} = 0.75 \times W_{str} = 17.5$in

4. Section Properties (Appendix B)

Moment of Inertia within effective width

$$I_x = 4 \times 7.552 + 6 \times 0.88065 = 35.5 in^4$$

$I_x = 18.417 in^4$ per foot of grating

Section Modulus

$$S_{top} = \frac{18.417}{2.22} = 8.29 in^3$$

$$S_{bot} = \frac{18.417}{2.78} = 6.62 in^3$$

5. Loads and Internal Forces

Dead Loads

Considering a simply supported beam

Moment due to the self-weight, $M_{DL} = 0.125 w_{deck} L^2 = 0.076$kip-ft

Shear due to self-weight, $VDL = 0.5 w_{deck} L = 0.062$kip

Live Loads

With an influence line analysis per effective width

Positive moments, $M_{pos} = (0.204 - 0.0250)\,\text{PL} = 14.32\,\text{kip-ft}$

Negative moments, $M_{neg} = (-0.1029 - 0.0789)\,\text{PL} = -14.54\,\text{kip-ft}$

Shear, V_{LL} = 16kips

With Impact factor for Strength, IM_{str} = 33%

Moments per foot of grating

$$M_{LL-pos} = \left(1 + \frac{IM_{str}}{100}\right) \times \frac{12}{23.125} \times M_{pos} = 9.60 \text{ kip-ft}$$

$$M_{LL-neg} = \left(1 + \frac{IM_{str}}{100}\right) \times \frac{12}{23.335} \times M_{neg} = 9.80\,\text{kip-ft}$$

Shear per effective width

$$V_{LL\_imp} = \left(1 + \frac{IM_{str}}{100}\right) \times V_{LL} = 21.28\,\text{kips}$$

6. Check for strength limit states

Moment, $M_u = 1.25M_{DL} + 1.75M_{LL}$

Positive moment = 16.895 kip-ft

Negative moment = 17.15 kip-ft

Nominal moment resistance

$\phi_f M_n = \phi_f F_y S_{bot} = 19.86\,\text{kip-ft} > M_u$, Moment OK

Shear, Vu = $1.25V_{DL}$ + 1.75VLL = 37.32kip

Shear Resistance with a factor of 1

$\phi_v V_n = 0.58\phi_v n_{bb} F_y D t_w = 145\,\text{kip} > \text{Vu}$, Shear OK

7. Check for Deflection

Using simply support span 1 and wheel load

$$\Delta = \frac{12}{W_{ser}}\left(1+\frac{IM_{str}}{100}\right)\frac{PL^3}{48EI} = 0.124\,\text{in}$$

$\frac{L}{400} = 0.15\,\text{in} > \Delta$, Deflection OK

8. Check for Fatigue

With Impact Factor for Fatigue, IM_{fat} = 15%

$$M_{LL-fat} = 0.75\left(1+\frac{IM_{fat}}{100}\right)\times\frac{12}{17.5}\times M_{neg} = 8.60\,\text{kip-ft}$$

$$\sigma_{fat} = \frac{M_{LL-fat}}{S_{top}} = 12.45\,\text{ksi}$$

Nominal fatigue resistance for the 37R5 L-series

Constant amplitude fatigue limit (ΔF_{TH}) = 12ksi

$\frac{\sigma_{fat} - \Delta F_{TH}}{\Delta F_{TH}} = 3.75\% \le 5\%$, Fatigue resistance OK

CHAPTER VIII

SUMMARY AND CONCLUSIONS

8.1 Summary and Conclusions

Two panels of the 37R5 lite were tested under H20 loading to study the nature of the stress distribution across the grating. A 3D finite element model was developed and results from the finite element analysis were compared with experimental results. A parametric study was performed on the gratings after finite element results correlated well with the experiments. Results from experimental testing and finite element analysis of the gratings have been used to establish the following;

(a) The stress distribution on heavy duty riveted gratings can accurately be calculated when bearing bars directly within the contact area of loading and the adjacent bearing bars are considered.

(b) The moment regions within the vicinity of loading have high strains as compared to other regions. For fatigue testing and analysis, the section might not be critical since they exist as base metal with no attachment or stress raisers. The negative moment regions over the supports where the riveted details with holes in the main bearing bars appear critical

(c) Intermediate bars provide some level of resistance to applied loads and must therefore be included when the structural capacity of a heavy duty riveted grating

is been estimated. During testing of the 37R5 lite panel, they provided about a quarter of the resistance provided by the adjacent main bearing bar. In the case of the 37R5 L-series, they provided about 25% of the resistance towards supporting applied loads.

(d) Stresses on bearing bars are lower if traffic is oriented parallel to the direction of bearing bars

(e) When the U shaped attachment plates are used as an attachment method, the welds to the bearing bars should be placed closer to the neutral axis.

(f) Finite element analysis can be used to study and predict the behavior of heavy duty riveted gratings and any modifications in geometry.

Results from both static testing and finite element analysis formed the basis towards the fatigue testing of the riveted grating. Two sets of tests were performed during fatigue evaluation. The first test involved fatigue testing of full size panels of the 37R5 lite and the 37R5 L-series under AASHTO H-20 loading. To better characterize the general fatigue behavior of the heavy duty riveted gratings, another set of tests on smaller panels were conducted under varying stress ranges. Results from the fatigue testing of both full and smaller size panels have been used to establish the following:

(g) The critical detail to be considered for the fatigue evaluation of the heavy duty riveted grating is the tension regions over supports where the riveted detail exists.

(h) The proposed S-N curve of the heavy duty riveted grating is close to that of category D in the AASHTO LRFD specifications for a 97.5% confidence level, but the constant amplitude fatigue limit of 12ksi should be used.

(i) Laboratory data occurred above category C, and was close to that of a category B for both full and smaller size panels of the heavy duty riveted grating.

(j) At lower stresses, no fatigue failures were observed even after 2 million cycles of loading.

Fracture mechanics principles were used to predict the fatigue life of the heavy duty riveted grating and produced results comparable to fatigue testing. Results from the fracture mechanics analysis is used to establish the following:

(k) Linear elastic fracture mechanics principles can be used to accurately predict the remaining fatigue life of a riveted grating when an initial crack is detected.

(l) The fatigue behavior of the riveted grating is between category C and D of the AASHTO LRFD specifications and in close proximity to the proposed S-N curve for heavy duty riveted steel gratings.

(m) The critical detail for evaluation of the fatigue behavior of riveted gratings is a bearing bar with a punched hole for rivets.

The following recommendations are made towards the design of a heavy duty riveted steel grating based on results of experiments and observations about the performance of gratings in service.

(n) The effect of increased primary strip width with increasing load is negligible for heavy duty riveted steel gratings.

(o) The effective width for strength is calculated based on the number of bearing bars within the primary strip width.

(p) A reduced effective width is used for the serviceability and fatigue limit states.

(q) Heavy duty riveted steel gratings should be designed for the strength (flexure and shear), serviceability (deflection) and fatigue limit states.

(r) Deflection limit for the heavy duty riveted grating should be taken as L/400.

8.2 Recommendations for future work

The following are recommendations made for future work on heavy duty riveted steel gratings

(a) Longer life tests should be run on the heavy duty riveted gratings at stress ranges between 14ksi and 18ksi

(b) A deck – stringer connection system for simply supported heavy duty riveted grating panels to eliminate the presence of the critical detail in negative bending over interior supports.

(c) Crack distribution effects on the load rating of heavy duty riveted steel decks.

(d) Alternative methods of attachment for the riveted grating -stringer system.

(e) Calibration of resistance factors for heavy duty riveted steel gratings based on field data and experiments.

(f) Fatigue behavior and design of partially filled riveted steel grating decks.

REFERENCES

1. American Association of State Highway and Transportation Officials (AASHTO), "Standard Specifications for Highway Bridges",(2002) 17th Ed.,Washington, D.C

2. American Association of State Highway and Transportation Officials (AASHTO), "LRFD Bridge Design Specifications" (2004), 3rd Ed.. Washington, D.C

3. ANSI / National Association of Architectural Metal Manufacturers (NAAMM), "Heavy Duty Metal Bar Grating Manual "MBG 532-09 (2009) , 5th Edition

4. ANSI / National Association of Architectural Metal Manufacturers (NAAMM), "Engineering Design Manual "MBG 534-12 (2012)

5. Baker, Tod H (1991) "Static and Fatigue Strength Determination of Design Properties for Grid Bridge Decks, Volume I- Plate stiffness constants for Concrete Filled grid decks." Research Report ST-9, Department of Civil Engineering, University of Pittsburgh

6. Barsom,J.M., and Rolfe, S.T (1996), "Fracture and fatigue control in stuctures-Application of fracture mechanics", 3rd Edition., ASTM, Philadelphia

7. Bejgum, M. (2006), "Testing and Analysis of Heavy Duty Riveted Gratings", Thesis submitted to The Graduate Faculty of The University of Akron, Akron

8. Cannon, J. (1969), "Yield line analysis and Design of Grid Systems." AISC Engineering Journal, October: 124 -129

9. DiBattista J., Adamson D., and Kulak G.(1998), "Fatigue Strength of Riveted Connections", Journal of Structural Engineering, Vol. 124, 792-797.

10. Fetzer, P. (2013), "Behavior of Open Grid Steel Decks under Service and Fatigue Loads", Thesis submitted to the Oregon State University, Corvallis

11. Fisher, J., Kulak G., and Smith I. (1998), "A fatigue primer for structural engineers", National Steel Bridge Alliance.

12. Higgins C., Turan T, Connor R and Lui J. (2011), "Unified Approach for LRFD Live Load Moments in Bridge Decks", Journal of Bridge Engineering, Vol 16, 804-811.

13. H.V.S. GangaRao, W. Seifert, and H. Kevork (1987), "Behavior and Design of Open Steel Grid Decks for Highway Bridges". Final Draft Report. West Virginia University, Morgantown, Oct. 1987

14. Huang H. (2001), "Behavior of Steel Grid Decks for Bridges", Dissertation submitted to the graduate Faculty of the University of Delaware for the Degree of Doctor of Philosophy.

15. Keating P. and Fisher J.(1986), " Review of Fatigue Tests and Design Criteria on Welded Details" Fritz Engineering Laboratory Report 488.1(86) , Lehigh University , Bethlehem, PA

16. Mahama F (2003), "Finite Element Analysis of Welded Steel Gratings", Thesis submitted to The University of Akron

17. Mangelsdorf, C.P (1996), "Static and Fatigue Strength Determination of Design Properties for Grid Bridge Decks", Volume 4 - Summary and Final Report. January 1996.

18. Menzemer, C and Apperson (2010), "Heavy Duty Riveted Bridge Deck AASHTO H20 Loading and Fatigue Testing", 13th Biennial Symposium of Heavy Movable Structures, Inc

19. Murakoshi, Takahashi, Arima, Fujiwara, "Fatigue Tests of Open Grid Steel Decks under Running Wheel Loads" Public Works Research Institute, Japan (2003)

20. Tada, W., Paris, P. C., and Irwin, G. R. (2000). "The stress analysis of cracks handbook", 3rd Ed., ASTM, New York.

21. Timoshenko, S. and Woinowsky-Krieger, S.(1959),"Theory of plates and shells", McGraw-Hill, New York

22. Vukov,A. (1986) "Limit Analysis and Plastic Design of Grid Systems." Engineering Journal/American Institute of Steel Construction, 2nd Quarter:77-83

23. White, Dave (2009), Laboratory Data for static testing of heavy duty riveted gratings, Department of Civil Engineering, The University of Akron

APPENDICES

APPENDIX A

SMALLER SIZE SAMPLES

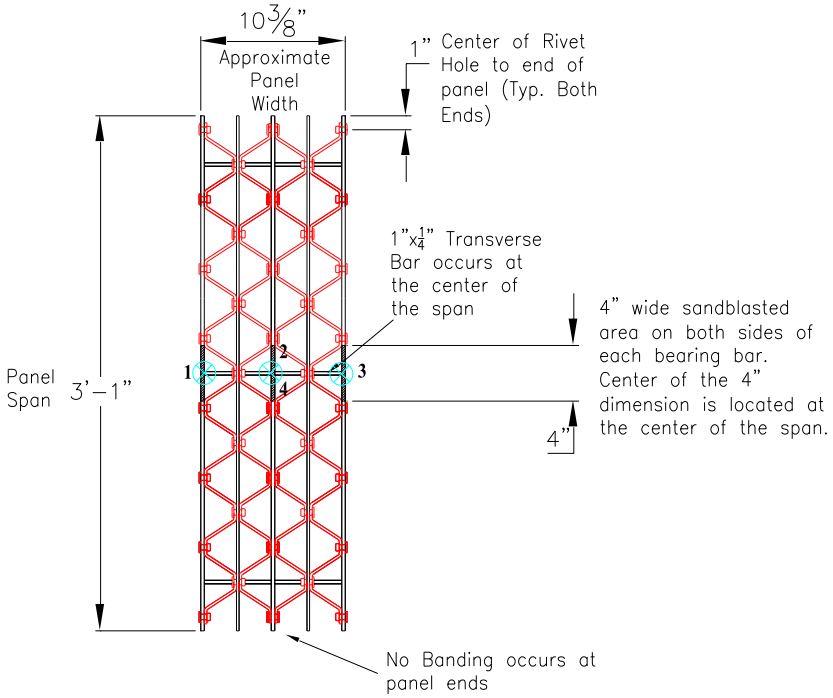

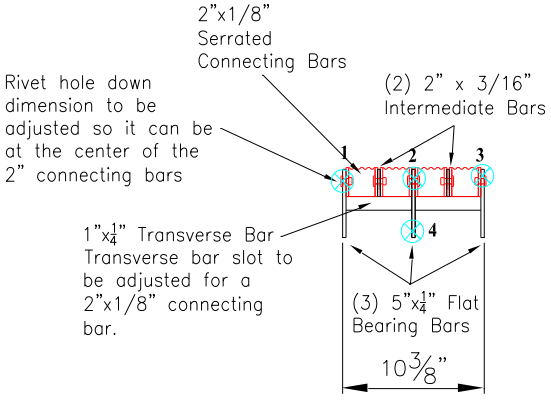

Sample B

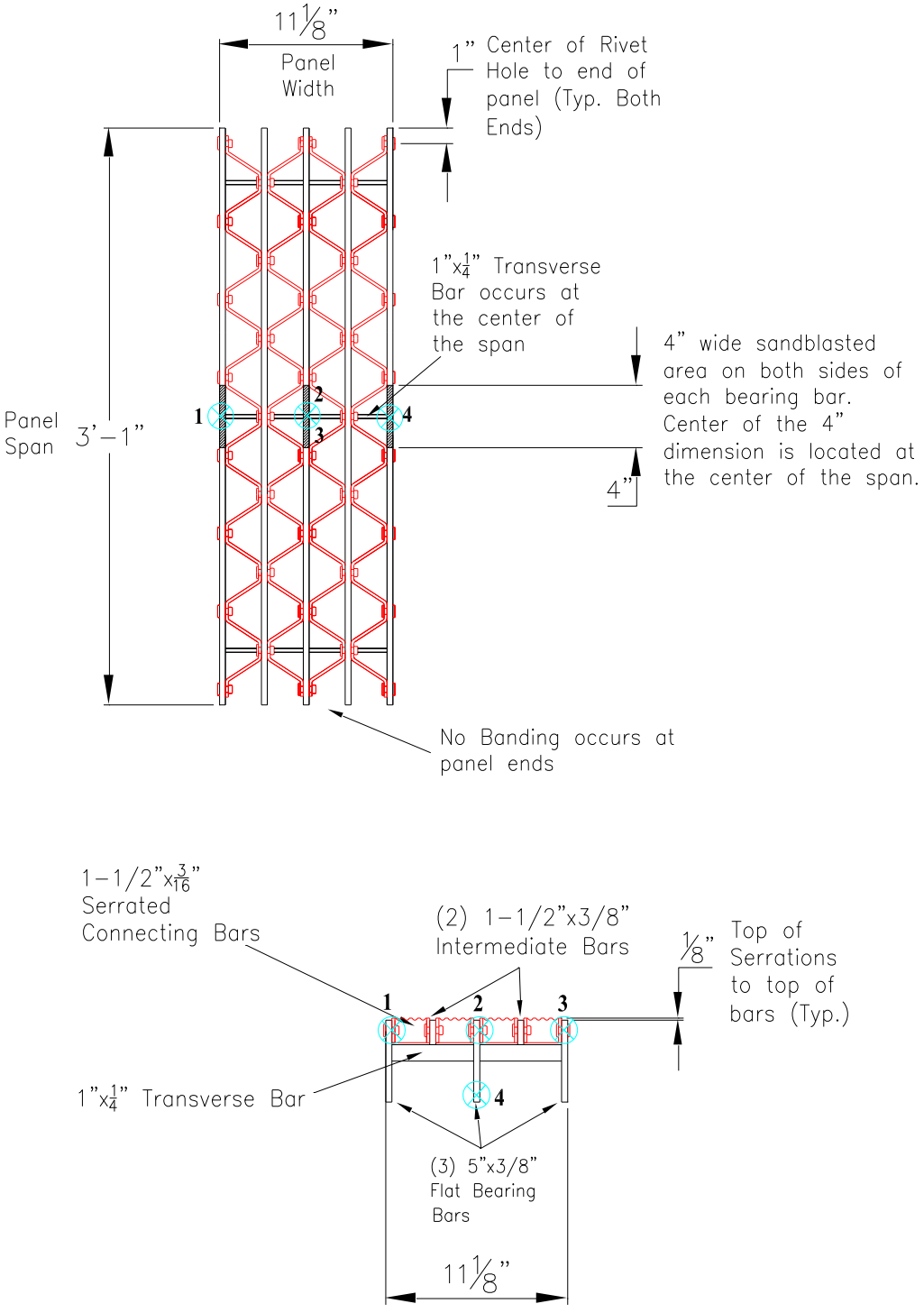
11 1/8"
Panel Width
1" Center of Rivet Hole to end of panel (Typ. Both Ends)
1"x1/4" Transverse Bar occurs at the center of the span
4" wide sandblasted area on both sides of each bearing bar. Center of the 4" dimension is located at the center of the span.
Panel Span
3'-1"
1
2
3
4
4"
No Banding occurs at panel ends
1-1/2"x3/16" Serrated Connecting Bars
(2) 1-1/2"x3/8" Intermediate Bars
1/8"
Top of Serrations to top of bars (Typ.)
1"x1/4" Transverse Bar
(3) 5"x3/8" Flat Bearing Bars
11 1/8"

Sample C

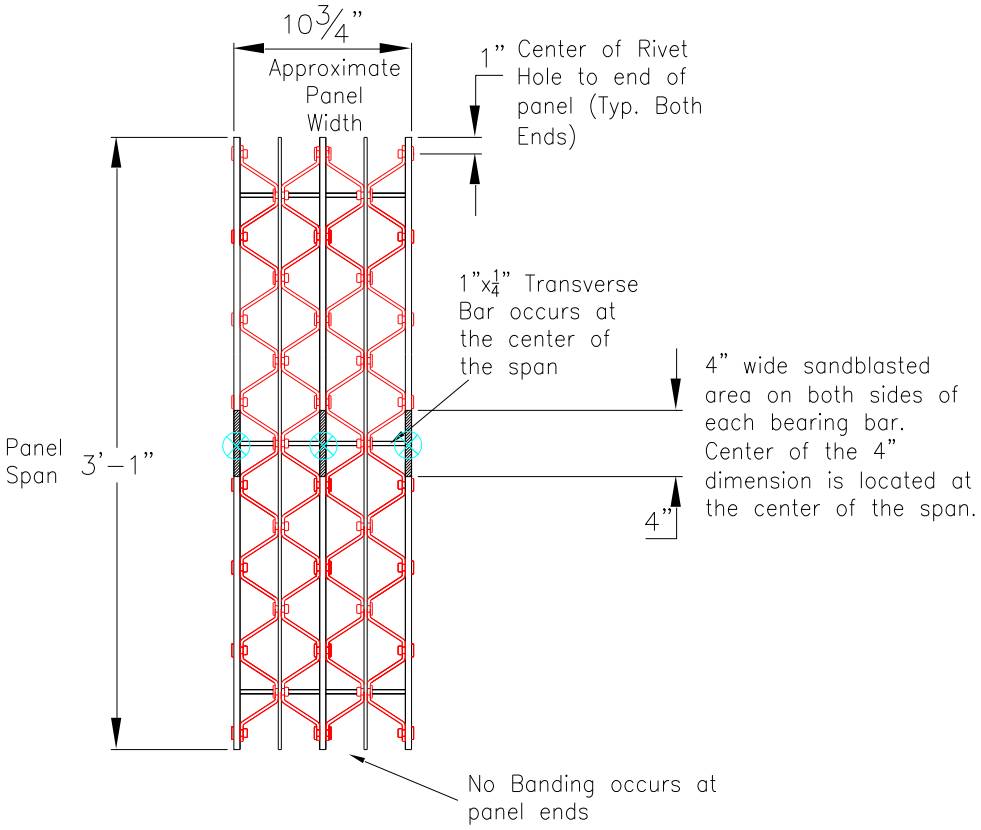
10¾"
Approximate Panel Width
1" Center of Rivet Hole to end of panel (Typ. Both Ends)
1"x¼" Transverse Bar occurs at the center of the span
4" wide sandblasted area on both sides of each bearing bar. Center of the 4" dimension is located at the center of the span.
4"
Panel Span 3'–1"
No Banding occurs at panel ends

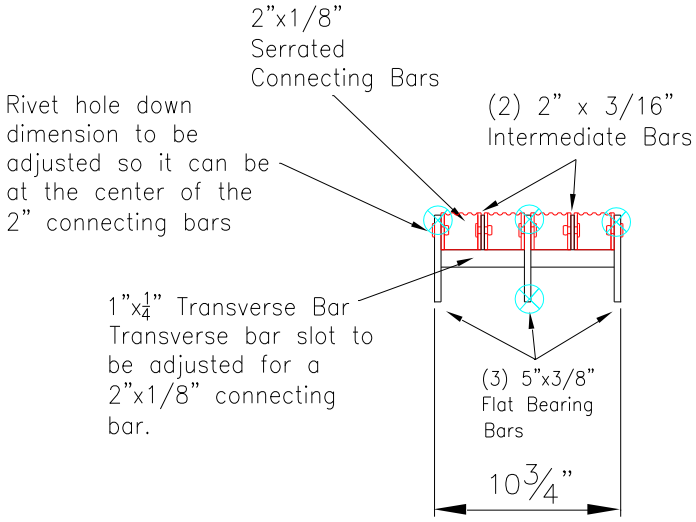
2"x1/8" Serrated Connecting Bars
(2) 2" x 3/16" Intermediate Bars
Rivet hole down dimension to be adjusted so it can be at the center of the 2" connecting bars
1"x¼" Transverse Bar Transverse bar slot to be adjusted for a 2"x1/8" connecting bar.
(3) 5"x3/8" Flat Bearing Bars
10¾"

Sample D

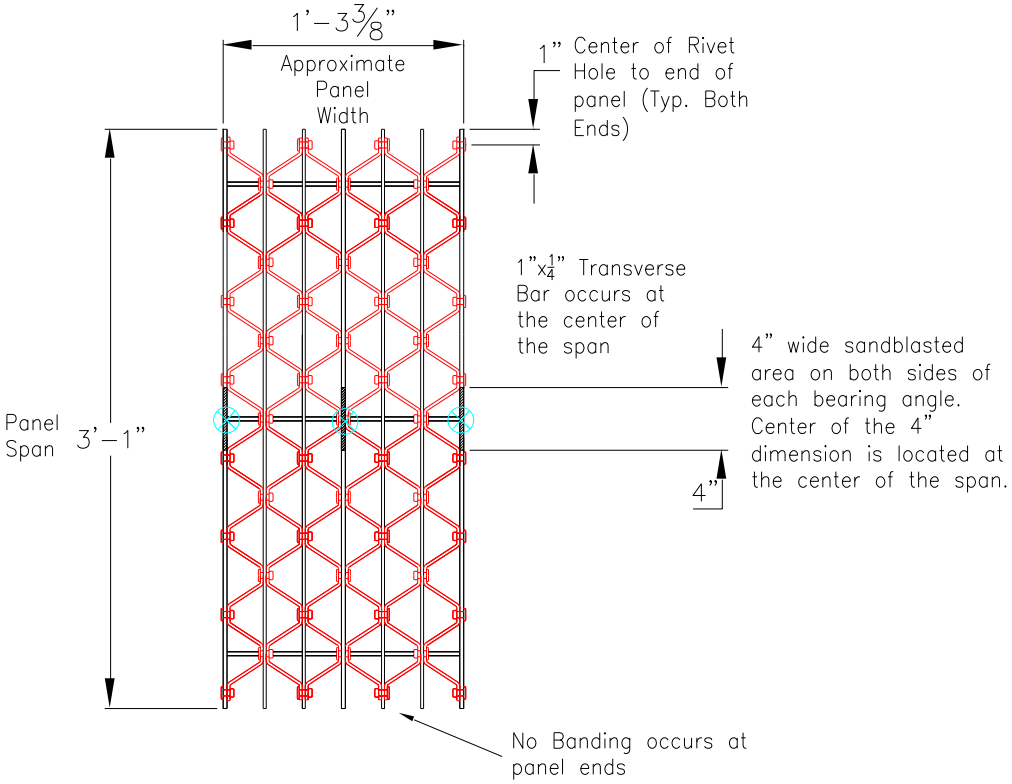
1'–3⅜"
Approximate Panel Width
1" Center of Rivet Hole to end of panel (Typ. Both Ends)
1"x¼" Transverse Bar occurs at the center of the span
4" wide sandblasted area on both sides of each bearing angle. Center of the 4" dimension is located at the center of the span.
Panel Span 3'–1"
4"
No Banding occurs at panel ends

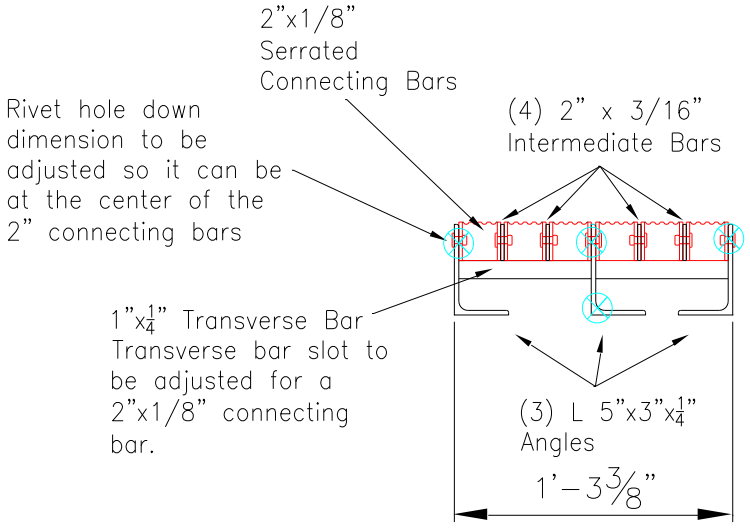
2"x1/8" Serrated Connecting Bars
Rivet hole down dimension to be adjusted so it can be at the center of the 2" connecting bars
(4) 2" x 3/16" Intermediate Bars
1"x¼" Transverse Bar Transverse bar slot to be adjusted for a 2"x1/8" connecting bar.
(3) L 5"x3"x¼" Angles
1'–3⅜"

Sample E

APPENDIX B

DESIGN CALCULATIONS

1. Weight of Open Grid Deck

Weight = cross section area x Density of steel

Weight = $490\left[1.9375\times 4+6\times 0.375+9\times 0.375\right]=45.51\text{lb/ ft}$ per effective width

Using a normalized width of 12in

Weight = $\frac{12}{23.125}\times 45.51=23.61\,\text{lb/ft}$

Assuming weight of Rivets = 1lb/ft^2

Weight of deck, w_{deck} = 23.61 + 1 = 24.61 lb/ft

2. Centroid within effective width

$$y_{bottom}=\frac{4\times 1.9375\times 1.657+1.5\times 0.25\times 4.25\times 6+1.5\times 0.25\times 4.375\times 9}{4\times 1.9375+1.5\times 0.25\times 6+1.5\times 0.25\times 9}=2.78in$$

3. Moment of Inertia

Moment of Inertia of a bearing angle with respect to centroidal axis

$$I_{C\_angle}=I_{angle}+Ah^2=5.109+1.9375\times(2.78-1.657)^2=7.552in^4$$

$$I_{C\_inter}=\frac{0.25\times 1.5^3}{12}+0.25\times 1.5\times(4.25-2.78)^2=0.88065in^4$$